Measurements of spin correlation in top-antitop quark events from proton-proton collisions at $\sqrt{s} = 7$ TeV using the ATLAS detector

G. Aad *et al.*[*]
(ATLAS Collaboration)

(Received 16 July 2014; published 24 December 2014)

Measurements of spin correlation in top quark pair production are presented using data collected with the ATLAS detector at the LHC with proton-proton collisions at a center-of-mass energy of 7 TeV, corresponding to an integrated luminosity of 4.6 fb^{-1}. Events are selected in final states with two charged leptons and at least two jets and in final states with one charged lepton and at least four jets. Four different observables sensitive to different properties of the top quark pair production mechanism are used to extract the correlation between the top and antitop quark spins. Some of these observables are measured for the first time. The measurements are in good agreement with the Standard Model prediction at next-to-leading-order accuracy.

DOI: 10.1103/PhysRevD.90.112016 PACS numbers: 14.65.Ha, 12.38.Qk, 13.85.Qk

I. INTRODUCTION

The top quark is the heaviest known elementary particle. Besides the high mass, it has the shortest lifetime of any quark, determined to be $(3.29^{+0.90}_{-0.63}) \times 10^{-25}$ s [1], which is shorter than the time scale for hadronization [2]. This implies that top quarks can be studied as bare quarks, i.e. quarks before hadronization, and the spin information of the top quark can be deduced from the angular distributions of its decay products.

In the Standard Model (SM) of particle physics, top quarks are produced at hadron colliders in pairs ($t\bar{t}$), predominantly via strong interactions, or singly via the electroweak interactions. At the Large Hadron Collider (LHC), which collided protons (pp) at a center-of-mass energy of 7 TeV in 2011, top quarks were mainly produced in pairs via gluon fusion. In the SM, $t\bar{t}$ pairs are produced essentially unpolarized at hadron colliders [3], as has been tested in recent measurements by the D0 Collaboration [4] and the ATLAS and CMS Collaborations [5,6]. Nonetheless, the correlation of the spin orientation of the top quark and the top antiquark can be studied, and is predicted to be nonzero [3,7–24].

New physics models beyond the SM (BSM) can alter the spin correlation of the top quark and top antiquark by modifying the production mechanism of the $t\bar{t}$ pair. Also, they can modify the $t\bar{t}$ decay by which the spin information is accessed. The first scenario occurs, for example, in BSM models where a $t\bar{t}$ pair is produced via a high-mass Z' boson [25,26] or via a heavy Higgs boson that decays into $t\bar{t}$ [27]. The second scenario occurs, for example, in supersymmetric models if a top quark decays into a spin zero particle like a charged Higgs boson, which then decays into a lepton and a neutrino [28,29]. Thus measuring the spin correlation in $t\bar{t}$ events can simultaneously probe top production and (indirectly) decay for potential effects due to new physics.

The measurements of the spin correlation between the top quark and the top antiquark presented in this paper rely on angular distributions of the top quark and top antiquark decay products. The charged leptons and the d-type quarks from the W boson decays are the most sensitive spin analyzers, and the b quark from top quark decay contains some information about the top quark polarization, too. Observables in the laboratory frame and in different top quark spin quantization bases are explored. These variables are used to measure the coefficient f_{SM}, which is related to the number of events where the t and $\bar{t}$ spins are correlated as predicted by the SM, assuming that $t\bar{t}$ production consists of events with spin correlation as in the SM or without spin correlation. The measured value of f_{SM} is translated into the spin correlation strength A, which is a measure for the number of events where the top quark and top antiquark spins are parallel minus the number of events where they are antiparallel with respect to a spin quantization axis, divided by the total number of events.

The spin correlation in $t\bar{t}$ events has been studied previously at the Tevatron and the LHC. The CDF and D0 Collaborations have performed a measurement of A by exploring the angular correlations of the charged leptons [30,31]. The D0 Collaboration has exploited a matrix element based approach [32] and reported the first evidence for nonvanishing $t\bar{t}$ spin correlation [33,34]. These measurements are limited by statistical uncertainties and are in good agreement with the SM prediction. Using the difference in azimuthal angles of the two leptons from the decays of the W bosons emerging from top quarks in the laboratory frame, $\Delta\phi$, the ATLAS Collaboration reported the first observation of nonvanishing $t\bar{t}$ spin correlation using

[*] Full author list given at the end of the article.

2.1 fb^{-1} of LHC data, taken at 7 TeV collision energy [35]. The CMS Collaboration also measured spin correlations in dileptonic final states at 7 TeV using angular correlations of the two charged leptons and the $\Delta\phi$ observable with 5.0 fb^{-1} of data [6], showing good agreement with the SM prediction.

In this paper, measurements of $t\bar{t}$ spin correlation using the full 7 TeV data sample of 4.6 fb^{-1} collected by the ATLAS Collaboration are presented. Using events with one or two isolated leptons in the final state, spin correlations are measured using $\Delta\phi$ between the lepton and one of the final-state jets or between the two leptons, respectively. Additional measurements are performed in the final state with two leptons, using observables that are sensitive to different types of sources of new physics in $t\bar{t}$ production. In particular, angular correlations between the charged leptons from top quark decays in two different spin quantization bases and a ratio of matrix elements in the dileptonic channel are also measured.

II. THE ATLAS DETECTOR

The ATLAS experiment [36] is a multipurpose particle physics detector. Its cylindrical geometry provides a solid angle coverage close to 4π.[1]

Closest to the interaction point is the inner detector, which covers a pseudorapidity range $|\eta| < 2.5$. It consists of multiple layers of silicon pixel and microstrip detectors and a straw-tube transition radiation tracker (TRT). Around the inner detector, a superconducting solenoid provides a 2 T axial magnetic field. The solenoid is surrounded by high-granularity lead/liquid-argon electromagnetic (EM) calorimeters and a steel/scintillator-tile hadronic calorimeter in the central region. In the forward region, end-cap liquid-argon calorimeters have either copper or tungsten absorbers.

The muon spectrometer is the outermost part of the detector. It consists of several layers of trigger and tracking chambers organized in three stations. A toroidal magnet system produces an azimuthal magnetic field to enable an independent measurement of the muon track momenta.

A three-level trigger system [37] is used for the ATLAS experiment. The first level is purely hardware-based and is followed by two software-based trigger levels.

III. OBJECT RECONSTRUCTION

In the SM, a top quark predominantly decays into a W boson and a b quark. For this analysis $t\bar{t}$ candidate events in two final states are selected. In the dilepton final state, both W bosons emerging from top and antitop quarks decay leptonically into $e\nu_e$, $\mu\nu_\mu$, or $\tau\nu_\tau$,[2] with the τ lepton decaying into an electron or a muon and the respective neutrinos. In the single-lepton channel, one W boson from the top or antitop quark decays leptonically, while the other W boson decays into a quark-antiquark pair.

Events are required to satisfy a single-electron or single-muon trigger with a minimum lepton transverse momentum (p_{T}) requirement that varies with the lepton flavor and the data-taking period to cope with the increasing instantaneous luminosity. During the 2011 data-taking period the average number of simultaneous pp interactions per beam crossing (pileup) at the beginning of a fill of the LHC increased from 6 to 17. The primary hard-scatter event vertex is defined as the reconstructed vertex with at least five associated tracks and the highest sum of the squared p_{T} values of the associated tracks with $p_{\mathrm{T}} > 0.4$ GeV.

Electron candidates [38] are reconstructed from energy deposits (clusters) in the electromagnetic calorimeter that are associated with reconstructed tracks in the inner detector. They are required to have a transverse energy, E_{T}, greater than 25 GeV and $|\eta_{\mathrm{cluster}}| < 2.47$, excluding the transition region $1.37 < |\eta_{\mathrm{cluster}}| < 1.52$ between sections of the electromagnetic calorimeters. The electron identification relies on a cut-based selection using calorimeter, tracking, and combined variables such as those describing shower shapes in the EM calorimeter's middle layer, track quality requirements and track-cluster matching, particle identification using the TRT, and discrimination against photon conversions via a hit requirement in the inner pixel detector layer and information about reconstructed conversion vertices. In addition, to reduce the background from nonprompt electrons, i.e. from decays of hadrons (including heavy flavor) produced in jets, electron candidates are required to be isolated from other activity in the calorimeter and in the tracking system. An η-dependent 90% efficient cut based on the transverse energy sum of cells around the direction of each candidate is made for a cone of size $\Delta R = \sqrt{(\Delta\phi)^2 + (\Delta\eta)^2} = 0.2$, after excluding cells associated with the electron cluster itself. A further 90% efficient isolation cut is made on the sum of track p_{T} in a cone of radius $\Delta R = 0.3$ around the electron track. The longitudinal impact parameter of the electron track with respect to the event primary vertex, z_0, is required to be less than 2 mm.

Muon candidates are reconstructed from track segments in various layers of the muon spectrometer and are matched with tracks found in the inner detector. The final muon candidates are refitted using the complete track information from both detector systems, and are required to have $p_{\mathrm{T}} > 20$ GeV and $|\eta| < 2.5$. Each muon candidate is required to be isolated from jets by a distance $\Delta R > 0.4$. In addition,

[1] ATLAS uses a right-handed coordinate system, with its origin at the nominal interaction point in the center of the detector. The z axis points along the beam direction, the x axis from the interaction point to the center of the LHC ring, and the y axis upwards. In the transverse plane, cylindrical coordinates (r, ϕ) are used, where ϕ is the azimuthal angle around the beam direction. The pseudorapidity η is defined via the polar angle θ as $\eta = -\ln\ \tan(\theta/2)$.

[2] We use the notation $e\nu_e$ for both $e^+\nu_e$ and $e^-\bar{\nu}_e$. The same applies to $\mu\nu_\mu$ and $\tau\nu_\tau$.

muon isolation requires that the transverse energy in the calorimeter within a cone of $\Delta R = 0.2$ is below 4 GeV after excluding the muon energy deposits in the calorimeter. Furthermore, muon isolation requires that the scalar sum of the track transverse momenta in a cone of $\Delta R = 0.3$ around the muon candidate is less than 2.5 GeV excluding the muon track. The efficiency of the muon isolation requirements depends weakly on the amount of pileup and is typically 85%.

Jets are reconstructed from clusters [36,39] built from energy deposits in the calorimeters using the anti-k_t algorithm [40–42] with a radius parameter $R = 0.4$. The jets are calibrated using energy- and η-dependent calibration factors, derived from simulations, to the mean energy of stable particles inside the jets. Additional corrections to account for the difference between simulation and data are derived from *in situ* techniques [39].

Calibrated jets with $p_{\mathrm{T}} > 25$ GeV and $|\eta| < 2.5$ are selected. To reduce the background from other pp interactions within the same bunch crossing, the scalar sum of the p_{T} of tracks matched to the jet and originating from the primary vertex must be at least 75% of the scalar sum of the p_{T} of all tracks matched to the jet.

If there are jets within a cone of $\Delta R = 0.2$ around a selected electron, the jet closest to the electron is discarded. This avoids double counting of electrons as jets. Finally, electrons are removed if they are within $\Delta R = 0.4$ of a selected jet.

Jets originating from or containing b quarks are selected in the single-lepton final state, making use of the long lifetime of b hadrons. Variables using the properties of the secondary vertex and displaced tracks associated with the jet are combined by a neural network used for b-jet identification [43]. A working point with a 70% b-tagging efficiency is used to select $t\bar{t}$ events [44] in the single-lepton channel.

The magnitude of the missing transverse momentum ($E_{\mathrm{T}}^{\mathrm{miss}}$) is reconstructed from the vector sum of all calorimeter cell energies associated with topological clusters with $|\eta| < 4.5$ [45]. Contributions from the calorimeter energy clusters matched with either a reconstructed lepton or jet are corrected to the corresponding energy scale. The term accounting for the p_{T} of any selected muon is included in the $E_{\mathrm{T}}^{\mathrm{miss}}$ calculation.

IV. EVENT SELECTION

A. Dilepton channel

To select $t\bar{t}$ candidate events with leptonic W decays, two leptons of opposite charge ($\ell^+\ell^- = e^+e^-$, $\mu^+\mu^-$, or $e^\pm\mu^\mp$) and at least two jets are required. For the $\mu^+\mu^-$ final state, events containing a muon pair consistent with a cosmic-ray muon signature are rejected. In particular, events are rejected if two muon tracks are back to back in ϕ, they have the same sign pseudorapidity, and the point of closest approach to the primary vertex of each track is greater than 5 mm. Since the same-flavor leptonic channels e^+e^- and $\mu^+\mu^-$ suffer from a large background from the leptonic decays of hadronic resonances, such as the J/ψ and Υ, the invariant mass of the two leptons, $m_{\ell\ell}$, is required to be larger than 15 GeV. A contribution from the Drell-Yan production of Z/γ^* bosons in association with jets ($Z/\gamma^* + \text{jets}$ production) to these channels is suppressed by rejecting events where $m_{\ell\ell}$ is close to the Z boson mass m_Z; i.e. $|m_{\ell\ell} - m_Z| > 10$ GeV is required. In addition, large missing transverse momentum, $E_{\mathrm{T}}^{\mathrm{miss}} > 60$ GeV, is required to account for the two neutrinos from the leptonic decays of the two W bosons. Events with at least two jets, $|m_{\ell\ell} - m_Z| < 10$ GeV, and $E_{\mathrm{T}}^{\mathrm{miss}} > 30$ GeV are used as a control region to validate modeling of the spin observables (see Sec. VII A).

The $e^\pm\mu^\mp$ channel does not suffer from an overwhelming Drell-Yan background. Therefore the $m_{\ell\ell}$ cut is not applied. To suppress the remaining background from $Z/\gamma^* \times (\rightarrow \tau^+\tau^-) + \text{jets}$ production a cut on the scalar sum of the transverse energy of leptons and jets, $H_{\mathrm{T}} > 130$ GeV, is applied instead of the $E_{\mathrm{T}}^{\mathrm{miss}}$ cut. The purity of the $t\bar{t}$ sample after the dilepton selection is about 85%.

B. Single-lepton channel

To select $t\bar{t}$ candidate events in the single-lepton final state, exactly one isolated lepton (electron or muon), at least four jets and high $E_{\mathrm{T}}^{\mathrm{miss}}$ are required. The $E_{\mathrm{T}}^{\mathrm{miss}}$ has to be larger than 30 GeV (20 GeV) in the $e + \text{jets}$ ($\mu + \text{jets}$) final state to account for the neutrino from the leptonic decay of a W boson. To suppress the contribution of QCD multijet events a cut on the W boson transverse mass,[3] $m_{\mathrm{T}}(W) > 30$ GeV, is applied in the $e + \text{jets}$ final state while in the $\mu + \text{jets}$ final state, $m_{\mathrm{T}}(W) + E_{\mathrm{T}}^{\mathrm{miss}}$ is required to be larger than 60 GeV. In both channels, at least one of the jets has to be identified as a b jet by the b-tagging algorithm, resulting in a 78% ($e + \text{jets}$) and 76% ($\mu + \text{jets}$) pure $t\bar{t}$ sample.

V. SAMPLE COMPOSITION AND MODELING

After event selection, the sample is composed of $t\bar{t}$ signal and various backgrounds. In the following, the sample composition of the dilepton and single-lepton channels are discussed.

A. Dilepton channel

Backgrounds to same-flavor dilepton $t\bar{t}$ production arise from the Drell-Yan $Z/\gamma^* + \text{jets}$ production process with the Z/γ^* boson decaying into e^+e^- or $\mu^+\mu^-$. In the $e^\pm\mu^\mp$

[3] In events with a leptonic decay of a W boson, $m_{\mathrm{T}}(W) = \sqrt{2p_{\mathrm{T}}^{\ell}p_{\mathrm{T}}^{\nu}(1 - \cos(\phi^{\ell} - \phi^{\nu}))}$ where p_{T}^{ℓ} and p_{T}^{ν} (ϕ^{ℓ} and ϕ^{ν}) are the transverse momenta (azimuthal angle) of the charged lepton and neutrino, respectively. The measured $E_{\mathrm{T}}^{\mathrm{miss}}$ vector provides the neutrino information.

channel, one of the main backgrounds is due to $Z/\gamma^* +$ jets production with decays $Z/\gamma^* \to \tau^+\tau^-$, followed by leptonic decays of the τ leptons. Other backgrounds in dilepton channels are due to diboson production, associated production of a single top quark, and a W boson (Wt), $t\bar{t}$ production with a single-lepton in the final state, single top quark production via s- or t-channel exchange of a W boson, and the production of a W boson in association with jets. The latter three processes contain nonprompt leptons that pass the lepton isolation requirement or misidentified leptons arising from jets. The contributions from these processes are estimated using data-driven methods.

Drell-Yan events are generated using the ALPGEN v2.13 [46] generator including leading-order (LO) matrix elements with up to five additional partons. The CTEQ6L1 parton distribution function (PDF) set [47] is used, and the cross section is normalized to the next-to-next-to-leading-order (NNLO) prediction [48]. Parton showering and fragmentation are modeled by HERWIG v6.520 [49], and the underlying event is simulated by JIMMY [50]. To avoid double counting of partonic configurations generated by both the matrix-element calculation and the parton-shower evolution, a parton-jet matching scheme ("MLM matching") [51] is employed. The yields of dielectron and dimuon Drell-Yan events predicted by the Monte Carlo (MC) simulation are compared to the data in $Z/\gamma^* +$ jets-dominated control regions. Correction factors are derived and applied to the predicted yields in the signal region, to account for the difference between the simulation prediction and data. The correction increases the $Z/\gamma^* \to e^+e^- +$ jets contribution by 3% and the $Z/\gamma^* \to \mu^+\mu^- +$ jets contribution by 13% relative to the prediction from simulation.

Single top quark background arises from the associated Wt production, when both the W boson emerging from the top quark and the W boson from the hard interaction decay leptonically. This contribution is modeled with MC@NLO v4.01 [52–54] using the CT10 PDF set [55] and normalized to the approximate NNLO theoretical cross section [56].

Finally, the diboson backgrounds are modeled using ALPGEN v2.13 interfaced with HERWIG using the MRST LO** PDF set [57] and normalized to the theoretical calculation at next-to-leading-order (NLO) in QCD [58].

The background arising from the misidentified and nonprompt leptons (collectively referred to as "fake leptons") is determined from data using the "matrix method," which was previously used in the measurement described in Refs. [59,60].

The SM $t\bar{t}$ signal events are modeled using the MC@NLO v4.01 generator. Top quarks and the subsequent W bosons are decayed conserving the spin correlation information. The decay products are interfaced with HERWIG, which showers the b quarks and W boson daughters, and with JIMMY to simulate multiparton interactions. A top quark mass of 172.5 GeV is assumed. The CT10 PDF set is used.

The generation chain can be modified such that top quarks are decayed by HERWIG rather than MC@NLO. In this case the top quark spin information is not propagated to the decay products, and therefore the spins between the top quarks are uncorrelated. This technique has a side effect that the top quarks in the uncorrelated case are treated as being on shell, and hence they do not have an intrinsic width. The effect of this limitation is found to be negligible.

All MC samples use a GEANT4-based simulation to model the ATLAS detector [61,62]. For each MC process, pileup is overlaid using simulated minimum-bias events from the PYTHIA generator. The number of additional pp interactions is reweighted to the number of interactions observed in data.

In Table I the observed yields in data are compared to the expected background and the $t\bar{t}$ signal normalized to $\sigma_{t\bar{t}} = 177^{+10}_{-11}$ pb calculated at NNLO in QCD including resummation of next-to-next-to-leading logarithmic soft gluon terms [63–67] with TOP++ v2.0 [68] for a top quark mass of 172.5 GeV. A significantly lower yield in the dielectron channel compared to the dimuon channel is due to the stringent isolation criteria and higher p_{T} cut on the electrons. The yield difference between $t\bar{t}$ signal with SM spin correlation and without spin correlation is found to be negligible in the $e^{\pm}\mu^{\mp}$ channel but not in the e^+e^- or $\mu^+\mu^-$ channels. Here, the cut on the invariant mass of the dilepton system used to suppress backgrounds also preferentially selects uncorrelated $t\bar{t}$ pairs over correlated pairs. This is due to the fact that on average uncorrelated $t\bar{t}$ pairs have larger values of $\Delta\phi(\ell,\ell)$, which translates into larger values of $m_{\ell\ell}$ and therefore more events passing the $|m_{\ell\ell} - m_Z| > 10$ GeV selection cut. This effect is accounted for in the analysis.

TABLE I. Observed numbers of events in data compared to the expectation after the selection in the dilepton channels. Backgrounds and signal estimated from simulation are indicated with the (MC) suffix, whereas backgrounds estimated using data-driven techniques are indicated with a (DD) suffix. Quoted uncertainties include the statistical uncertainty on the yield and the uncertainty on the theoretical cross sections used for MC normalization. The uncertainty on the DD estimate is statistical only.

	e^+e^-	$\mu^+\mu^-$	$e^{\pm}\mu^{\mp}$
$Z(\to \ell^+\ell^-) +$ jets (DD/MC)	21 ± 3	83 ± 9	$\cdots$
$Z(\to \tau^+\tau^-) +$ jets (MC)	18 ± 6	67 ± 23	172 ± 59
Fake leptons (DD)	20 ± 7	29 ± 4	101 ± 15
Single top (MC)	31 ± 3	83 ± 7	224 ± 17
Diboson (MC)	23 ± 8	60 ± 21	174 ± 59
Total (non-$t\bar{t}$)	112 ± 13	322 ± 33	671 ± 87
$t\bar{t}$ (MC)	610 ± 37	1750 ± 110	4610 ± 280
Expected	721 ± 39	2070 ± 110	5280 ± 290
Observed	736	2057	5320

B. Single-lepton channel

In the single-lepton channel the main background is due to $W+$jets production, where the W boson decays leptonically. Other background contributions arise from Z/γ^*+jets production, where the Z boson decays into a pair of leptons and one of the leptons does not pass the selection requirements, from electroweak processes (diboson and single top quark production in the s, t channel, and Wt processes) and from multijets events, where a lepton from the decay of a heavy-flavor quark appears isolated or a jet mimics an electron. Additional background arising from $t\bar{t}$ events with two leptons in the final state, where one lepton lies outside the acceptance, is studied with MC@NLO MC simulation and treated as part of the signal. The diboson, single top quark and Z/γ^*+jets backgrounds are estimated using simulated events normalized to the theoretical cross sections. The $W+$jets events are generated with ALPGEN v2.13, using the CTEQ6L1 PDF set with up to five additional partons. Separate samples are generated for $W+b\bar{b}$, $W+c\bar{c}$, and $W+c$ production at the matrix-element level. The normalization of the $W+$jets background and its heavy-flavor content are extracted from data by a method exploiting the $W+$jets production charge asymmetry [59]. Single top quark s-channel and Wt-channel production is generated using MC@NLO, where the diagram removal scheme is invoked in the Wt-channel production to avoid overlap between single top quark and $t\bar{t}$ final states [69]. For the t channel, ACERMC [70] with PYTHIA parton shower and modified LO PDFs (MRST LO** [71]) is used.

The QCD multijet background is estimated from data using the same matrix method as in the dilepton channel [59,60].

Table II shows the observed yields in data, compared to the expectation from the background and the $t\bar{t}$ signal. The expectation is in good agreement with the data.

TABLE II. Observed numbers of events in data compared to the expectation after the selection in the single-lepton channels. Backgrounds and signal are estimated from simulation (MC) or from data-driven techniques (DD). Quoted uncertainties include the statistical uncertainty on the yield and the uncertainty on the theoretical cross sections used for MC normalization. The uncertainty on the DD estimate is statistical only.

$n_{\text{jets}} \geq 4$, $n_{b\text{-tags}} \geq 1$	$e+$jets	$\mu+$jets
$W+$jets (DD/MC)	2320 ± 390	4840 ± 770
$Z+$jets (MC)	450 ± 210	480 ± 230
Fake leptons (DD)	840 ± 420	1830 ± 340
Single top (MC)	1186 ± 55	1975 ± 83
Diboson (MC)	46 ± 2	73 ± 4
Total (non-$t\bar{t}$)	4830 ± 620	9200 ± 890
$t\bar{t}$ (MC, $\ell+$jets)	15130 ± 900	25200 ± 1500
$t\bar{t}$ (MC, dilepton)	2090 ± 120	3130 ± 190
Expected	22100 ± 1100	37500 ± 1800
Observed	21770	37645

VI. SPIN CORRELATION OBSERVABLES

The spin correlation of pair-produced top quarks is extracted from the angular distributions of the top quark decay products in $t \to Wb$ followed by $W \to \ell\nu$ or $W \to q\bar{q}$. The single differential angular distribution of the top decay width Γ is given by

$$\frac{1}{\Gamma}\frac{d\Gamma}{d\cos(\theta_i)} = (1+\alpha_i|\mathbf{P}|\cos(\theta_i))/2, \tag{1}$$

where θ_i is the angle between the momentum direction of decay product i of the top (antitop) quark and the top (antitop) quark polarization three-vector $\mathbf{P}$, $0 \leq |\mathbf{P}| \leq 1$. The factor α_i is the spin-analyzing power, which must be between -1 and 1. At NLO, the factor α_i is predicted to be $\alpha_{\ell^+} = +0.998$ for positively charged leptons [19,72,73], $\alpha_d = -0.966$ for down quarks, $\alpha_b = -0.393$ for bottom quarks [72–74], and the same α_i value with opposite sign for the respective antiparticles.

In the SM, the polarization of the pair-produced top quarks in pp collisions is negligible [24]. Ignoring it, the correlation between the decay products of the top quark (denoted with subscript $+$) and the top antiquark (denoted with subscript $-$) can be expressed by

$$\frac{1}{\sigma}\frac{d\sigma}{d\cos(\theta_+)d\cos(\theta_-)} = \frac{1}{4}(1+A\alpha_+\alpha_-\cos(\theta_+)\cos(\theta_-)), \tag{2}$$

with

$$A = \frac{N_{\text{like}} - N_{\text{unlike}}}{N_{\text{like}} + N_{\text{unlike}}} = \frac{N(\uparrow\uparrow) + N(\downarrow\downarrow) - N(\uparrow\downarrow) - N(\downarrow\uparrow)}{N(\uparrow\uparrow) + N(\downarrow\downarrow) + N(\uparrow\downarrow) + N(\downarrow\uparrow)}, \tag{3}$$

where $N_{\text{like}} = N(\uparrow\uparrow) + N(\downarrow\downarrow)$ is the number of events where the top quark and top antiquark spins are parallel, and $N_{\text{unlike}} = N(\uparrow\downarrow) + N(\downarrow\uparrow)$ is the number of events where they are antiparallel with respect to the spin quantization axis. The strength of the spin correlation is defined by

$$C = -A\alpha_+\alpha_-. \tag{4}$$

Using the mean of the doubly differential cross section in Eq. (2), C can be extracted as

$$C = -9\langle\cos(\theta_+)\cos(\theta_-)\rangle. \tag{5}$$

In this paper, however, the full distribution of $\cos(\theta_+)\cos(\theta_-)$, as defined in Eq. (2), is used. In dilepton final states where the spin-analyzing power is effectively 100%, $C \approx A$. To allow for a comparison to previous analyses, the results are given both in terms of f_{SM} defined in Sec. VII C and in terms of A.

Four observables are used to extract the spin correlation strength. The first variable is used in both the dilepton and

the single-lepton final states, and the latter three variables are only used in the dilepton final state.

(i) The azimuthal opening angle, $\Delta\phi$, between the momentum directions of a top quark decay product and an antitop quark decay product in the laboratory frame. In the dilepton final state, $\Delta\phi$ between the charged lepton momentum directions, $\Delta\phi(\ell^+,\ell^-)$, is explored. This observable is straightforward to measure and very sensitive because like-helicity gluon-gluon initial states dominate [75]. It was used in Ref. [35] to observe a nonvanishing spin correlation, consistent with the SM prediction. In the single-lepton channel, $\Delta\phi$ between the charged lepton momentum direction and either the down-type jet from W boson decay, $\Delta\phi(\ell, d)$, or the b jet from the hadronically decaying top quark, $\Delta\phi(\ell, b)$, are analyzed. Since this requires the identification of the jets from the W boson and hadronically decaying top quark, full event reconstruction is necessary, making the measurement of $\Delta\phi$ in the single-lepton channel more challenging. Moreover, there is a need to identify the jet emerging from the down-type quark from W boson decay (see Sec. VII B for more details).

(ii) The "S ratio" of matrix elements $\mathcal{M}$ for top quark production and decay from the fusion of like-helicity gluons $[g_R g_R + g_L g_L \to t\bar{t} \to (b\ell^+\nu)(\bar{b}\ell^-\bar{\nu})]$ with SM spin correlation and without spin correlation at LO [75],

$$S = \frac{(|\mathcal{M}|^2_{\mathrm{RR}} + |\mathcal{M}|^2_{\mathrm{LL}})_{\mathrm{corr}}}{(|\mathcal{M}|^2_{\mathrm{RR}} + |\mathcal{M}|^2_{\mathrm{LL}})_{\mathrm{uncorr}}} = \frac{m_t^2\{(t\cdot\ell^+)(t\cdot\ell^-) + (\bar{t}\cdot\ell^+)(\bar{t}\cdot\ell^-) - m_t^2(\ell^+\cdot\ell^-)\}}{(t\cdot\ell^+)(\bar{t}\cdot\ell^-)(t\cdot\bar{t})}, \tag{6}$$

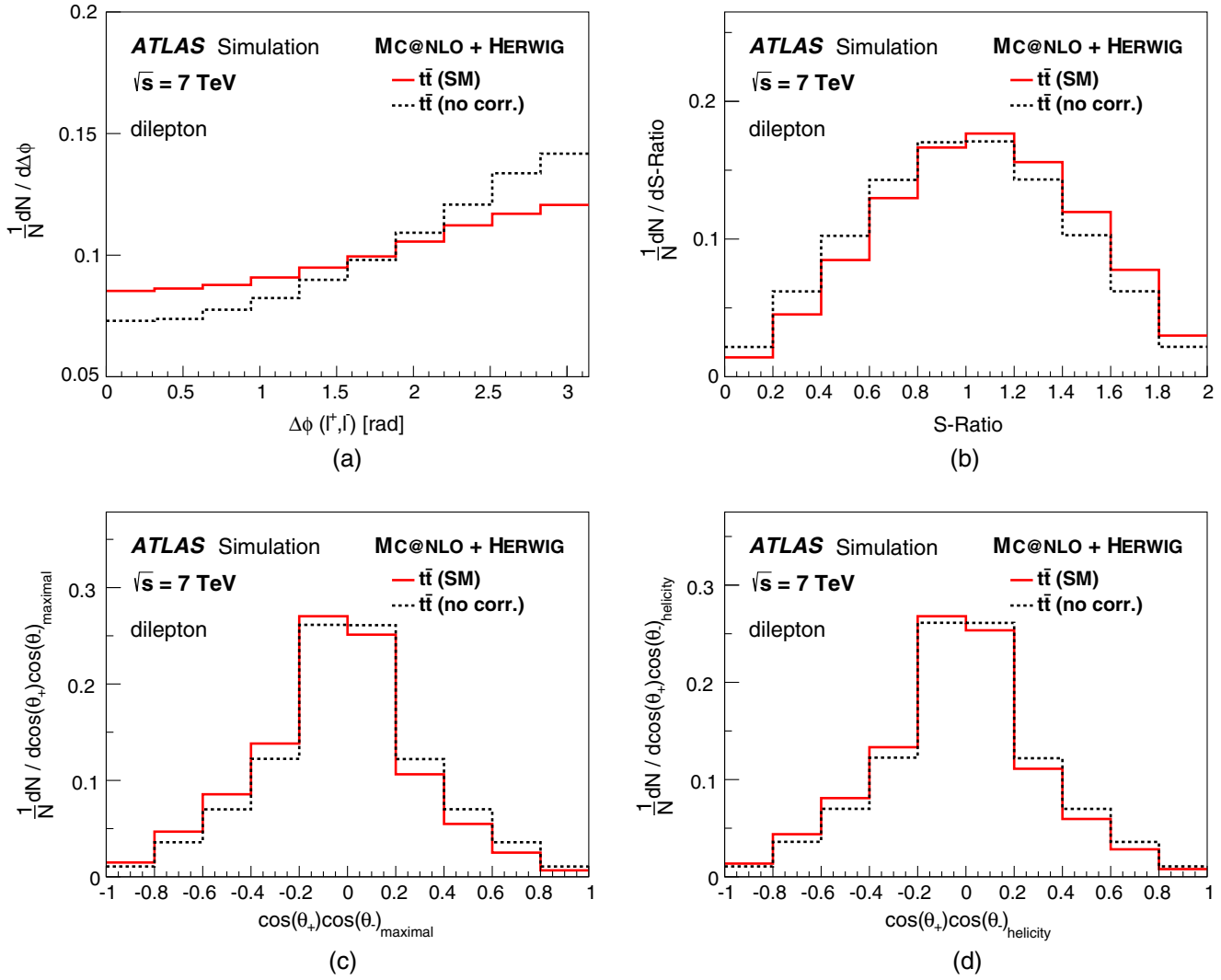

FIG. 1 (color online). Distributions of several observables for generated charged leptons from top quark decay and top quarks: (a) $\Delta\phi(\ell^+,\ell^-)$; (b) S ratio, as defined in Eq. (6); (c) $\cos(\theta_+)\cos(\theta_-)$, as defined in Eq. (2) in the helicity basis; (d) in the maximal basis. The normalized distributions show predictions for SM spin correlation (red solid lines) and no spin correlation (black dotted lines).

where t, $\bar{t}$, ℓ^+, and ℓ^- are the 4-momenta of the top quarks and the charged leptons. Since the like-helicity gluon-gluon matrix elements are used for the construction of the S ratio, it is particularly sensitive to like-helicity gluon-gluon initial states. To measure this observable, and the two others described below, the top quark and the top antiquark have to be fully reconstructed.

(iii) The double differential distribution [Eq. (2)], where the top direction in the $t\bar{t}$ rest frame is used as the spin quantization axis. The measurement of this distribution allows for a direct extraction of the spin correlation strength A_{helicity} [3], as defined in Eq. (3). The SM prediction is $A^{\text{SM}}_{\text{helicity}} = 0.31$, which was calculated including NLO QCD corrections to $t\bar{t}$ production and decay and mixed weak-QCD corrections to the production amplitudes in Ref. [24]. MC@NLO, which includes NLO QCD corrections to $t\bar{t}$ production but not to top quark decay, reproduces the same value after adding parton shower simulated by HERWIG.

(iv) The double differential distribution [Eq. (2)], using the "maximal" basis as the top spin quantization axis. For the gluon-gluon fusion process, which is a mixture of like-helicity and unlike-helicity initial states, no optimal axis exists where the spin correlation strength is 100%. This is in contrast to the quark-antiquark annihilation process where an optimal "off-diagonal" basis was first identified by Ref. [76]. However, event by event a quantization axis that maximizes spin correlation and is called the maximal basis can be constructed for the gluon fusion process [77]. A prediction for the $t\bar{t}$ spin correlation using this observable is not yet available for 7 TeV pp collisions. Therefore, the prediction is calculated using the MC@NLO+HERWIG simulation resulting in $A^{\text{SM}}_{\text{maximal}} = 0.44$.

Figure 1 shows all four observables for 1(a) generated charged leptons from top quark decay and 1(b), 1(c), 1(d) top quarks in the dilepton final state, calculated with MC@NLO under the assumption of SM $t\bar{t}$ spin correlation and no spin correlation, as defined in Sec. V.

The measurement of the four variables in the dilepton final state does not comprise redundant information. It can be shown that the hadronic $t\bar{t}$ production density matrices at tree level can be decomposed into different terms analyzing top quark spin-independent effects, top quark polarization, and $t\bar{t}$ spin correlations [78]. Using rotational invariance, these terms can be structured according to their discrete symmetry properties. In this way four independent C-even and P-even spin correlation coefficients that are functions of the partonic center-of-mass energy and the production angle are introduced. The four observables investigated here depend on different linear combinations of these four coefficient functions.

In the single-lepton final state, $\Delta\phi(\ell, d)$ and $\Delta\phi(\ell, b)$ are used in the analysis. Their distributions are shown in Fig. 2 for generated leptons and quarks and are identical in the absence of spin correlation. The presence of spin correlation causes a split into two distributions such that the $\Delta\phi(\ell, b)$ distribution becomes steeper while the trend is opposite for $\Delta\phi(\ell, d)$. At parton level the separation between the distribution with SM spin correlation and without spin correlation for $\Delta\phi(\ell, d)$ is similar to the one for $\Delta\phi(\ell, \ell)$ in the dilepton channel while the separation is significantly smaller for $\Delta\phi(\ell, b)$.

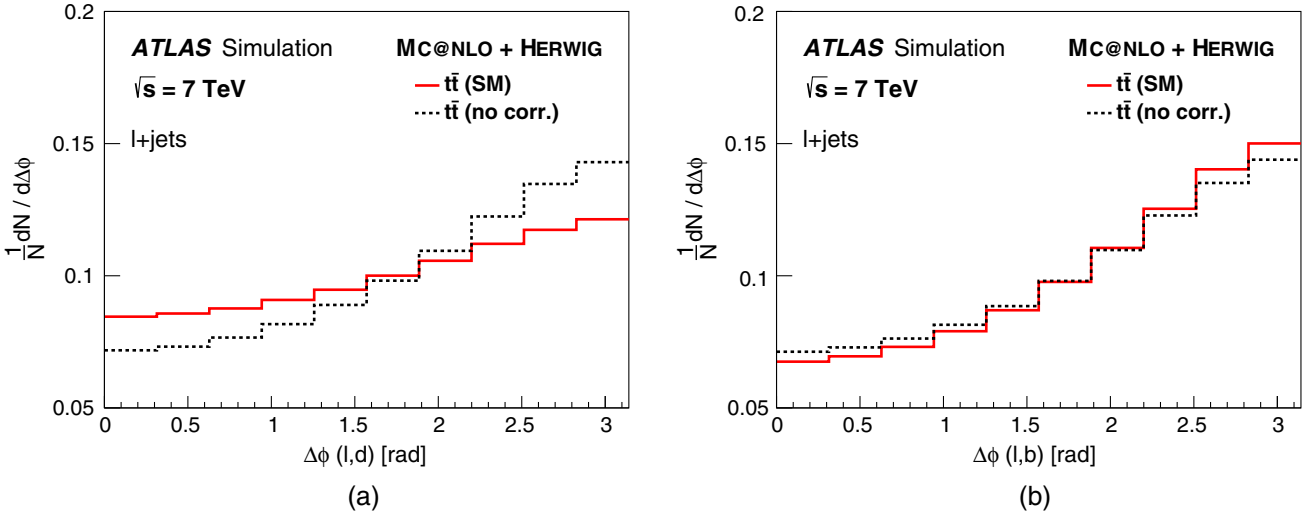

FIG. 2 (color online). Distribution of $\Delta\phi$: (a) between lepton and d quark; (b) between lepton and b quark, for generated top quark decay products. The normalized distributions show predictions for SM spin correlation (red solid lines) and no spin correlation (black dotted lines).

VII. MEASUREMENT PROCEDURE

After selecting a $t\bar{t}$-enriched data sample and estimating the signal and background composition, the spin correlation observables, as defined in Sec. VI, are measured and used to extract the strength of the $t\bar{t}$ spin correlation.

In the dilepton final state, the $\Delta\phi(\ell,\ell)$ observable is the absolute value of the difference in ϕ of the two leptons; i.e. it is measured in the laboratory frame. Figures 3(a) and 4(a) show this distribution in the e^+e^- and $\mu^+\mu^-$ channels, respectively, in a control region dominated by $Z/\gamma^* +$ jets

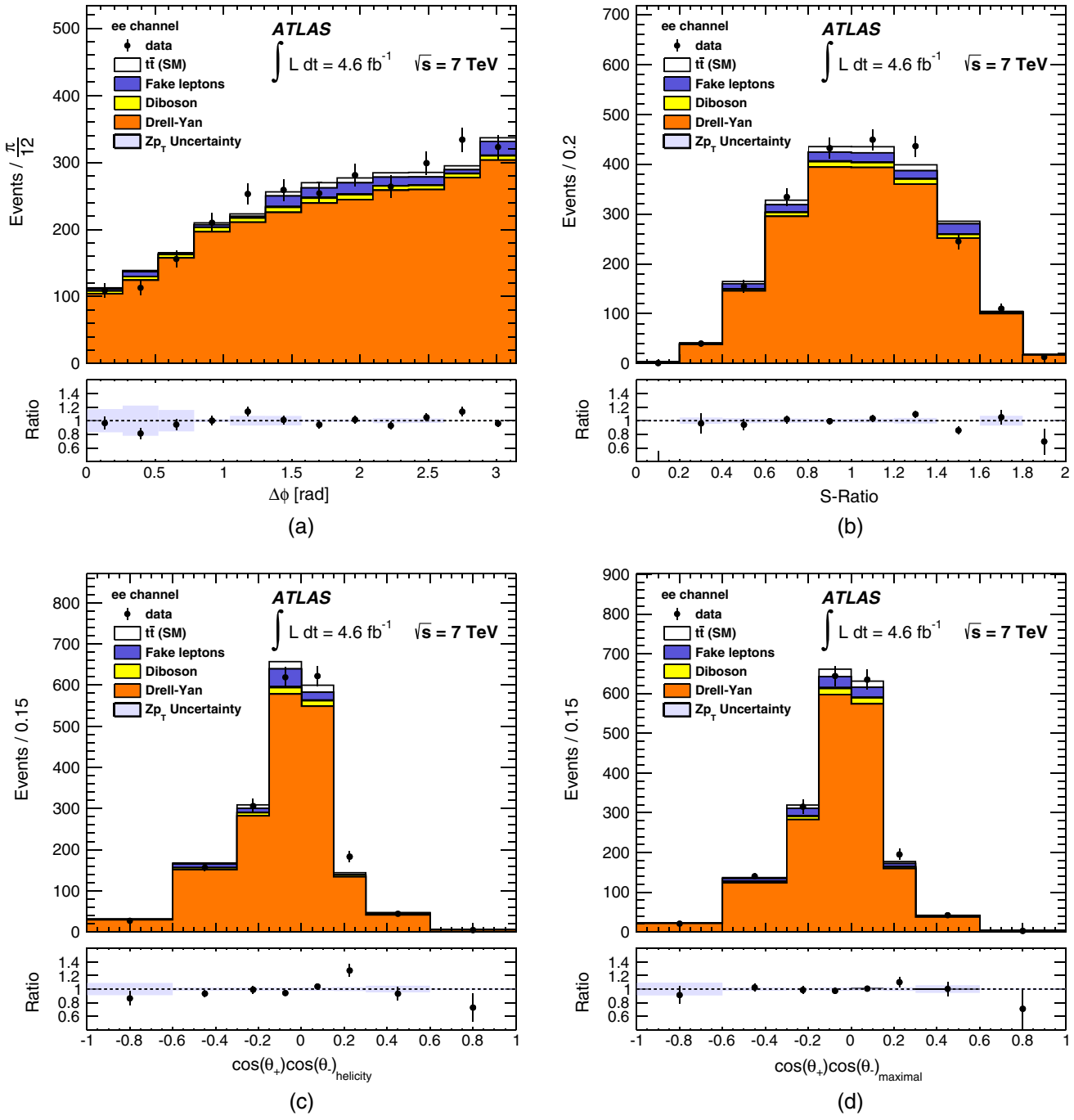

FIG. 3 (color online). Distributions of observables sensitive to $t\bar{t}$ spin correlation in the e^+e^- channel in a control region dominated by $Z/\gamma^* +$ jets background: (a) the azimuthal angle $\Delta\phi(\ell,\ell)$ between the two charged leptons, (b) the S ratio, as defined in Eq. (6), (c) $\cos(\theta_+)\cos(\theta_-)$, as defined in Eq. (2) in the helicity basis, and (d) in the maximal basis. The $Z/\gamma^* +$ jets background is normalized to the data in the control region. The contributions from single top and $Z \to \tau^+\tau^- +$ jets are not included in the legend as their contribution in this region is negligible. The uncertainties shown in the ratio are the systematic uncertainty due to the modeling of the Z transverse momentum, which is a dominant effect in this control region.

production. This region is selected using the same requirements as for the signal sample selection, but inverting the Z mass window cut, defined in Sec. IV. The other observables in the dilepton final state, $\cos(\theta_+)\cos(\theta_-)$ and the S ratio, require the reconstruction of the full kinematics of the $t\bar{t}$ system discussed in Sec. VII A.

In the single-lepton final state, two observables for the spin correlation measurement are used, $\Delta\phi(\ell, d)$ and $\Delta\phi(\ell, b)$, that both require event reconstruction to identify the jets from W-boson and top quark decay. Furthermore, a larger sensitivity to the modeling of the kinematics of $t\bar{t}$ events requires a somewhat different approach than in the

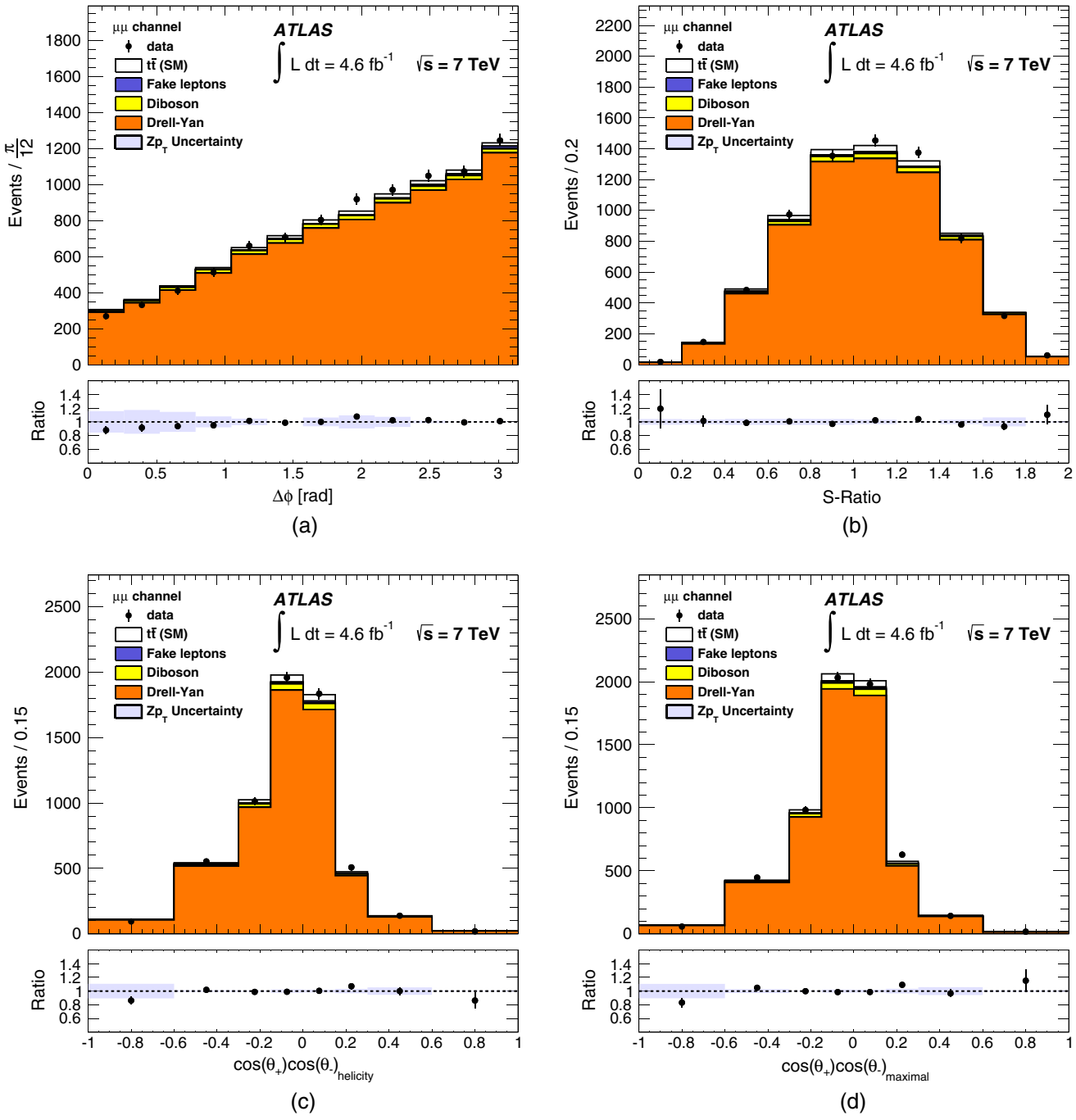

FIG. 4 (color online). Distributions of observables sensitive to $t\bar{t}$ spin correlation in the $\mu^+\mu^-$ channel in a $Z/\gamma^* +$ jets background dominated control region: (a) the azimuthal angle $\Delta\phi(\ell, \ell)$ between the two charged leptons, (b) the S ratio, as defined in Eq. (6), (c) $\cos(\theta_+)\cos(\theta_-)$, as defined in Eq. (2) in the helicity basis, and (d) in the maximal basis. The $Z/\gamma^* +$ jets background is normalized to the data in the control region. The contributions from single top and $Z \to \tau^+\tau^- +$ jets are not included in the legend as their contribution in this region is negligible. The uncertainties shown in the ratio are the systematic uncertainty due to the modeling of the Z transverse momentum, which is a dominant effect in this control region.

dilepton final state: instead of fitting $\Delta\phi(\ell, d)$ and $\Delta\phi(\ell, b)$ separately, a fit to the combination of both observables is used.

A. Kinematic reconstruction of the $t\bar{t}$ system in the dilepton final state

The two neutrinos from W-boson decays in dilepton final states cannot be measured but can only be inferred from the measured missing transverse momentum in the event. Since only the sum of the missing transverse momenta of the two neutrinos is measured, the system is underconstrained.

In this analysis a method known as the "neutrino weighting technique" [79] is employed. To solve the event kinematics and assign the final-state objects to the decay products of the top quark and top antiquarks, the invariant mass calculated from the reconstructed charged lepton and the assumed neutrino has to correspond to the W-boson mass, and the invariant mass of the jet-lepton-neutrino combination is constrained to the top quark mass. To fully solve the kinematics, the pseudorapidities η_1 and η_2 of the two neutrinos are sampled from a fit of a Gaussian function to the respective distributions in a simulated sample of $t\bar{t}$ events. It was verified that the η_1 and η_2 distributions in $t\bar{t}$ events do not change for different $t\bar{t}$ spin correlation strengths. Fifty values are chosen for each neutrino η, with $-4 < \eta_{1,2} < 4$ taken independently of each other.

By scanning over all η_1 and η_2 configurations taken from the simulation, all possible solutions of how to assign the charged leptons, neutrinos, and jets to their parent top quarks are accounted for. In addition, the energies of the reconstructed jets are smeared according to the experimental resolution [80], and the solutions are recalculated for every smearing step. If no solution is found, the event is discarded. Around 95% of simulated $t\bar{t}$ events have at least one solution. This fraction is considerably lower for the backgrounds, leading to an increase by 25% in the signal-to-background ratio when requiring at least one solution. Each solution is assigned a weight, defined by

$$w = \prod_{i=x,y} \exp\left(\frac{-(E_i^{\text{miss,calc}} - E_i^{\text{miss,obs}})^2}{2(\sigma_{E_{\text{T}}^{\text{miss}}})^2}\right), \qquad (7)$$

where $E_{x,y}^{\text{miss,calc}}$ ($E_{x,y}^{\text{miss,obs}}$) is the calculated (observed) missing transverse momentum component in the x or y direction. Solutions that fit better to the expected $t\bar{t}$ event kinematics are assigned a higher weight. The measured resolution of the missing transverse momentum $\sigma_{E_{\text{T}}^{\text{miss}}}$ is taken from Ref. [45] as a function of the sum of the transverse energy in the event. For example, for an event with a total sum of transverse momentum of 100 GeV, the resolution is taken to be 6.6 GeV. The weights of all solutions define a weight distribution for each observable per event. For each event, the weighted mean value of the respective observable is used for the measurement.

Figures 3(b)–3(d) and 4(b)–4(d) show distributions of spin correlation observables that use the $t\bar{t}$ event reconstruction with the neutrino weighting method. For the e^+e^- and $\mu^+\mu^-$ channels, in a control region dominated by $Z/\gamma^* +$ jets production, the S ratio and $\cos(\theta_+)\cos(\theta_-)$ in two different spin quantization bases are presented. Good agreement between data and the prediction is observed confirming a reliable description of observables sensitive to $t\bar{t}$ spin correlations with and without $t\bar{t}$ event reconstruction in the Drell-Yan background.

B. Kinematic reconstruction of the $t\bar{t}$ system in the single-lepton channel

In the single-lepton events, there is one missing neutrino from the $W \to \ell\nu$ decay. Therefore, the W-boson mass and the top quark mass can be used as constraints to solve the kinematics and to assign the reconstructed objects (jets, leptons, and $E_{\text{T}}^{\text{miss}}$) to the corresponding partons (quarks, leptons, and the neutrino). The main challenge for the event reconstruction in this final state is the presence of at least four jets, providing a large number of possible permutations when assigning objects to partons.

To perform the kinematic reconstruction, the Kinematic Likelihood Fitter (KLFitter) algorithm [81] is applied. The likelihood function is defined as a product of individual likelihood terms describing the kinematics of the $t\bar{t}$ signature including constraints from the masses of the two W bosons and the two top quarks. Detector resolutions for energy measurements are described in terms of transfer functions that map initial parton kinematics to those of reconstructed jets and leptons. The transfer functions are derived for electrons, muons, light-quark (u, d, s, c) jets, and b-quark jets, using a simulated $t\bar{t}$ sample generated with MC@NLO, and are parametrized in p_{T} (for muons) or energy in several η regions of the detector. The angular variables of each reconstructed object are measured with a negligible uncertainty.

The likelihood is maximized taking into account all possible permutations of the objects. The maximized likelihood of each permutation is extended to a normalized event probability by adding information from b-jet identification. This enhances the probability to choose the correct assignment of the reconstructed objects. The likelihood itself is invariant under the exchange of jets from down-type and up-type quarks from the W-boson decay. To enhance the probability to correctly assign the jets to down-type and up-type quarks from the W-boson decay, two additional quantities are incorporated into the likelihood. The first quantity is the weight assigned to the jet by the b-jet tagging algorithm. This takes advantage of the fact that 50% of the W-boson decays contain charm quarks, which have higher b-tag weights than other light quarks. The second quantity is the reconstructed jet p_{T}. Because of the $V - A$ structure of the W-boson decay, down-type jets have on average a lower p_{T} than up-type jets. A two-dimensional

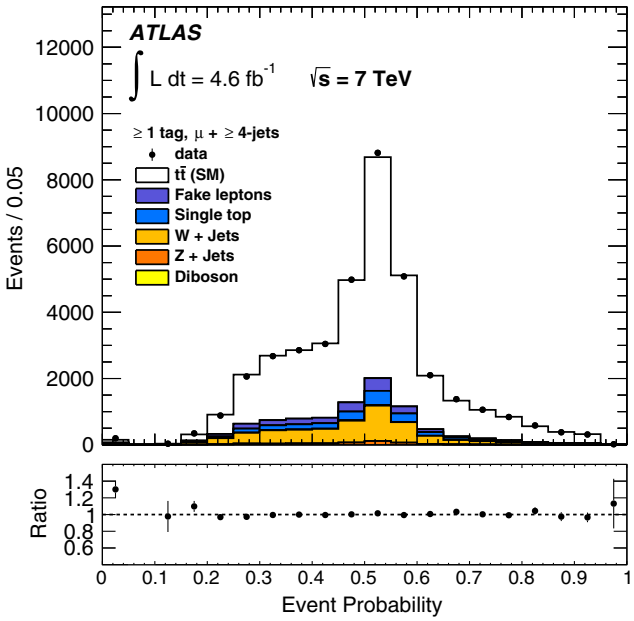

FIG. 5 (color online). Event probability distribution in the $\mu +$ jets channel for the most likely permutation.

probability distribution of the reconstructed jet p_{T} and the weight assigned to a jet by the b-jet tagging algorithm are used in the event probability. Figure 5 shows the event probability distribution for the permutation with the highest value in the $\mu +$ jets channel.

If the p_{T} and b-tagging weights of the two light jets are similar, no additional separation power is obtained and both permutations have an equal event probability of not larger than 0.5. In case the event probability reaches values above 0.5, one permutation matches the model better than all others, implying additional separation power between the two light jets. For the construction of the $\Delta\phi(\ell, d)$ and $\Delta\phi(\ell, b)$ observables, the permutation with the highest event probability is chosen.

Figure 6 shows distributions of $\Delta\phi(\ell, d)$ and $\Delta\phi(\ell, b)$ after selection and $t\bar{t}$ kinematic reconstruction for the SM spin correlation and no spin correlation scenarios in a subchannel of single-lepton events containing one muon and five jets, two of which are b tagged. One can see a significant deterioration of the separation between the two distributions compared to the parton-level results in Fig. 2. This is mainly due to misreconstruction of the top quarks which leads to a loss of the spin information. Because of a more reliable identification of b-quark jets compared to d-quark jets, the separation becomes comparable between the $\Delta\phi(\ell, d)$ and $\Delta\phi(\ell, b)$ observables in the single-lepton final state, motivating the use of both observables for the measurement.

C. Extraction of spin correlation

To extract the spin correlation strength from the distributions of the respective observables in data, templates are constructed and a binned maximum likelihood fit is performed. For each background contribution, one template for every observable is constructed. For the $t\bar{t}$ signal, one template is constructed from a MC@NLO sample with SM spin correlation and another using MC@NLO without spin correlation. The templates are fitted to the data. The predicted number of events per template bin i is written as a function of the coefficient f_{SM} as

$$m^i = f_{\mathrm{SM}} \times m^i_{A=\mathrm{SM}}(\sigma_{t\bar{t}}) + (1 - f_{\mathrm{SM}}) \times m^i_{A=0}(\sigma_{t\bar{t}}) + \sum_{j=1}^{N_{\mathrm{bkg}}} m^i_j, \quad (8)$$

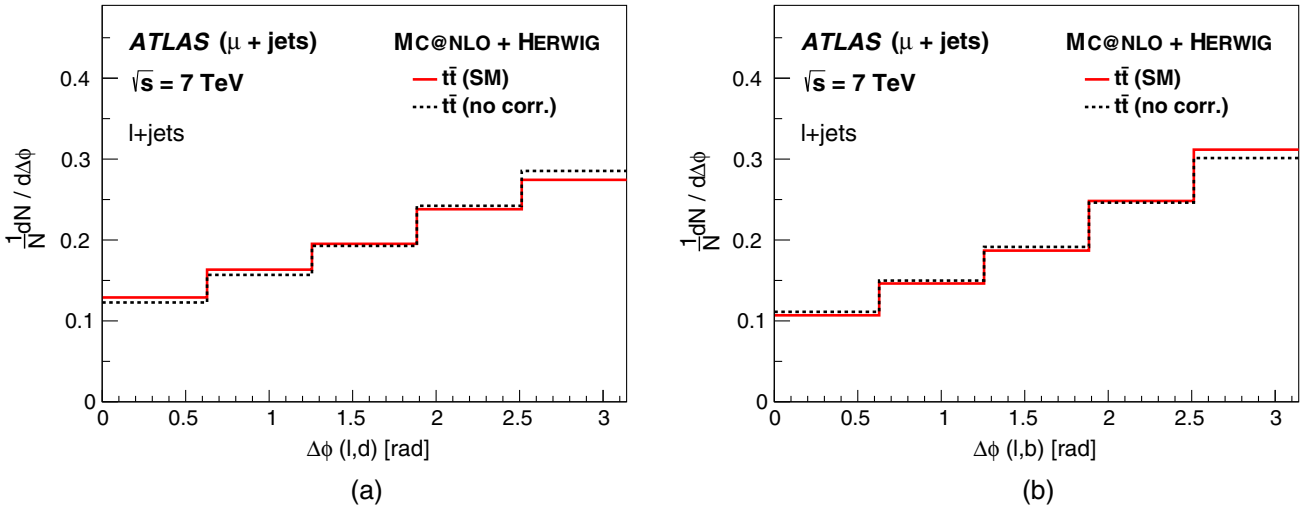

FIG. 6 (color online). Distributions of $\Delta\phi(\ell, d)$ between (a) the lepton and the jet from the down-type quark and (b) $\Delta\phi(\ell, b)$ between the lepton and the jet from the b quark after event selection and reconstruction for MC@NLO samples with SM spin correlation and no spin correlation.

where $m^i_{A=\mathrm{SM}}(\sigma_{t\bar{t}})$ and $m^i_{A=0}(\sigma_{t\bar{t}})$ is the predicted number of signal events in bin i for the signal template obtained with the SM MC@NLO sample and with the MC@NLO sample with spin correlation turned off, respectively, and $\sum_{j=1}^{N_{\mathrm{bkg}}} m^i_j$ is the sum over all background contributions N_{bkg}. To reduce the influence of systematic uncertainties sensitive to the normalization of the signal, the $t\bar{t}$ cross section $\sigma_{t\bar{t}}$ is included as a free parameter in the fit.

The negative logarithm of the likelihood function L

$$L = \prod_{i=1}^{N} \mathcal{P}(n^i, m^i) \tag{9}$$

is minimized with $\mathcal{P}(n^i, m^i)$ representing the Poisson probability to observe n^i events in bin i with m^i events expected. The number of bins N used for the fit depends on the variable and the channel.

To maximize sensitivity in the single-lepton channel by taking advantage of different $t\bar{t}$ signal purities, the preselected sample is split into subsamples of different lepton flavors with exactly one and more than one b-tagged jet and exactly four and at least five jets, thus giving eight subchannels in the likelihood fit. Moreover, since the power of the two variables $\Delta\phi(\ell, b)$ and $\Delta\phi(\ell, d)$ to discriminate between the SM spin correlation and no spin correlation scenarios is comparable, and the correlation between them is at most 10%, both are included in the fit as independent subchannels. This approach not only allows an effective doubling of the information used in the fit but also takes advantage of the opposite behavior of the ratios between the spin correlation and no spin correlation scenarios in the two observables. This in turn leads to opposite trends with respect to the signal-modeling systematic uncertainties resulting in significant cancellation effects.

To demonstrate a reduced sensitivity of the simultaneous fit using $\Delta\phi(\ell, b)$ and $\Delta\phi(\ell, d)$ to the choice of the signal model, pseudodata $t\bar{t}$ events simulated with POWHEG interfaced to HERWIG with spin correlation included ($f_{\mathrm{SM}} = 1$) were generated and the fit was performed using the default templates, simulated with MC@NLO interfaced to HERWIG. The measured f_{SM} is $f_{\mathrm{SM}} = 1.26 \pm 0.14(\mathrm{stat})$ when using the $\Delta\phi(\ell, d)$ observable, and $f_{\mathrm{SM}} = 0.64 \pm 0.18(\mathrm{stat})$ for $\Delta\phi(\ell, b)$. Fitting both distributions simultaneously resulted in a value of f_{SM} compatible with the true value, namely $f_{\mathrm{SM}} = 1.02 \pm 0.11(\mathrm{stat})$. The difference is explained to a large extent by the difference of the top quark p_{T} distributions in POWHEG and MC@NLO. The recent measurements by the ATLAS [82] and CMS [83] Collaborations indicate that the top quark p_{T} distributions vary between the generators and that the top quark p_{T} distribution in data is better described by POWHEG interfaced with HERWIG [82]. Ensemble tests performed using templates produced after reweighting the top quark p_{T} in the MC@NLO sample to the distribution in POWHEG show a reduced difference between the results obtained using different analyzers: $f_{\mathrm{SM}} = 1.13 \pm 0.14(\mathrm{stat})$ when using $\Delta\phi(\ell, d)$, $f_{\mathrm{SM}} = 0.77 \pm 0.18(\mathrm{stat})$ for $\Delta\phi(\ell, b)$, and $f_{\mathrm{SM}} = 0.99 \pm 0.11(\mathrm{stat})$ if the simultaneous fit to both observables is performed. Figures 7(a) and 7(b) demonstrate the effect of top quark p_{T} reweighting on the

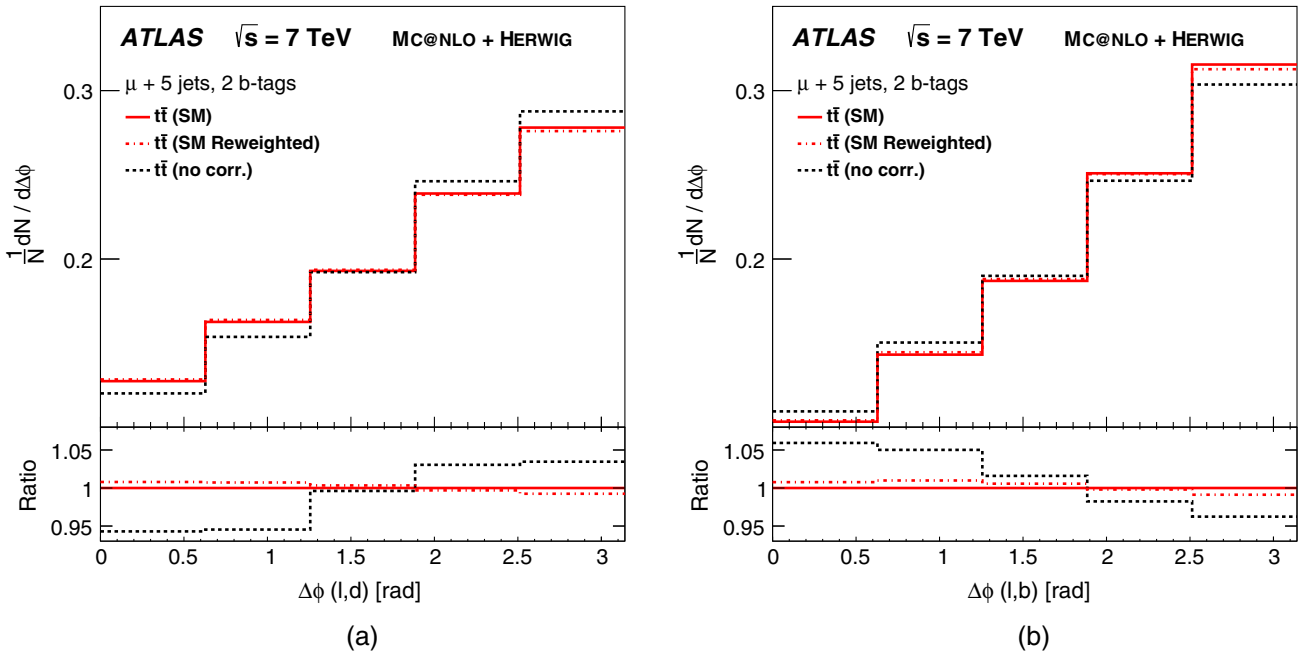

FIG. 7 (color online). Comparison of the difference of SM spin correlation and no spin correlation for (a) $\Delta\phi(\ell, b)$ and (b) $\Delta\phi(\ell, d)$ distributions for the nominal and reweighted-to- POWHEG top quark p_{T} distributions in the MC@NLO SM spin correlation sample. The "Ratio" shows the ratio of each distribution to that of the SM spin sample.

$\Delta\phi(\ell, d)$ and $\Delta\phi(\ell, b)$ distributions, respectively, for the SM spin correlation sample. One can see that top quark p_{T} reweighting causes the same trend, but it has the opposite direction with respect to the no spin correlation and SM spin correlation hypotheses for the $\Delta\phi(\ell, d)$ and $\Delta\phi(\ell, b)$ distributions: for $\Delta\phi(\ell, d)$ the reweighting leads to a shape corresponding to larger spin correlation strength than in the SM, while for $\Delta\phi(\ell, b)$ the shape corresponds to a smaller spin correlation strength.

VIII. SYSTEMATIC UNCERTAINTIES

Several classes of systematic uncertainties were considered: uncertainties related to the detector model and to $t\bar{t}$ signal and background models. Each source can affect the normalization of the signal and the background and/or the shape of the distributions used to measure the spin correlation strength. Normalization uncertainties typically have a small effect on the extracted spin correlation strength since the $t\bar{t}$ cross section is included as a free parameter in the fit and the contribution of backgrounds is small.

Systematic uncertainties are evaluated either by performing pseudoexperiments or by including them in the fit via nuisance parameters represented by Gaussian distributions [84]. The former is used when no continuous behavior of an uncertainty is expected. The majority of the uncertainties associated with the modeling of signal and background are of noncontinuous nature and fall into this category. Uncertainties associated with the modeling of reconstruction, identification, and calibration of all physics objects used in the analysis are included in the fit in the single-lepton channel, allowing data to constrain some important uncertainties and thus improve sensitivity. In the dilepton channel the effect of the detector modeling uncertainties was found to be small and was evaluated by performing pseudoexperiments.

Pseudoexperiments are created according to the following procedure. For each source of uncertainty templates corresponding to the respective up and down variation are created for both the SM and the uncorrelated spin templates, taking into account the change of the acceptance and shape of the observable due to the source under study. Pseudodata sets are generated by mixing these templates according to the measured f_{SM} and applying Poisson fluctuations to each bin. Then the nominal and varied templates are used to perform a fit to the same pseudodata. This procedure is repeated many times for each source of systematic uncertainty, and the means of the differences between the central fit values and the up and down variations are symmetrized and quoted as the systematic uncertainty from this source. Systematic uncertainties arising from the same source are treated as correlated between different dilepton or single-lepton channels.

Uncertainties in the detector model include uncertainties associated with the objects used in the event selection. Lepton uncertainties (quoted as "Lepton reconstruction" in Table III) include trigger efficiency and identification uncertainties for electrons and muons, and uncertainties due to electron (muon) energy (momentum) calibration and resolution. Uncertainty associated with the jet energy calibration is referred to as "Jet energy scale," while jet reconstruction efficiency and resolution uncertainties are combined and quoted as "Jet reconstruction" in Table III. Uncertainties on the $E_{\mathrm{T}}^{\mathrm{miss}}$ include uncertainties due to the pileup modeling and the modeling of energy deposits not associated with the reconstructed objects.

TABLE III. Systematic uncertainties on f_{SM} for the various observables in the dilepton final state.

Source of uncertainty	$\Delta\phi(\ell, \ell)$	S ratio	$\cos(\theta_+)\cos(\theta_-)_{\mathrm{helicity}}$	$\cos(\theta_+)\cos(\theta_-)_{\mathrm{maximal}}$
Detector modeling				
Lepton reconstruction	± 0.01	± 0.02	± 0.05	± 0.03
Jet energy scale	± 0.02	± 0.04	± 0.12	± 0.08
Jet reconstruction	< 0.01	± 0.03	± 0.08	± 0.01
$E_{\mathrm{T}}^{\mathrm{miss}}$	± 0.01	± 0.01	± 0.03	± 0.02
Fake leptons	± 0.03	± 0.03	± 0.06	± 0.04
Signal and background modeling				
Renormalization/factorization scale	± 0.09	± 0.08	± 0.08	± 0.07
Parton shower and fragmentation	± 0.02	< 0.01	± 0.01	± 0.08
ISR/FSR	± 0.08	± 0.05	± 0.08	± 0.01
Underlying event	± 0.04	± 0.06	± 0.01	< 0.01
Color reconnection	± 0.01	± 0.02	± 0.07	± 0.07
PDF uncertainty	± 0.05	± 0.03	± 0.03	± 0.05
Background	± 0.04	± 0.01	± 0.02	± 0.02
MC statistics	± 0.03	± 0.03	± 0.08	± 0.04
Top p_{T} reweighting	± 0.09	± 0.03	± 0.03	< 0.01
Total systematic uncertainty	± 0.18	± 0.14	± 0.23	± 0.18
Data statistics	± 0.09	± 0.11	± 0.19	± 0.14

A number of systematic uncertainties affecting the $t\bar{t}$ modeling are considered. Systematic uncertainty associated with the choice of factorization and renormalization scales in MC@NLO is evaluated by varying the default scales by a factor of 2 up and down simultaneously. The uncertainty due to the choice of parton shower and hadronization model is determined by comparing two alternative samples simulated with the POWHEG (HVQ V4) [85] generator interfaced with PYTHIA 6.425 [86] and HERWIG v6.520. The uncertainty on the amount of initial- and final-state radiation (ISR and FSR) in the simulated $t\bar{t}$ sample is assessed by comparing ALPGEN, showered with PYTHIA, with varied amounts of initial- and final-state radiation. The size of the variation is compatible with the recent measurements of additional jet activity in $t\bar{t}$ events [87]. The uncertainty due to the choice of the underlying event model is estimated by comparing a POWHEG-generated sample showered by PYTHIA with the PERUGIA 2011 tune to one with the PERUGIA 2011 MPIHI tune [88]. The latter is a variation of the PYTHIA 2011 tune with more semihard multiple parton interactions. The impact of the color reconnection model of the partons that enter hadronization is assessed by comparing samples generated with POWHEG and showered by PYTHIA with the PERUGIA 2011 tune and the PERUGIA 2011 NOCR tune [88]. To investigate the effect of the choice of PDF used in the analysis, the uncertainties from the nominal CT10 PDF set and from the NNPDF2.3 [89] and MSTW2008 [90] NLO PDF sets are considered, and the envelope of these uncertainties is taken as the uncertainty estimate. The dependence of the measured f_{SM} on the top quark mass is evaluated by changing the value of 172.5 GeV used in the simulation and performing a linear fit of the dependency of the considered observable on the top quark mass within the mass range 172.5 ± 5 GeV.

Uncertainties on the backgrounds (quoted as "Background" in Table III), evaluated using simulation, arise from the limited knowledge of the theoretical cross sections for single top, diboson, and $Z \to \tau^+\tau^-$ production, from the modeling of additional jets in these samples and from the integrated luminosity. The uncertainty of the latter amounts to $\pm 1.8\%$ [91]. Systematic uncertainties on the $Z \to e^+e^-$ and $Z \to \mu^+\mu^-$ backgrounds result from the uncertainty of their normalization to data in control regions and modeling of the Z-boson transverse momentum. It was checked that these uncertainties cover the small differences between data and prediction seen in Figs. 3(a) and 4(a). The uncertainty on the W + jets background in the single-lepton channel arises from the normalization uncertainty and from the uncertainty on the flavor composition given by the charge asymmetry method. The uncertainty on the fake lepton background ("Fake leptons" in Table III) arises mainly from uncertainties on the measurement of lepton misidentification rates in different control samples.

Finally, an uncertainty on the method to extract the spin correlation strength arises from the limited size of the MC samples used to create the templates.

As discussed in Sec. VII, top quark p_{T} modeling has an effect on f_{SM}. The effect on f_{SM} of reweighting of the top quark p_{T} to match the distribution in unfolded data is listed separately in Sec. VII C. To avoid double counting, the uncertainty due to the choice of parton shower and hadronization model is evaluated after the top quark p_{T} distribution in POWHEG+PYTHIA is corrected to be consistent with POWHEG+HERWIG.

IX. RESULTS

In the following, the results for the spin correlation measurements in the dilepton and single-lepton final states are discussed.

A. Dilepton channel

For each of the four observables, the maximum likelihood fit in each of the three individual channels (e^+e^-, $e^\pm\mu^\mp$, and $\mu^+\mu^-$) and their combination is performed. The observable with the largest statistical separation power between the no spin correlation and the SM spin correlation hypotheses is $\Delta\phi$. The measured values of f_{SM} for $\Delta\phi(\ell,\ell)$, the S ratio, and $\cos(\theta_+)\cos(\theta_-)$ in the helicity and maximal bases are summarized in Table IV. The systematic uncertainties and their effect on the measurement of f_{SM} in the dilepton channel are listed in Table III. Because of the different methods of constructing the four observables, they have different sensitivities to the various sources of systematic uncertainty and to the various physics effects. Some of the given uncertainties are limited by the size of the samples used for their extraction. The dependence of f_{SM} on the top quark mass m_t is parametrized as $\Delta f_{\mathrm{SM}} = -1.55 \times 10^{-5}(m_t/\mathrm{GeV} - 172.5)$ for $\Delta\phi(\ell,\ell)$, $\Delta f_{\mathrm{SM}} = -0.010(m_t/\mathrm{GeV} - 172.5)$ for the S ratio, $\Delta f_{\mathrm{SM}} = 0.015(m_t/\mathrm{GeV} - 172.5)$ for $\cos(\theta_+)\cos(\theta_-)$ in

TABLE IV. Summary of f_{SM} measurements in the individual dilepton channels and in the combined dilepton channel for the four different observables. The uncertainties quoted are first statistical and then systematic.

Channel	$f_{\mathrm{SM}}(\Delta\phi(\ell,\ell))$	$f_{\mathrm{SM}}(S$ ratio$)$	$f_{\mathrm{SM}}(\cos(\theta_+)\cos(\theta_-)_{\mathrm{helicity}})$	$f_{\mathrm{SM}}(\cos(\theta_+)\cos(\theta_-)_{\mathrm{maximal}})$
e^+e^-	$0.87 \pm 0.35 \pm 0.50$	$0.81 \pm 0.35 \pm 0.40$	$1.72 \pm 0.57 \pm 0.75$	$0.48 \pm 0.41 \pm 0.52$
$e^\pm\mu^\mp$	$1.24 \pm 0.11 \pm 0.13$	$0.95 \pm 0.12 \pm 0.13$	$0.76 \pm 0.23 \pm 0.25$	$0.86 \pm 0.16 \pm 0.20$
$\mu^+\mu^-$	$1.11 \pm 0.20 \pm 0.22$	$0.53 \pm 0.26 \pm 0.39$	$0.31 \pm 0.42 \pm 0.58$	$0.97 \pm 0.33 \pm 0.44$
Dilepton	$1.19 \pm 0.09 \pm 0.18$	$0.87 \pm 0.11 \pm 0.14$	$0.75 \pm 0.19 \pm 0.23$	$0.83 \pm 0.14 \pm 0.18$

the helicity basis, and $\Delta f_{\mathrm{SM}} = 0.016(m_t/\mathrm{GeV} - 172.5)$ for $\cos(\theta_+)\cos(\theta_-)$ in the maximal basis.

Figure 8 shows the distribution of the four observables in the data, the prediction for SM spin correlation and no spin correlation, and the result of the fit.

The analysis of the $\cos(\theta_+)\cos(\theta_-)$ observable allows a direct measurement of the spin correlation strength A, because A is defined by the $\cos(\theta_+)\cos(\theta_-)$ distribution according to Eq. (2). This becomes obvious in Eqs. (4) and (5), which show that the expectation value of $\cos(\theta_+)\cos(\theta_-)$ is equal to A modulo constant factors. Therefore, the extraction of f_{SM} using the full distribution in a template method is equivalent to extracting the spin correlation in the respective spin quantization basis $A_{\mathrm{basis}}^{\mathrm{measured}}$. The relation is given by

$$A_{\mathrm{basis}}^{\mathrm{measured}} = f_{\mathrm{SM}} A_{\mathrm{basis}}^{\mathrm{SM}}, \tag{10}$$

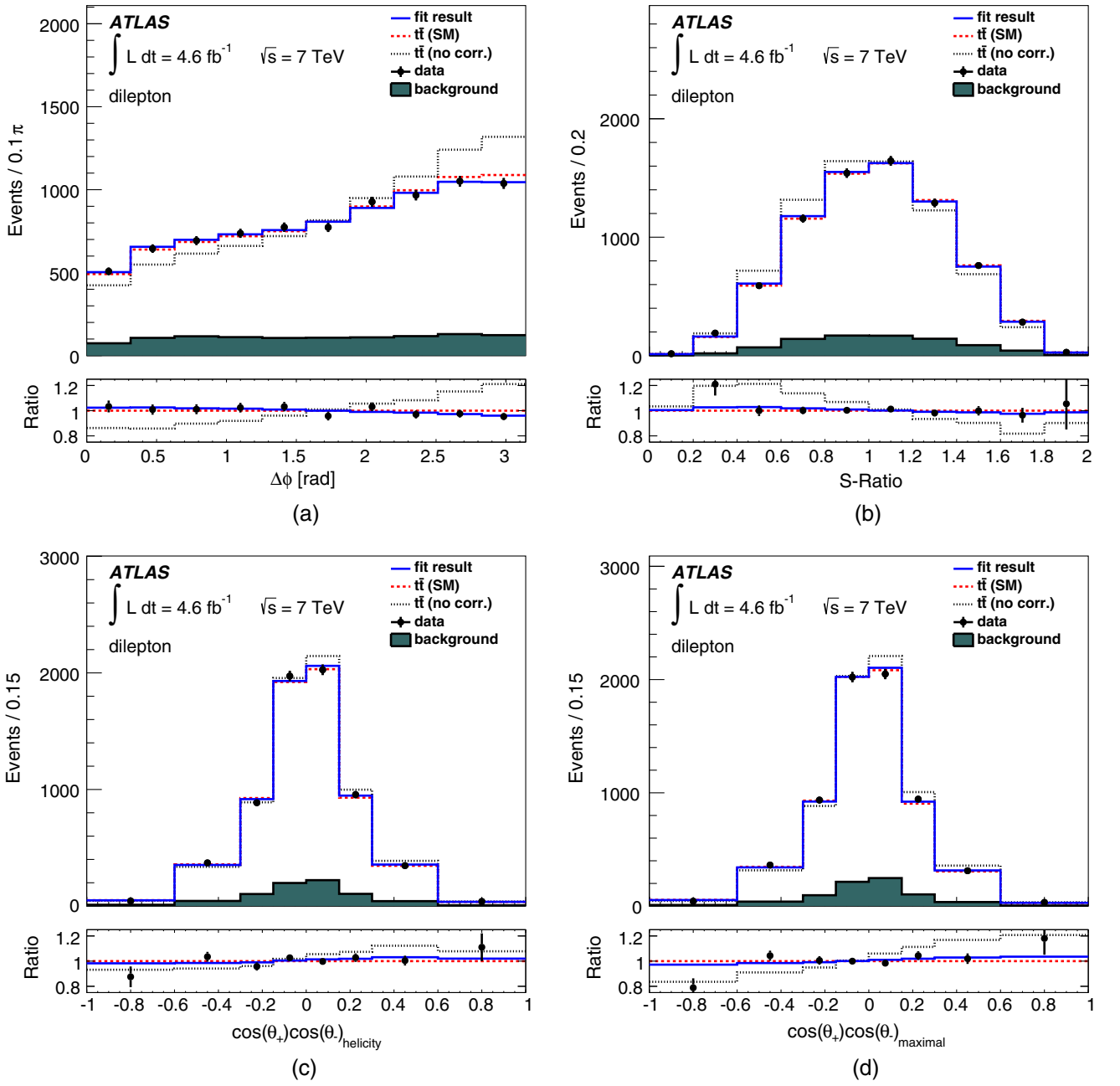

FIG. 8 (color online). Distributions of (a) $\Delta\phi(\ell,\ell)$, (b) S ratio, (c) $\cos(\theta_+)\cos(\theta_-)$ in the helicity basis, and (d) $\cos(\theta_+)\cos(\theta_-)$ in the maximal basis in the dilepton final state. The result of the fit to data (blue lines) is compared to the templates for background plus $t\bar{t}$ signal with SM spin correlation (red dashed lines) and without spin correlation (black dotted lines). The bottom panel shows the ratio of the data (black points), the best fit (blue solid lines) and the no spin prediction to the SM prediction.

TABLE V. Summary of measurements of the spin correlation strength A in the helicity and maximal bases in the combined dilepton channel for the four different observables. For the indirect extractions using $\Delta\phi(\ell,\ell)$ and the S ratio, A is given in both the helicity and the maximal bases. For the direct measurements using $\cos(\theta_+)\cos(\theta_-)$, only results for the basis utilized for the measurement are given. The uncertainties quoted are first statistical and then systematic. The SM predictions are $A^{\mathrm{SM}}_{\mathrm{helicity}} = 0.31$ and $A^{\mathrm{SM}}_{\mathrm{maximal}} = 0.44$.

	$\Delta\phi(\ell,\ell)$	S ratio	$\cos(\theta_+)\cos(\theta_-)_{\mathrm{helicity}}$	$\cos(\theta_+)\cos(\theta_-)_{\mathrm{maximal}}$
	Indirect extraction		Direct extraction	
$A^{\mathrm{measured}}_{\mathrm{helicity}}$	$0.37 \pm 0.03 \pm 0.06$	$0.27 \pm 0.03 \pm 0.04$	$0.23 \pm 0.06 \pm 0.07$	$\cdots$
$A^{\mathrm{measured}}_{\mathrm{maximal}}$	$0.52 \pm 0.04 \pm 0.08$	$0.38 \pm 0.05 \pm 0.06$	$\cdots$	$0.36 \pm 0.06 \pm 0.08$

with the SM predictions being $A^{\mathrm{SM}}_{\mathrm{helicity}} = 0.31$ and $A^{\mathrm{SM}}_{\mathrm{maximal}} = 0.44$, respectively, as discussed in Sec. VI.

Combining all three final states in the measurement of $\cos(\theta_+)\cos(\theta_-)$ in the helicity basis, a direct measurement of $A^{\mathrm{measured}}_{\mathrm{helicity}} = 0.23 \pm 0.06\,(\mathrm{stat}) \pm 0.07\,(\mathrm{syst})$ is derived, which is in good agreement with the SM value of $A^{\mathrm{SM}}_{\mathrm{helicity}} = 0.31$.

The combined result using $\cos(\theta_+)\cos(\theta_-)$ in the maximal basis gives a direct measurement of $A^{\mathrm{measured}}_{\mathrm{maximal}} = 0.37 \pm 0.06\,(\mathrm{stat}) \pm 0.08\,(\mathrm{syst})$, in good agreement with the SM value of $A^{\mathrm{SM}}_{\mathrm{maximal}} = 0.44$.

The analysis of $\Delta\phi(\ell,\ell)$ and the S ratio allows an indirect extraction of A under the assumption that the $t\bar{t}$ sample is composed of top quark pairs as predicted by the SM, either with or without spin correlation, but does not contain contributions beyond the SM. In that case, a change in the fraction f_{SM} will lead to a linear change of A according to Eq. (2). This has been verified in pseudoexperiments. Under these conditions, the measured f_{SM} can be translated into values of $A^{\mathrm{measured}}_{\mathrm{basis}}$ via Eq. (10), giving $A^{\mathrm{measured}}_{\mathrm{helicity}} = 0.37 \pm 0.03\,(\mathrm{stat}) \pm 0.06\,(\mathrm{syst})$ and $A^{\mathrm{measured}}_{\mathrm{maximal}} = 0.52 \pm 0.04\,(\mathrm{stat}) \pm 0.08\,(\mathrm{syst})$. These results are limited by systematic uncertainties, in particular by uncertainties due to signal modeling. The influence of the dominant systematic uncertainties in the previous ATLAS measurement performed on a smaller data set (2.1 fb^{-1}), giving $A_{\mathrm{helicity}} = 0.40^{+0.09}_{-0.08}\,(\mathrm{stat}\oplus\mathrm{syst})$ [35], has been reduced due to a better model of the fake lepton background and improved understanding of the jet energy scale. The two results are in agreement with each other.

The analysis of the S ratio results in $A^{\mathrm{measured}}_{\mathrm{helicity}} = 0.27 \pm 0.03\,(\mathrm{stat}) \pm 0.04\,(\mathrm{syst})$ and $A^{\mathrm{measured}}_{\mathrm{maximal}} = 0.38 \pm 0.05\,(\mathrm{stat}) \pm 0.06\,(\mathrm{syst})$.

All results are summarized in Table V. Within uncertainties, all values are in agreement with the SM prediction and with each other.

B. Single-lepton channel

The measured value of f_{SM} using the simultaneous fit to the $\Delta\phi(\ell,d)$ and $\Delta\phi(\ell,b)$ variables in the single-lepton channel is $f_{\mathrm{SM}} = 1.12 \pm 0.11(\mathrm{stat}) \pm 0.22(\mathrm{syst})$. Again, under the assumption that there is only SM $t\bar{t}$ spin correlation, vanishing $t\bar{t}$ spin correlation, or any mixture of both, this results in an indirect extraction of $A^{\mathrm{measured}}_{\mathrm{helicity}} = 0.35 \pm 0.03(\mathrm{stat}) \pm 0.08(\mathrm{syst})$. The systematic uncertainties and their effect on the measurement of f_{SM} are listed in Table VI. Part of the detector modeling uncertainties were determined using nuisance parameters, corresponding to the uncertainties on lepton identification, b-jet tagging, and jet energy calibration (denoted "Detector modeling I" in Table VI). Uncertainties due to lepton reconstruction, jet reconstruction and resolution, and multijet background shape are evaluated using ensemble tests and are included in the "Detector modeling II" entry. In the single-lepton channel, the main systematic uncertainty arises from parton showering and fragmentation. The parametrization of f_{SM} versus the top quark mass is $\Delta f_{\mathrm{SM}} = 0.024(m_t/\mathrm{GeV} - 172.5)$.

Figure 9 shows the observables including the result of the fit to data.

TABLE VI. Systematic uncertainties on f_{SM} determined from the simultaneous fit to $\Delta\phi(\ell,d)$ and $\Delta\phi(\ell,b)$. Uncertainty on the background normalization is included in the statistical uncertainty of the fit while uncertainty on the background shape is included into "Detector modeling I" and "Detector modeling II." The detector modeling uncertainties are split into nuisance parameter uncertainties (I) and uncertainties evaluated via ensemble tests (II).

Source of uncertainty	
Detector modeling	
Detector modeling I	± 0.09
Detector modeling II	± 0.02
Signal and background modeling	
Renormalization/factorization scale	± 0.06
Parton shower and fragmentation	± 0.16
ISR/FSR	± 0.07
Underlying event	± 0.05
Color reconnection	± 0.01
PDF uncertainty	± 0.02
MC statistics	± 0.05
Top p_{T} reweighting	± 0.02
Total systematic uncertainty	± 0.22
Data statistics	± 0.11

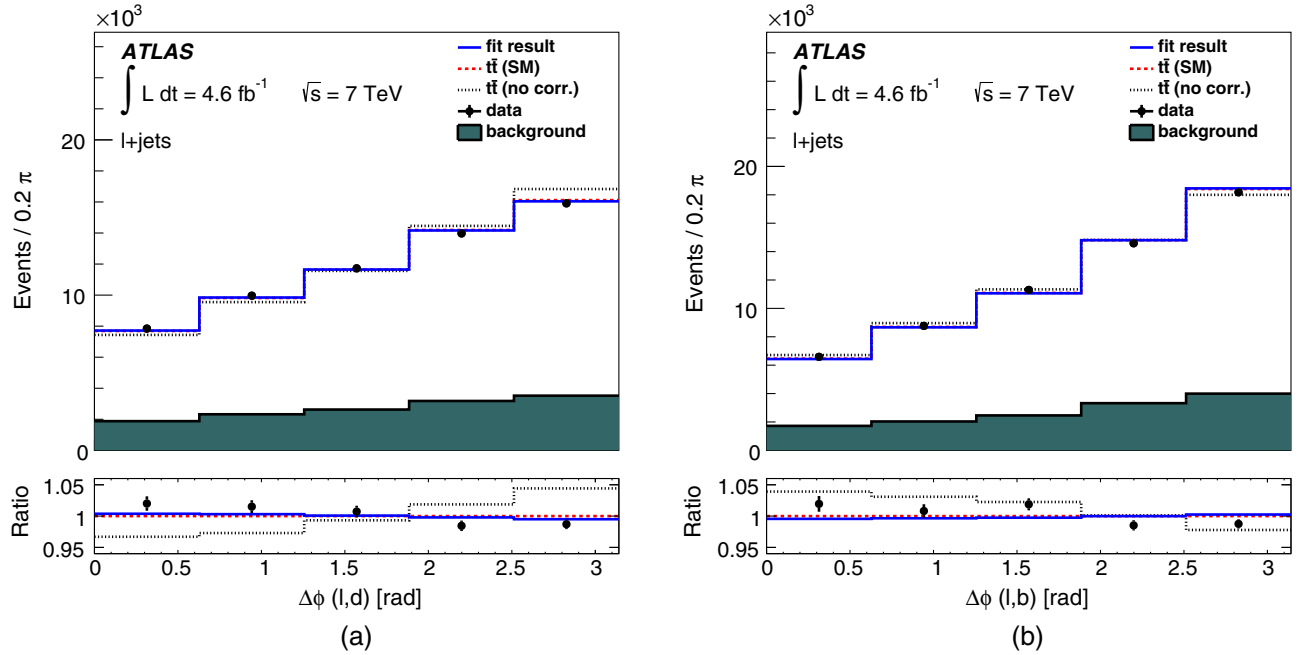

FIG. 9 (color online). Distributions of (a) $\Delta\phi(\ell, d)$ and (b) $\Delta\phi(\ell, b)$ in the single-lepton final sate. The result of the fit to data (blue lines) is compared to the templates for background plus $t\bar{t}$ signal with SM spin correlation (red dashed lines) and without spin correlation (black dotted lines). The bottom panel shows the ratio of the data (black points), of the best fit (blue solid lines) and of the no spin prediction to the SM prediction.

Figure 10 summarizes the f_{SM} values measured using various observables in the dilepton and single-lepton final states. All measurements agree with the SM prediction of $f_{\mathrm{SM}} = 1$.

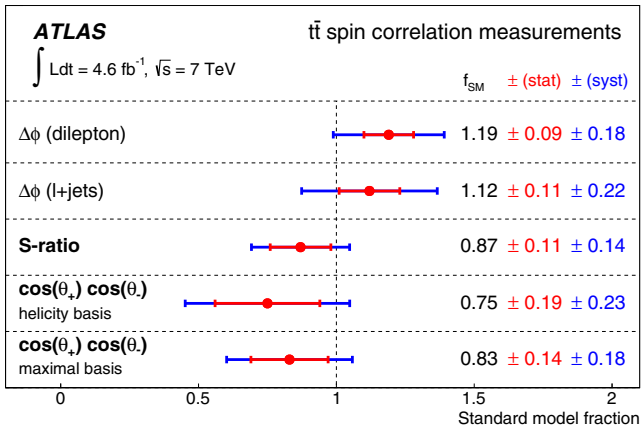

FIG. 10 (color online). Summary of the measurements of the fraction of $t\bar{t}$ events corresponding to the SM spin correlation hypothesis, f_{SM}, in the dilepton final state, using four spin correlation observables sensitive to different properties of the production mechanism, and in the single-lepton final state. Dashed vertical line at $f_{\mathrm{SM}} = 1$ indicates the SM prediction. The inner, red error bars indicate statistical uncertainties, the outer, blue error bars indicate the contribution of the systematic uncertainties to the total uncertainties.

X. CONCLUSIONS

The $t\bar{t}$ spin correlation in dilepton and single-lepton final states is measured utilizing ATLAS data, corresponding to an integrated luminosity of 4.6 fb^{-1}, recorded in proton-proton scattering at the LHC at a center-of-mass energy of 7 TeV.

In dilepton final states, four observables are used with different sensitivities to like-helicity gluon-gluon initial states and unlike-helicity gluon-gluon or $q\bar{q}$ initial states. For the first time, the measurement of $t\bar{t}$ spin correlation is performed using the S ratio. Also, a direct measurement of the spin correlation strengths A_{helicity} and A_{maximal} is performed using $\cos\theta_+ \cos\theta_-$ in the helicity and maximal bases, respectively. The measurement in the maximal basis is performed for the first time resulting in $A_{\mathrm{maximal}}^{\mathrm{measured}} = 0.36 \pm 0.10\,(\mathrm{stat} \oplus \mathrm{syst})$.

In the dilepton channel, the measurement of $t\bar{t}$ spin correlation using the azimuthal angle between the charged leptons, $\Delta\phi$, gives $f_{\mathrm{SM}} = 1.19 \pm 0.20\,(\mathrm{stat} \oplus \mathrm{syst})$. In the single-lepton channel, the $t\bar{t}$ spin correlation strength is measured for the first time at the LHC using a simultaneous fit to the azimuthal angle between charged lepton and d-quark $\Delta\phi(\ell, d)$ and between charged lepton and b-quark $\Delta\phi(\ell, b)$. The result is $f_{\mathrm{SM}} = 1.12 \pm 0.24\,(\mathrm{stat} \oplus \mathrm{syst})$. These measurements in the dilepton and single-lepton channels are in good agreement with the SM predictions.

ACKNOWLEDGMENTS

We thank CERN for the very successful operation of the LHC, as well as the support staff from our institutions without whom ATLAS could not be operated efficiently. We acknowledge the support of ANPCyT, Argentina; YerPhI, Armenia; ARC, Australia; BMWFW and FWF, Austria; ANAS, Azerbaijan; SSTC, Belarus; CNPq and FAPESP, Brazil; NSERC, NRC and CFI, Canada; CERN; CONICYT, Chile; CAS, MOST and NSFC, China; COLCIENCIAS, Colombia; MSMT CR, MPO CR and VSC CR, Czech Republic; DNRF, DNSRC and Lundbeck Foundation, Denmark; EPLANET, ERC and NSRF, European Union; IN2P3-CNRS, CEA-DSM/IRFU, France; GNSF, Georgia; BMBF, DFG, HGF, MPG and AvH Foundation, Germany; GSRT and NSRF, Greece; ISF, MINERVA, GIF, I-CORE and Benoziyo Center, Israel; INFN, Italy; MEXT and JSPS, Japan; CNRST, Morocco; FOM and NWO, Netherlands; BRF and RCN, Norway; MNiSW and NCN, Poland; GRICES and FCT, Portugal; MNE/IFA, Romania; MES of Russia and ROSATOM, Russian Federation; JINR; MSTD, Serbia; MSSR, Slovakia; ARRS and MIZŠ, Slovenia; DST/NRF, South Africa; MINECO, Spain; SRC and Wallenberg Foundation, Sweden; SER, SNSF and Cantons of Bern and Geneva, Switzerland; NSC, Taiwan; TAEK, Turkey; STFC, the Royal Society and Leverhulme Trust, United Kingdom; DOE and NSF, United States of America. The crucial computing support from all WLCG partners is acknowledged gratefully, in particular from CERN and the ATLAS Tier-1 facilities at TRIUMF (Canada), NDGF (Denmark, Norway, Sweden), CC-IN2P3 (France), KIT/GridKA (Germany), INFN-CNAF (Italy), NL-T1 (Netherlands), PIC (Spain), ASGC (Taiwan), RAL (UK) and BNL (USA) and in the Tier-2 facilities worldwide.

[1] V. M. Abazov *et al.* (D0 Collaboration), Phys. Rev. D **85**, 091104 (2012).
[2] R. H. Dalitz and G. R. Goldstein, Phys. Rev. D **45**, 1531 (1992); M. Jezabek and J. H. Kühn, Phys. Rev. D **48**, R1910 (1993).
[3] W. Bernreuther and Z. G. Si, Nucl. Phys. **B837**, 90 (2010).
[4] V. M. Abazov *et al.* (D0 Collaboration), Phys. Rev. D **87**, 011103 (2013).
[5] ATLAS Collaboration, Phys. Rev. Lett. **111**, 232002 (2013).
[6] CMS Collaboration, Phys. Rev. Lett. **112**, 182001 (2014).
[7] J. H. Kühn, Nucl. Phys. **B237**, 77 (1984).
[8] V. D. Barger, J. Ohnemus, and R. J. Phillips, Int. J. Mod. Phys. A **04**, 617 (1989).
[9] G. L. Kane, G. A. Ladinsky, and C. P. Yuan, Phys. Rev. D **45**, 124 (1992).
[10] T. Arens and L. M. Sehgal, Phys. Lett. B **302**, 501 (1993).
[11] G. Mahlon and S. J. Parke, Phys. Rev. D **53**, 4886 (1996).
[12] T. Stelzer and S. Willenbrock, Phys. Lett. B **374**, 169 (1996).
[13] A. Brandenburg, Phys. Lett. B **388**, 626 (1996).
[14] D. Chang, S.-C. Lee, and A. Sumarokov, Phys. Rev. Lett. **77**, 1218 (1996).
[15] W. Bernreuther, A. Brandenburg, and P. Uwer, Phys. Lett. B **368**, 153 (1996).
[16] W. G. Dharmaratna and G. R. Goldstein, Phys. Rev. D **53**, 1073 (1996).
[17] G. Mahlon and S. J. Parke, Phys. Lett. B **411**, 173 (1997).
[18] M. Beneke *et al.*, arXiv:hep-ph/0003033.
[19] W. Bernreuther, A. Brandenburg, Z. G. Si, and P. Uwer, Phys. Rev. Lett. **87**, 242002 (2001).
[20] W. Bernreuther, A. Brandenburg, Z. G. Si, and P. Uwer, Nucl. Phys. **B690**, 81 (2004).
[21] C. A. Nelson, E. G. Barbagiovanni, J. J. Berger, E. K. Pueschel, and J. R. Wickman, Eur. Phys. J. C **45**, 121 (2006).
[22] R. M. Godbole, S. D. Rindani, and R. K. Singh, J. High Energy Phys. 12 (2006) 021.
[23] W. Bernreuther, J. Phys. G **35**, 083001 (2008).
[24] W. Bernreuther and Z.-G. Si, Phys. Lett. B **725**, 115 (2013).
[25] R. M. Harris, C. T. Hill, and S. J. Parke, arXiv:hep-ph/9911288.
[26] M. Arai, N. Okada, K. Smolek, and V. Simak, Acta Phys. Pol. B **40**, 93 (2009).
[27] W. Bernreuther, M. Flesch, and P. Haberl, Phys. Rev. D **58**, 114031 (1998).
[28] J. S. Lee, Y. Peters, A. Pilaftsis, and C. Schwanenberger, Eur. Phys. J. C **66**, 261 (2010).
[29] M. S. Carena, S. Heinemeyer, C. E. M. Wagner, and G. Weiglein, Eur. Phys. J. C **26**, 601 (2003).
[30] V. M. Abazov *et al.* (D0 Collaboration), Phys. Lett. B **702**, 16 (2011).
[31] T. Aaltonen *et al.* (CDF Collaboration), Phys. Rev. D **83**, 031104 (2011).
[32] K. Melnikov and M. Schulze, Phys. Lett. B **700**, 17 (2011).
[33] V. M. Abazov *et al.* (D0 Collaboration), Phys. Rev. Lett. **107**, 032001 (2011).
[34] V. M. Abazov *et al.* (D0 Collaboration), Phys. Rev. Lett. **108**, 032004 (2012).
[35] ATLAS Collaboration, Phys. Rev. Lett. **108**, 212001 (2012).
[36] ATLAS Collaboration, JINST **3**, S08003 (2008).
[37] ATLAS Collaboration, Eur. Phys. J. C **72**, 1849 (2012).
[38] ATLAS Collaboration, Eur. Phys. J. C **74**, 2941 (2014).
[39] ATLAS Collaboration, Eur. Phys. J. C **73**, 2304 (2013).
[40] M. Cacciari, and G. P. Salam, Phys. Lett. B **641**, 57 (2006).
[41] M. Cacciari, G. P. Salam, and G. Soyez, J. High Energy Phys. 04 (2008) 063.
[42] M. Cacciari, G. P. Salam, and G. Soyez, Eur. Phys. J. C **72**, 1896 (2012).

[43] ATLAS Collaboration, Report No. ATLAS-CONF-2011-102, https://cds.cern.ch/record/1369219.
[44] ATLAS Collaboration, Report No. ATLAS-CONF-2012-097, https://cds.cern.ch/record/1460443.
[45] ATLAS Collaboration, Eur. Phys. J. C **72**, 1844 (2012).
[46] M. L. Mangano, F. Piccinini, A. D. Polosa, M. Moretti, and R. Pittau, J. High Energy Phys. 07 (2003) 001.
[47] P. Nadolsky, H.-L. Lai, Q.-H. Cao, J. Huston, J. Pumplin, D. Stump, W.-K. Tung, and C.-P. Yuan, Phys. Rev. D **78**, 013004 (2008).
[48] R. Hamberg, W. L. van Neerven, and T. Matsuura, Nucl. Phys. **B359**, 343 (1991); **B644**, 403(E) (2002).
[49] G. Corcella, I. G. Knowles, G. Marchesini, S. Moretti, K. Odagiri, P. Richardson, M. H. Seymour, and B. R. Webber, J. High Energy Phys. 01 (2001) 010.
[50] J. Butterworth, J. Forshaw, and M. Seymour, Z. Phys. C **72**, 637 (1996).
[51] M. L. Mangano, M. Moretti, and R. Pittau, Nucl. Phys. **B632**, 343 (2002).
[52] S. Frixione and B. R. Webber, J. High Energy Phys. 06 (2002) 029.
[53] S. Frixione, E. Laenen, P. Motylinski, and B. R. Webber, J. High Energy Phys. 03 (2006) 092.
[54] S. Frixione, E. Laenen, P. Motylinski, C. White, and B. R. Webber, J. High Energy Phys. 07 (2008) 029.
[55] H.-L. Lai, M. Guzzi, J. Huston, Z. Li, P. M. Nadolsky, J. Pumplin, and C.-P. Yuan, Phys. Rev. D **82**, 074024 (2010).
[56] N. Kidonakis, Phys. Rev. D **82**, 054018 (2010).
[57] A. Sherstnev and R. S. Thorne, Eur. Phys. J. C **55**, 553 (2008).
[58] J. M. Campbell and R. K. Ellis, Phys. Rev. D **60**, 113006 (1999).
[59] ATLAS Collaboration, Eur. Phys. J. C **71**, 1577 (2011).
[60] ATLAS Collaboration, J. High Energy Phys. 05 (2012) 059.
[61] S. Agostinelli *et al.* (GEANT4 Collaboration), Nucl. Instrum. Methods Phys. Res., Sect. A **506**, 250 (2003).
[62] ATLAS Collaboration, Eur. Phys. J. C **70**, 823 (2010).
[63] M. Cacciari, M. Czakon, M. Mangano, A. Mitov, and P. Nason, Phys. Lett. B **710**, 612 (2012).
[64] P. Bärnreuther, M. Czakon, and A. Mitov, Phys. Rev. Lett. **109**, 132001 (2012).
[65] M. Czakon and A. Mitov, J. High Energy Phys. 12 (2012) 054.
[66] M. Czakon and A. Mitov, J. High Energy Phys. 01 (2013) 080.
[67] M. Czakon, P. Fiedler, and A. Mitov, Phys. Rev. Lett. **110**, 252004 (2013).
[68] M. Czakon and A. Mitov, Comput. Phys. Commun. **185**, 2930 (2014).
[69] S. Frixione, E. Laenen, P. Motylinski, B. R. Webber, and C. D. White, J. High Energy Phys. 07 (2008) 029.
[70] B. Kersevan and E. Richter-Was, Comput. Phys. Commun. **184**, 919 (2013).
[71] A. Sherstnev and R. S. Thorne, Eur. Phys. J. C **55**, 553 (2008).
[72] M. Jezabek and J. H. Kühn, Nucl. Phys. **B320**, 20 (1989); A. Czarnecki, M. Jezabek, and J. H. Kühn, Nucl. Phys. **B351**, 70 (1991).
[73] S. J. Parke, Nuovo Cimento Soc. Ital. Fis. C **035N3**, 111 (2012).
[74] A. Brandenburg, Z. G. Si, and P. Uwer, Phys. Lett. B **539**, 235 (2002).
[75] G. Mahlon and S. J. Parke, Phys. Rev. D **81**, 074024 (2010).
[76] S. J. Parke and Y. Shadmi, Phys. Lett. B **387**, 199 (1996).
[77] P. Uwer, Phys. Lett. B **609**, 271 (2005).
[78] W. Bernreuther (private communication).
[79] B. Abbott *et al.* (D0 Collaboration), Phys. Rev. Lett. **80**, 2063 (1998).
[80] ATLAS Collaboration, Eur. Phys. J. C **73**, 2306 (2013).
[81] J. Erdmann, S. Guindon, K. Kröninger, B. Lemmer, O. Nackenhorst, A. Quadt, and P. Stolte, Nucl. Instrum. Methods Phys. Res., Sect. A **748**, 18 (2014).
[82] ATLAS Collaboration, arXiv:1407.0891.
[83] CMS Collaboration, Eur. Phys. J. C **73**, 2339 (2013).
[84] N. Reid and D. A. S. Fraser, in *Proceedings of PHYSTAT 2003*, edited by L. Lyons, R. P. Mount, and R. Reitmeyer (SLAC, Stanford, 2003), p. 265.
[85] P. Nason, J. High Energy Phys. 11 (2004) 040.
[86] T. Sjostrand, S. Mrenna, and P. Skands, J. High Energy Phys. 05 (2006) 026.
[87] ATLAS Collaboration, Eur. Phys. J. C **72**, 2043 (2012).
[88] P. Skands, Phys. Rev. D **82**, 074018 (2010).
[89] R. D. Ball, V. Bertone, F. Cerutti, L. Del Debbio, S. Forte, A. Guffanti, J. I. Latorre, J. Rojo, and M. Ubiali, Nucl. Phys. **B855**, 153 (2012).
[90] A. Martin, W. Stirling, R. Thorne, and G. Watt, Phys. Rev. D **60**, 113006 (1999).
[91] ATLAS Collaboration, Eur. Phys. J. C **73**, 2518 (2013).

G. Aad,[84] B. Abbott,[112] J. Abdallah,[152] S. Abdel Khalek,[116] O. Abdinov,[11] R. Aben,[106] B. Abi,[113] M. Abolins,[89] O. S. AbouZeid,[159] H. Abramowicz,[154] H. Abreu,[153] R. Abreu,[30] Y. Abulaiti,[147a,147b] B. S. Acharya,[165a,165b,b] L. Adamczyk,[38a] D. L. Adams,[25] J. Adelman,[177] S. Adomeit,[99] T. Adye,[130] T. Agatonovic-Jovin,[13a] J. A. Aguilar-Saavedra,[125a,125f] M. Agustoni,[17] S. P. Ahlen,[22] F. Ahmadov,[64,c] G. Aielli,[134a,134b] H. Akerstedt,[147a,147b] T. P. A. Åkesson,[80] G. Akimoto,[156] A. V. Akimov,[95] G. L. Alberghi,[20a,20b] J. Albert,[170] S. Albrand,[55] M. J. Alconada Verzini,[70] M. Aleksa,[30] I. N. Aleksandrov,[64] C. Alexa,[26a] G. Alexander,[154] G. Alexandre,[49] T. Alexopoulos,[10] M. Alhroob,[165a,165c] G. Alimonti,[90a] L. Alio,[84] J. Alison,[31] B. M. M. Allbrooke,[18] L. J. Allison,[71] P. P. Allport,[73] J. Almond,[83] A. Aloisio,[103a,103b] A. Alonso,[36] F. Alonso,[70] C. Alpigiani,[75] A. Altheimer,[35] B. Alvarez Gonzalez,[89] M. G. Alviggi,[103a,103b] K. Amako,[65] Y. Amaral Coutinho,[24a] C. Amelung,[23] D. Amidei,[88] S. P. Amor Dos Santos,[125a,125c] A. Amorim,[125a,125b]

S. Amoroso,[48] N. Amram,[154] G. Amundsen,[23] C. Anastopoulos,[140] L. S. Ancu,[49] N. Andari,[30] T. Andeen,[35] C. F. Anders,[58b] G. Anders,[30] K. J. Anderson,[31] A. Andreazza,[90a,90b] V. Andrei,[58a] X. S. Anduaga,[70] S. Angelidakis,[9] I. Angelozzi,[106] P. Anger,[44] A. Angerami,[35] F. Anghinolfi,[30] A. V. Anisenkov,[108] N. Anjos,[125a] A. Annovi,[47] A. Antonaki,[9] M. Antonelli,[47] A. Antonov,[97] J. Antos,[145b] F. Anulli,[133a] M. Aoki,[65] L. Aperio Bella,[18] R. Apolle,[119,d] G. Arabidze,[89] I. Aracena,[144] Y. Arai,[65] J. P. Araque,[125a] A. T. H. Arce,[45] J-F. Arguin,[94] S. Argyropoulos,[42] M. Arik,[19a] A. J. Armbruster,[30] O. Arnaez,[30] V. Arnal,[81] H. Arnold,[48] M. Arratia,[28] O. Arslan,[21] A. Artamonov,[96] G. Artoni,[23] S. Asai,[156] N. Asbah,[42] A. Ashkenazi,[154] B. Åsman,[147a,147b] L. Asquith,[6] K. Assamagan,[25] R. Astalos,[145a] M. Atkinson,[166] N. B. Atlay,[142] B. Auerbach,[6] K. Augsten,[127] M. Aurousseau,[146b] G. Avolio,[30] G. Azuelos,[94,e] Y. Azuma,[156] M. A. Baak,[30] A. Baas,[58a] C. Bacci,[135a,135b] H. Bachacou,[137] K. Bachas,[155] M. Backes,[30] M. Backhaus,[30] J. Backus Mayes,[144] E. Badescu,[26a] P. Bagiacchi,[133a,133b] P. Bagnaia,[133a,133b] Y. Bai,[33a] T. Bain,[35] J. T. Baines,[130] O. K. Baker,[177] P. Balek,[128] F. Balli,[137] E. Banas,[39] Sw. Banerjee,[174] A. A. E. Bannoura,[176] V. Bansal,[170] H. S. Bansil,[18] L. Barak,[173] S. P. Baranov,[95] E. L. Barberio,[87] D. Barberis,[50a,50b] M. Barbero,[84] T. Barillari,[100] M. Barisonzi,[176] T. Barklow,[144] N. Barlow,[28] B. M. Barnett,[130] R. M. Barnett,[15] Z. Barnovska,[5] A. Baroncelli,[135a] G. Barone,[49] A. J. Barr,[119] F. Barreiro,[81] J. Barreiro Guimarães da Costa,[57] R. Bartoldus,[144] A. E. Barton,[71] P. Bartos,[145a] V. Bartsch,[150] A. Bassalat,[116] A. Basye,[166] R. L. Bates,[53] L. Batkova,[145a] J. R. Batley,[28] M. Battaglia,[138] M. Battistin,[30] F. Bauer,[137] H. S. Bawa,[144,f] T. Beau,[79] P. H. Beauchemin,[162] R. Beccherle,[123a,123b] P. Bechtle,[21] H. P. Beck,[17] K. Becker,[176] S. Becker,[99] M. Beckingham,[171] C. Becot,[116] A. J. Beddall,[19c] A. Beddall,[19c] S. Bedikian,[177] V. A. Bednyakov,[64] C. P. Bee,[149] L. J. Beemster,[106] T. A. Beermann,[176] M. Begel,[25] K. Behr,[119] C. Belanger-Champagne,[86] P. J. Bell,[49] W. H. Bell,[49] G. Bella,[154] L. Bellagamba,[20a] A. Bellerive,[29] M. Bellomo,[85] K. Belotskiy,[97] O. Beltramello,[30] O. Benary,[154] D. Benchekroun,[136a] K. Bendtz,[147a,147b] N. Benekos,[166] Y. Benhammou,[154] E. Benhar Noccioli,[49] J. A. Benitez Garcia,[160b] D. P. Benjamin,[45] J. R. Bensinger,[23] K. Benslama,[131] S. Bentvelsen,[106] D. Berge,[106] E. Bergeaas Kuutmann,[16] N. Berger,[5] F. Berghaus,[170] J. Beringer,[15] C. Bernard,[22] P. Bernat,[77] C. Bernius,[78] F. U. Bernlochner,[170] T. Berry,[76] P. Berta,[128] C. Bertella,[84] G. Bertoli,[147a,147b] F. Bertolucci,[123a,123b] D. Bertsche,[112] M. I. Besana,[90a] G. J. Besjes,[105] O. Bessidskaia,[147a,147b] M. F. Bessner,[42] N. Besson,[137] C. Betancourt,[48] S. Bethke,[100] W. Bhimji,[46] R. M. Bianchi,[124] L. Bianchini,[23] M. Bianco,[30] O. Biebel,[99] S. P. Bieniek,[77] K. Bierwagen,[54] J. Biesiada,[15] M. Biglietti,[135a] J. Bilbao De Mendizabal,[49] H. Bilokon,[47] M. Bindi,[54] S. Binet,[116] A. Bingul,[19c] C. Bini,[133a,133b] C. W. Black,[151] J. E. Black,[144] K. M. Black,[22] D. Blackburn,[139] R. E. Blair,[6] J.-B. Blanchard,[137] T. Blazek,[145a] I. Bloch,[42] C. Blocker,[23] W. Blum,[82,a] U. Blumenschein,[54] G. J. Bobbink,[106] V. S. Bobrovnikov,[108] S. S. Bocchetta,[80] A. Bocci,[45] C. Bock,[99] C. R. Boddy,[119] M. Boehler,[48] T. T. Boek,[176] J. A. Bogaerts,[30] A. G. Bogdanchikov,[108] A. Bogouch,[91,a] C. Bohm,[147a] J. Bohm,[126] V. Boisvert,[76] T. Bold,[38a] V. Boldea,[26a] A. S. Boldyrev,[98] M. Bomben,[79] M. Bona,[75] M. Boonekamp,[137] A. Borisov,[129] G. Borissov,[71] M. Borri,[83] S. Borroni,[42] J. Bortfeldt,[99] V. Bortolotto,[135a,135b] K. Bos,[106] D. Boscherini,[20a] M. Bosman,[12] H. Boterenbrood,[106] J. Boudreau,[124] J. Bouffard,[2] E. V. Bouhova-Thacker,[71] D. Boumediene,[34] C. Bourdarios,[116] N. Bousson,[113] S. Boutouil,[136d] A. Boveia,[31] J. Boyd,[30] I. R. Boyko,[64] J. Bracinik,[18] A. Brandt,[8] G. Brandt,[15] O. Brandt,[58a] U. Bratzler,[157] B. Brau,[85] J. E. Brau,[115] H. M. Braun,[176,a] S. F. Brazzale,[165a,165c] B. Brelier,[159] K. Brendlinger,[121] A. J. Brennan,[87] R. Brenner,[167] S. Bressler,[173] K. Bristow,[146c] T. M. Bristow,[46] D. Britton,[53] F. M. Brochu,[28] I. Brock,[21] R. Brock,[89] C. Bromberg,[89] J. Bronner,[100] G. Brooijmans,[35] T. Brooks,[76] W. K. Brooks,[32b] J. Brosamer,[15] E. Brost,[115] J. Brown,[55] P. A. Bruckman de Renstrom,[39] D. Bruncko,[145b] R. Bruneliere,[48] S. Brunet,[60] A. Bruni,[20a] G. Bruni,[20a] M. Bruschi,[20a] L. Bryngemark,[80] T. Buanes,[14] Q. Buat,[143] F. Bucci,[49] P. Buchholz,[142] R. M. Buckingham,[119] A. G. Buckley,[53] S. I. Buda,[26a] I. A. Budagov,[64] F. Buehrer,[48] L. Bugge,[118] M. K. Bugge,[118] O. Bulekov,[97] A. C. Bundock,[73] H. Burckhart,[30] S. Burdin,[73] B. Burghgrave,[107] S. Burke,[130] I. Burmeister,[43] E. Busato,[34] D. Büscher,[48] V. Büscher,[82] P. Bussey,[53] C. P. Buszello,[167] B. Butler,[57] J. M. Butler,[22] A. I. Butt,[3] C. M. Buttar,[53] J. M. Butterworth,[77] P. Butti,[106] W. Buttinger,[28] A. Buzatu,[53] M. Byszewski,[10] S. Cabrera Urbán,[168] D. Caforio,[20a,20b] O. Cakir,[4a] P. Calafiura,[15] A. Calandri,[137] G. Calderini,[79] P. Calfayan,[99] R. Calkins,[107] L. P. Caloba,[24a] D. Calvet,[34] S. Calvet,[34] R. Camacho Toro,[49] S. Camarda,[42] D. Cameron,[118] L. M. Caminada,[15] R. Caminal Armadans,[12] S. Campana,[30] M. Campanelli,[77] A. Campoverde,[149] V. Canale,[103a,103b] A. Canepa,[160a] M. Cano Bret,[75] J. Cantero,[81] R. Cantrill,[76] T. Cao,[40] M. D. M. Capeans Garrido,[30] I. Caprini,[26a] M. Caprini,[26a] M. Capua,[37a,37b] R. Caputo,[82] R. Cardarelli,[134a] T. Carli,[30] G. Carlino,[103a] L. Carminati,[90a,90b] S. Caron,[105] E. Carquin,[32a] G. D. Carrillo-Montoya,[146c] J. R. Carter,[28] J. Carvalho,[125a,125c] D. Casadei,[77] M. P. Casado,[12] M. Casolino,[12] E. Castaneda-Miranda,[146b] A. Castelli,[106] V. Castillo Gimenez,[168] N. F. Castro,[125a] P. Catastini,[57] A. Catinaccio,[30] J. R. Catmore,[118] A. Cattai,[30] G. Cattani,[134a,134b] S. Caughron,[89] V. Cavaliere,[166] D. Cavalli,[90a] M. Cavalli-Sforza,[12] V. Cavasinni,[123a,123b] F. Ceradini,[135a,135b] B. Cerio,[45] K. Cerny,[128]

A. S. Cerqueira,[24b] A. Cerri,[150] L. Cerrito,[75] F. Cerutti,[15] M. Cerv,[30] A. Cervelli,[17] S. A. Cetin,[19b] A. Chafaq,[136a] D. Chakraborty,[107] I. Chalupkova,[128] P. Chang,[166] B. Chapleau,[86] J. D. Chapman,[28] D. Charfeddine,[116] D. G. Charlton,[18] C. C. Chau,[159] C. A. Chavez Barajas,[150] S. Cheatham,[86] A. Chegwidden,[89] S. Chekanov,[6] S. V. Chekulaev,[160a] G. A. Chelkov,[64,g] M. A. Chelstowska,[88] C. Chen,[63] H. Chen,[25] K. Chen,[149] L. Chen,[33d,h] S. Chen,[33c] X. Chen,[146c] Y. Chen,[35] H. C. Cheng,[88] Y. Cheng,[31] A. Cheplakov,[64] R. Cherkaoui El Moursli,[136e] V. Chernyatin,[25,a] E. Cheu,[7] L. Chevalier,[137] V. Chiarella,[47] G. Chiefari,[103a,103b] J. T. Childers,[6] A. Chilingarov,[71] G. Chiodini,[72a] A. S. Chisholm,[18] R. T. Chislett,[77] A. Chitan,[26a] M. V. Chizhov,[64] S. Chouridou,[9] B. K. B. Chow,[99] D. Chromek-Burckhart,[30] M. L. Chu,[152] J. Chudoba,[126] J. J. Chwastowski,[39] L. Chytka,[114] G. Ciapetti,[133a,133b] A. K. Ciftci,[4a] R. Ciftci,[4a] D. Cinca,[53] V. Cindro,[74] A. Ciocio,[15] P. Cirkovic,[13b] Z. H. Citron,[173] M. Citterio,[90a] M. Ciubancan,[26a] A. Clark,[49] P. J. Clark,[46] R. N. Clarke,[15] W. Cleland,[124] J. C. Clemens,[84] C. Clement,[147a,147b] Y. Coadou,[84] M. Cobal,[165a,165c] A. Coccaro,[139] J. Cochran,[63] L. Coffey,[23] J. G. Cogan,[144] J. Coggeshall,[166] B. Cole,[35] S. Cole,[107] A. P. Colijn,[106] J. Collot,[55] T. Colombo,[58c] G. Colon,[85] G. Compostella,[100] P. Conde Muiño,[125a,125b] E. Coniavitis,[48] M. C. Conidi,[12] S. H. Connell,[146b] I. A. Connelly,[76] S. M. Consonni,[90a,90b] V. Consorti,[48] S. Constantinescu,[26a] C. Conta,[120a,120b] G. Conti,[57] F. Conventi,[103a,i] M. Cooke,[15] B. D. Cooper,[77] A. M. Cooper-Sarkar,[119] N. J. Cooper-Smith,[76] K. Copic,[15] T. Cornelissen,[176] M. Corradi,[20a] F. Corriveau,[86,j] A. Corso-Radu,[164] A. Cortes-Gonzalez,[12] G. Cortiana,[100] G. Costa,[90a] M. J. Costa,[168] D. Costanzo,[140] D. Côté,[8] G. Cottin,[28] G. Cowan,[76] B. E. Cox,[83] K. Cranmer,[109] G. Cree,[29] S. Crépé-Renaudin,[55] F. Crescioli,[79] W. A. Cribbs,[147a,147b] M. Crispin Ortuzar,[119] M. Cristinziani,[21] V. Croft,[105] G. Crosetti,[37a,37b] C.-M. Cuciuc,[26a] T. Cuhadar Donszelmann,[140] J. Cummings,[177] M. Curatolo,[47] C. Cuthbert,[151] H. Czirr,[142] P. Czodrowski,[3] Z. Czyczula,[177] S. D'Auria,[53] M. D'Onofrio,[73] M. J. Da Cunha Sargedas De Sousa,[125a,125b] C. Da Via,[83] W. Dabrowski,[38a] A. Dafinca,[119] T. Dai,[88] O. Dale,[14] F. Dallaire,[94] C. Dallapiccola,[85] M. Dam,[36] A. C. Daniells,[18] M. Dano Hoffmann,[137] V. Dao,[105] G. Darbo,[50a] S. Darmora,[8] J. A. Dassoulas,[42] A. Dattagupta,[60] W. Davey,[21] C. David,[170] T. Davidek,[128] E. Davies,[119,d] M. Davies,[154] O. Davignon,[79] A. R. Davison,[77] P. Davison,[77] Y. Davygora,[58a] E. Dawe,[143] I. Dawson,[140] R. K. Daya-Ishmukhametova,[85] K. De,[8] R. de Asmundis,[103a] S. De Castro,[20a,20b] S. De Cecco,[79] N. De Groot,[105] P. de Jong,[106] H. De la Torre,[81] F. De Lorenzi,[63] L. De Nooij,[106] D. De Pedis,[133a] A. De Salvo,[133a] U. De Sanctis,[165a,165b] A. De Santo,[150] J. B. De Vivie De Regie,[116] W. J. Dearnaley,[71] R. Debbe,[25] C. Debenedetti,[138] B. Dechenaux,[55] D. V. Dedovich,[64] I. Deigaard,[106] J. Del Peso,[81] T. Del Prete,[123a,123b] F. Deliot,[137] C. M. Delitzsch,[49] M. Deliyergiyev,[74] A. Dell'Acqua,[30] L. Dell'Asta,[22] M. Dell'Orso,[123a,123b] M. Della Pietra,[103a,i] D. della Volpe,[49] M. Delmastro,[5] P. A. Delsart,[55] C. Deluca,[106] S. Demers,[177] M. Demichev,[64] A. Demilly,[79] S. P. Denisov,[129] D. Derendarz,[39] J. E. Derkaoui,[136d] F. Derue,[79] P. Dervan,[73] K. Desch,[21] C. Deterre,[42] P. O. Deviveiros,[106] A. Dewhurst,[130] S. Dhaliwal,[106] A. Di Ciaccio,[134a,134b] L. Di Ciaccio,[5] A. Di Domenico,[133a,133b] C. Di Donato,[103a,103b] A. Di Girolamo,[30] B. Di Girolamo,[30] A. Di Mattia,[153] B. Di Micco,[135a,135b] R. Di Nardo,[47] A. Di Simone,[48] R. Di Sipio,[20a,20b] D. Di Valentino,[29] F. A. Dias,[46] M. A. Diaz,[32a] E. B. Diehl,[88] J. Dietrich,[42] T. A. Dietzsch,[58a] S. Diglio,[84] A. Dimitrievska,[13a] J. Dingfelder,[21] C. Dionisi,[133a,133b] P. Dita,[26a] S. Dita,[26a] F. Dittus,[30] F. Djama,[84] T. Djobava,[51b] M. A. B. do Vale,[24c] A. Do Valle Wemans,[125a,125g] T. K. O. Doan,[5] D. Dobos,[30] C. Doglioni,[49] T. Doherty,[53] T. Dohmae,[156] J. Dolejsi,[128] Z. Dolezal,[128] B. A. Dolgoshein,[97,a] M. Donadelli,[24d] S. Donati,[123a,123b] P. Dondero,[120a,120b] J. Donini,[34] J. Dopke,[130] A. Doria,[103a] M. T. Dova,[70] A. T. Doyle,[53] M. Dris,[10] J. Dubbert,[88] S. Dube,[15] E. Dubreuil,[34] E. Duchovni,[173] G. Duckeck,[99] O. A. Ducu,[26a] D. Duda,[176] A. Dudarev,[30] F. Dudziak,[63] L. Duflot,[116] L. Duguid,[76] M. Dührssen,[30] M. Dunford,[58a] H. Duran Yildiz,[4a] M. Düren,[52] A. Durglishvili,[51b] M. Dwuznik,[38a] M. Dyndal,[38a] J. Ebke,[99] W. Edson,[2] N. C. Edwards,[46] W. Ehrenfeld,[21] T. Eifert,[144] G. Eigen,[14] K. Einsweiler,[15] T. Ekelof,[167] M. El Kacimi,[136c] M. Ellert,[167] S. Elles,[5] F. Ellinghaus,[82] N. Ellis,[30] J. Elmsheuser,[99] M. Elsing,[30] D. Emeliyanov,[130] Y. Enari,[156] O. C. Endner,[82] M. Endo,[117] R. Engelmann,[149] J. Erdmann,[177] A. Ereditato,[17] D. Eriksson,[147a] G. Ernis,[176] J. Ernst,[2] M. Ernst,[25] J. Ernwein,[137] D. Errede,[166] S. Errede,[166] E. Ertel,[82] M. Escalier,[116] H. Esch,[43] C. Escobar,[124] B. Esposito,[47] A. I. Etienvre,[137] E. Etzion,[154] H. Evans,[60] A. Ezhilov,[122] L. Fabbri,[20a,20b] G. Facini,[31] R. M. Fakhrutdinov,[129] S. Falciano,[133a] R. J. Falla,[77] J. Faltova,[128] Y. Fang,[33a] M. Fanti,[90a,90b] A. Farbin,[8] A. Farilla,[135a] T. Farooque,[12] S. Farrell,[164] S. M. Farrington,[171] P. Farthouat,[30] F. Fassi,[136e] P. Fassnacht,[30] D. Fassouliotis,[9] A. Favareto,[50a,50b] L. Fayard,[116] P. Federic,[145a] O. L. Fedin,[122,k] W. Fedorko,[169] M. Fehling-Kaschek,[48] S. Feigl,[30] L. Feligioni,[84] C. Feng,[33d] E. J. Feng,[6] H. Feng,[88] A. B. Fenyuk,[129] S. Fernandez Perez,[30] S. Ferrag,[53] J. Ferrando,[53] A. Ferrari,[167] P. Ferrari,[106] R. Ferrari,[120a] D. E. Ferreira de Lima,[53] A. Ferrer,[168] D. Ferrere,[49] C. Ferretti,[88] A. Ferretto Parodi,[50a,50b] M. Fiascaris,[31] F. Fiedler,[82] A. Filipčič,[74] M. Filipuzzi,[42] F. Filthaut,[105] M. Fincke-Keeler,[170] K. D. Finelli,[151] M. C. N. Fiolhais,[125a,125c] L. Fiorini,[168] A. Firan,[40] A. Fischer,[2] J. Fischer,[176] W. C. Fisher,[89]

E. A. Fitzgerald,[23] M. Flechl,[48] I. Fleck,[142] P. Fleischmann,[88] S. Fleischmann,[176] G. T. Fletcher,[140] G. Fletcher,[75] T. Flick,[176] A. Floderus,[80] L. R. Flores Castillo,[174,l] A. C. Florez Bustos,[160b] M. J. Flowerdew,[100] A. Formica,[137] A. Forti,[83] D. Fortin,[160a] D. Fournier,[116] H. Fox,[71] S. Fracchia,[12] P. Francavilla,[79] M. Franchini,[20a,20b] S. Franchino,[30] D. Francis,[30] M. Franklin,[57] S. Franz,[61] M. Fraternali,[120a,120b] S. T. French,[28] C. Friedrich,[42] F. Friedrich,[44] D. Froidevaux,[30] J. A. Frost,[28] C. Fukunaga,[157] E. Fullana Torregrosa,[82] B. G. Fulsom,[144] J. Fuster,[168] C. Gabaldon,[55] O. Gabizon,[173] A. Gabrielli,[20a,20b] A. Gabrielli,[133a,133b] S. Gadatsch,[106] S. Gadomski,[49] G. Gagliardi,[50a,50b] P. Gagnon,[60] C. Galea,[105] B. Galhardo,[125a,125c] E. J. Gallas,[119] V. Gallo,[17] B. J. Gallop,[130] P. Gallus,[127] G. Galster,[36] K. K. Gan,[110] R. P. Gandrajula,[62] J. Gao,[33b,h] Y. S. Gao,[144,f] F. M. Garay Walls,[46] F. Garberson,[177] C. García,[168] J. E. García Navarro,[168] M. Garcia-Sciveres,[15] R. W. Gardner,[31] N. Garelli,[144] V. Garonne,[30] C. Gatti,[47] G. Gaudio,[120a] B. Gaur,[142] L. Gauthier,[94] P. Gauzzi,[133a,133b] I. L. Gavrilenko,[95] C. Gay,[169] G. Gaycken,[21] E. N. Gazis,[10] P. Ge,[33d] Z. Gecse,[169] C. N. P. Gee,[130] D. A. A. Geerts,[106] Ch. Geich-Gimbel,[21] K. Gellerstedt,[147a,147b] C. Gemme,[50a] A. Gemmell,[53] M. H. Genest,[55] S. Gentile,[133a,133b] M. George,[54] S. George,[76] D. Gerbaudo,[164] A. Gershon,[154] H. Ghazlane,[136b] N. Ghodbane,[34] B. Giacobbe,[20a] S. Giagu,[133a,133b] V. Giangiobbe,[12] P. Giannetti,[123a,123b] F. Gianotti,[30] B. Gibbard,[25] S. M. Gibson,[76] M. Gilchriese,[15] T. P. S. Gillam,[28] D. Gillberg,[30] G. Gilles,[34] D. M. Gingrich,[3,e] N. Giokaris,[9] M. P. Giordani,[165a,165c] R. Giordano,[103a,103b] F. M. Giorgi,[20a] F. M. Giorgi,[16] P. F. Giraud,[137] D. Giugni,[90a] C. Giuliani,[48] M. Giulini,[58b] B. K. Gjelsten,[118] S. Gkaitatzis,[155] I. Gkialas,[155,m] L. K. Gladilin,[98] C. Glasman,[81] J. Glatzer,[30] P. C. F. Glaysher,[46] A. Glazov,[42] G. L. Glonti,[64] M. Goblirsch-Kolb,[100] J. R. Goddard,[75] J. Godfrey,[143] J. Godlewski,[30] C. Goeringer,[82] S. Goldfarb,[88] T. Golling,[177] D. Golubkov,[129] A. Gomes,[125a,125b,125d] L. S. Gomez Fajardo,[42] R. Gonçalo,[125a] J. Goncalves Pinto Firmino Da Costa,[137] L. Gonella,[21] S. González de la Hoz,[168] G. Gonzalez Parra,[12] S. Gonzalez-Sevilla,[49] L. Goossens,[30] P. A. Gorbounov,[96] H. A. Gordon,[25] I. Gorelov,[104] B. Gorini,[30] E. Gorini,[72a,72b] A. Gorišek,[74] E. Gornicki,[39] A. T. Goshaw,[6] C. Gössling,[43] M. I. Gostkin,[64] M. Gouighri,[136a] D. Goujdami,[136c] M. P. Goulette,[49] A. G. Goussiou,[139] C. Goy,[5] S. Gozpinar,[23] H. M. X. Grabas,[137] L. Graber,[54] I. Grabowska-Bold,[38a] P. Grafström,[20a,20b] K-J. Grahn,[42] J. Gramling,[49] E. Gramstad,[118] S. Grancagnolo,[16] V. Grassi,[149] V. Gratchev,[122] H. M. Gray,[30] E. Graziani,[135a] O. G. Grebenyuk,[122] Z. D. Greenwood,[78,n] K. Gregersen,[77] I. M. Gregor,[42] P. Grenier,[144] J. Griffiths,[8] A. A. Grillo,[138] K. Grimm,[71] S. Grinstein,[12,o] Ph. Gris,[34] Y. V. Grishkevich,[98] J.-F. Grivaz,[116] J. P. Grohs,[44] A. Grohsjean,[42] E. Gross,[173] J. Grosse-Knetter,[54] G. C. Grossi,[134a,134b] J. Groth-Jensen,[173] Z. J. Grout,[150] L. Guan,[33b] F. Guescini,[49] D. Guest,[177] O. Gueta,[154] C. Guicheney,[34] E. Guido,[50a,50b] T. Guillemin,[116] S. Guindon,[2] U. Gul,[53] C. Gumpert,[44] J. Gunther,[127] J. Guo,[35] S. Gupta,[119] P. Gutierrez,[112] N. G. Gutierrez Ortiz,[53] C. Gutschow,[77] N. Guttman,[154] C. Guyot,[137] C. Gwenlan,[119] C. B. Gwilliam,[73] A. Haas,[109] C. Haber,[15] H. K. Hadavand,[8] N. Haddad,[136e] P. Haefner,[21] S. Hageböck,[21] Z. Hajduk,[39] H. Hakobyan,[178] M. Haleem,[42] D. Hall,[119] G. Halladjian,[89] K. Hamacher,[176] P. Hamal,[114] K. Hamano,[170] M. Hamer,[54] A. Hamilton,[146a] S. Hamilton,[162] P. G. Hamnett,[42] L. Han,[33b] K. Hanagaki,[117] K. Hanawa,[156] M. Hance,[15] P. Hanke,[58a] R. Hanna,[137] J. B. Hansen,[36] J. D. Hansen,[36] P. H. Hansen,[36] K. Hara,[161] A. S. Hard,[174] T. Harenberg,[176] F. Hariri,[116] S. Harkusha,[91] D. Harper,[88] R. D. Harrington,[46] O. M. Harris,[139] P. F. Harrison,[171] F. Hartjes,[106] S. Hasegawa,[102] Y. Hasegawa,[141] A. Hasib,[112] S. Hassani,[137] S. Haug,[17] M. Hauschild,[30] R. Hauser,[89] M. Havranek,[126] C. M. Hawkes,[18] R. J. Hawkings,[30] A. D. Hawkins,[80] T. Hayashi,[161] D. Hayden,[89] C. P. Hays,[119] H. S. Hayward,[73] S. J. Haywood,[130] S. J. Head,[18] T. Heck,[82] V. Hedberg,[80] L. Heelan,[8] S. Heim,[121] T. Heim,[176] B. Heinemann,[15] L. Heinrich,[109] J. Hejbal,[126] L. Helary,[22] C. Heller,[99] M. Heller,[30] S. Hellman,[147a,147b] D. Hellmich,[21] C. Helsens,[30] J. Henderson,[119] R. C. W. Henderson,[71] Y. Heng,[174] C. Hengler,[42] A. Henrichs,[177] A. M. Henriques Correia,[30] S. Henrot-Versille,[116] C. Hensel,[54] G. H. Herbert,[16] Y. Hernández Jiménez,[168] R. Herrberg-Schubert,[16] G. Herten,[48] R. Hertenberger,[99] L. Hervas,[30] G. G. Hesketh,[77] N. P. Hessey,[106] R. Hickling,[75] E. Higón-Rodriguez,[168] E. Hill,[170] J. C. Hill,[28] K. H. Hiller,[42] S. Hillert,[21] S. J. Hillier,[18] I. Hinchliffe,[15] E. Hines,[121] M. Hirose,[158] D. Hirschbuehl,[176] J. Hobbs,[149] N. Hod,[106] M. C. Hodgkinson,[140] P. Hodgson,[140] A. Hoecker,[30] M. R. Hoeferkamp,[104] J. Hoffman,[40] D. Hoffmann,[84] J. I. Hofmann,[58a] M. Hohlfeld,[82] T. R. Holmes,[15] T. M. Hong,[121] L. Hooft van Huysduynen,[109] J-Y. Hostachy,[55] S. Hou,[152] A. Hoummada,[136a] J. Howard,[119] J. Howarth,[42] M. Hrabovsky,[114] I. Hristova,[16] J. Hrivnac,[116] T. Hryn'ova,[5] C. Hsu,[146c] P. J. Hsu,[82] S.-C. Hsu,[139] D. Hu,[35] X. Hu,[25] Y. Huang,[42] Z. Hubacek,[30] F. Hubaut,[84] F. Huegging,[21] T. B. Huffman,[119] E. W. Hughes,[35] G. Hughes,[71] M. Huhtinen,[30] T. A. Hülsing,[82] M. Hurwitz,[15] N. Huseynov,[64,c] J. Huston,[89] J. Huth,[57] G. Iacobucci,[49] G. Iakovidis,[10] I. Ibragimov,[142] L. Iconomidou-Fayard,[116] E. Ideal,[177] P. Iengo,[103a] O. Igonkina,[106] T. Iizawa,[172] Y. Ikegami,[65] K. Ikematsu,[142] M. Ikeno,[65] Y. Ilchenko,[31,p] D. Iliadis,[155] N. Ilic,[159] Y. Inamaru,[66] T. Ince,[100] P. Ioannou,[9] M. Iodice,[135a] K. Iordanidou,[9] V. Ippolito,[57] A. Irles Quiles,[168] C. Isaksson,[167] M. Ishino,[67] M. Ishitsuka,[158] R. Ishmukhametov,[110] C. Issever,[119] S. Istin,[19a] J. M. Iturbe Ponce,[83] R. Iuppa,[134a,134b] J. Ivarsson,[80] W. Iwanski,[39] H. Iwasaki,[65] J. M. Izen,[41]

V. Izzo,[103a] B. Jackson,[121] M. Jackson,[73] P. Jackson,[1] M. R. Jaekel,[30] V. Jain,[2] K. Jakobs,[48] S. Jakobsen,[30] T. Jakoubek,[126] J. Jakubek,[127] D. O. Jamin,[152] D. K. Jana,[78] E. Jansen,[77] H. Jansen,[30] J. Janssen,[21] M. Janus,[171] G. Jarlskog,[80] N. Javadov,[64,c] T. Javůrek,[48] L. Jeanty,[15] J. Jejelava,[51a,q] G.-Y. Jeng,[151] D. Jennens,[87] P. Jenni,[48,r] J. Jentzsch,[43] C. Jeske,[171] S. Jézéquel,[5] H. Ji,[174] W. Ji,[82] J. Jia,[149] Y. Jiang,[33b] M. Jimenez Belenguer,[42] S. Jin,[33a] A. Jinaru,[26a] O. Jinnouchi,[158] M. D. Joergensen,[36] K. E. Johansson,[147a,147b] P. Johansson,[140] K. A. Johns,[7] K. Jon-And,[147a,147b] G. Jones,[171] R. W. L. Jones,[71] T. J. Jones,[73] J. Jongmanns,[58a] P. M. Jorge,[125a,125b] K. D. Joshi,[83] J. Jovicevic,[148] X. Ju,[174] C. A. Jung,[43] R. M. Jungst,[30] P. Jussel,[61] A. Juste Rozas,[12,o] M. Kaci,[168] A. Kaczmarska,[39] M. Kado,[116] H. Kagan,[110] M. Kagan,[144] E. Kajomovitz,[45] C. W. Kalderon,[119] S. Kama,[40] A. Kamenshchikov,[129] N. Kanaya,[156] M. Kaneda,[30] S. Kaneti,[28] V. A. Kantserov,[97] J. Kanzaki,[65] B. Kaplan,[109] A. Kapliy,[31] D. Kar,[53] K. Karakostas,[10] N. Karastathis,[10] M. Karnevskiy,[82] S. N. Karpov,[64] Z. M. Karpova,[64] K. Karthik,[109] V. Kartvelishvili,[71] A. N. Karyukhin,[129] L. Kashif,[174] G. Kasieczka,[58b] R. D. Kass,[110] A. Kastanas,[14] Y. Kataoka,[156] A. Katre,[49] J. Katzy,[42] V. Kaushik,[7] K. Kawagoe,[69] T. Kawamoto,[156] G. Kawamura,[54] S. Kazama,[156] V. F. Kazanin,[108] M. Y. Kazarinov,[64] R. Keeler,[170] R. Kehoe,[40] M. Keil,[54] J. S. Keller,[42] J. J. Kempster,[76] H. Keoshkerian,[5] O. Kepka,[126] B. P. Kerševan,[74] S. Kersten,[176] K. Kessoku,[156] J. Keung,[159] F. Khalil-zada,[11] H. Khandanyan,[147a,147b] A. Khanov,[113] A. Khodinov,[97] A. Khomich,[58a] T. J. Khoo,[28] G. Khoriauli,[21] A. Khoroshilov,[176] V. Khovanskiy,[96] E. Khramov,[64] J. Khubua,[51b] H. Y. Kim,[8] H. Kim,[147a,147b] S. H. Kim,[161] N. Kimura,[172] O. Kind,[16] B. T. King,[73] M. King,[168] R. S. B. King,[119] S. B. King,[169] J. Kirk,[130] A. E. Kiryunin,[100] T. Kishimoto,[66] D. Kisielewska,[38a] F. Kiss,[48] T. Kittelmann,[124] K. Kiuchi,[161] E. Kladiva,[145b] M. Klein,[73] U. Klein,[73] K. Kleinknecht,[82] P. Klimek,[147a,147b] A. Klimentov,[25] R. Klingenberg,[43] J. A. Klinger,[83] T. Klioutchnikova,[30] P. F. Klok,[105] E.-E. Kluge,[58a] P. Kluit,[106] S. Kluth,[100] E. Kneringer,[61] E. B. F. G. Knoops,[84] A. Knue,[53] D. Kobayashi,[158] T. Kobayashi,[156] M. Kobel,[44] M. Kocian,[144] P. Kodys,[128] P. Koevesarki,[21] T. Koffas,[29] E. Koffeman,[106] L. A. Kogan,[119] S. Kohlmann,[176] Z. Kohout,[127] T. Kohriki,[65] T. Koi,[144] H. Kolanoski,[16] I. Koletsou,[5] J. Koll,[89] A. A. Komar,[95,a] Y. Komori,[156] T. Kondo,[65] N. Kondrashova,[42] K. Köneke,[48] A. C. König,[105] S. König,[82] T. Kono,[65,s] R. Konoplich,[109,t] N. Konstantinidis,[77] R. Kopeliansky,[153] S. Koperny,[38a] L. Köpke,[82] A. K. Kopp,[48] K. Korcyl,[39] K. Kordas,[155] A. Korn,[77] A. A. Korol,[108,u] I. Korolkov,[12] E. V. Korolkova,[140] V. A. Korotkov,[129] O. Kortner,[100] S. Kortner,[100] V. V. Kostyukhin,[21] V. M. Kotov,[64] A. Kotwal,[45] C. Kourkoumelis,[9] V. Kouskoura,[155] A. Koutsman,[160a] R. Kowalewski,[170] T. Z. Kowalski,[38a] W. Kozanecki,[137] A. S. Kozhin,[129] V. Kral,[127] V. A. Kramarenko,[98] G. Kramberger,[74] D. Krasnopevtsev,[97] M. W. Krasny,[79] A. Krasznahorkay,[30] J. K. Kraus,[21] A. Kravchenko,[25] S. Kreiss,[109] M. Kretz,[58c] J. Kretzschmar,[73] K. Kreutzfeldt,[52] P. Krieger,[159] K. Kroeninger,[54] H. Kroha,[100] J. Kroll,[121] J. Kroseberg,[21] J. Krstic,[13a] U. Kruchonak,[64] H. Krüger,[21] T. Kruker,[17] N. Krumnack,[63] Z. V. Krumshteyn,[64] A. Kruse,[174] M. C. Kruse,[45] M. Kruskal,[22] T. Kubota,[87] S. Kuday,[4a] S. Kuehn,[48] A. Kugel,[58c] A. Kuhl,[138] T. Kuhl,[42] V. Kukhtin,[64] Y. Kulchitsky,[91] S. Kuleshov,[32b] M. Kuna,[133a,133b] J. Kunkle,[121] A. Kupco,[126] H. Kurashige,[66] Y. A. Kurochkin,[91] R. Kurumida,[66] V. Kus,[126] E. S. Kuwertz,[148] M. Kuze,[158] J. Kvita,[114] A. La Rosa,[49] L. La Rotonda,[37a,37b] C. Lacasta,[168] F. Lacava,[133a,133b] J. Lacey,[29] H. Lacker,[16] D. Lacour,[79] V. R. Lacuesta,[168] E. Ladygin,[64] R. Lafaye,[5] B. Laforge,[79] T. Lagouri,[177] S. Lai,[48] H. Laier,[58a] L. Lambourne,[77] S. Lammers,[60] C. L. Lampen,[7] W. Lampl,[7] E. Lançon,[137] U. Landgraf,[48] M. P. J. Landon,[75] V. S. Lang,[58a] A. J. Lankford,[164] F. Lanni,[25] K. Lantzsch,[30] S. Laplace,[79] C. Lapoire,[21] J. F. Laporte,[137] T. Lari,[90a] M. Lassnig,[30] P. Laurelli,[47] W. Lavrijsen,[15] A. T. Law,[138] P. Laycock,[73] B. T. Le,[55] O. Le Dortz,[79] E. Le Guirriec,[84] E. Le Menedeu,[12] T. LeCompte,[6] F. Ledroit-Guillon,[55] C. A. Lee,[152] H. Lee,[106] J. S. H. Lee,[117] S. C. Lee,[152] L. Lee,[177] G. Lefebvre,[79] M. Lefebvre,[170] F. Legger,[99] C. Leggett,[15] A. Lehan,[73] M. Lehmacher,[21] G. Lehmann Miotto,[30] X. Lei,[7] W. A. Leight,[29] A. Leisos,[155] A. G. Leister,[177] M. A. L. Leite,[24d] R. Leitner,[128] D. Lellouch,[173] B. Lemmer,[54] K. J. C. Leney,[77] T. Lenz,[106] G. Lenzen,[176] B. Lenzi,[30] R. Leone,[7] S. Leone,[123a,123b] K. Leonhardt,[44] C. Leonidopoulos,[46] S. Leontsinis,[10] C. Leroy,[94] C. G. Lester,[28] C. M. Lester,[121] M. Levchenko,[122] J. Levêque,[5] D. Levin,[88] L. J. Levinson,[173] M. Levy,[18] A. Lewis,[119] G. H. Lewis,[109] A. M. Leyko,[21] M. Leyton,[41] B. Li,[33b,v] B. Li,[84] H. Li,[149] H. L. Li,[31] L. Li,[45] L. Li,[33e] S. Li,[45] Y. Li,[33c,w] Z. Liang,[138] H. Liao,[34] B. Liberti,[134a] P. Lichard,[30] K. Lie,[166] J. Liebal,[21] W. Liebig,[14] C. Limbach,[21] A. Limosani,[87] S. C. Lin,[152,x] T. H. Lin,[82] F. Linde,[106] B. E. Lindquist,[149] J. T. Linnemann,[89] E. Lipeles,[121] A. Lipniacka,[14] M. Lisovyi,[42] T. M. Liss,[166] D. Lissauer,[25] A. Lister,[169] A. M. Litke,[138] B. Liu,[152] D. Liu,[152] J. B. Liu,[33b] K. Liu,[33b,y] L. Liu,[88] M. Liu,[45] M. Liu,[33b] Y. Liu,[33b] M. Livan,[120a,120b] S. S. A. Livermore,[119] A. Lleres,[55] J. Llorente Merino,[81] S. L. Lloyd,[75] F. Lo Sterzo,[152] E. Lobodzinska,[42] P. Loch,[7] W. S. Lockman,[138] T. Loddenkoetter,[21] F. K. Loebinger,[83] A. E. Loevschall-Jensen,[36] A. Loginov,[177] C. W. Loh,[169] T. Lohse,[16] K. Lohwasser,[42] M. Lokajicek,[126] V. P. Lombardo,[5] B. A. Long,[22] J. D. Long,[88] R. E. Long,[71] L. Lopes,[125a] D. Lopez Mateos,[57] B. Lopez Paredes,[140] I. Lopez Paz,[12] J. Lorenz,[99] N. Lorenzo Martinez,[60] M. Losada,[163] P. Loscutoff,[15] X. Lou,[41] A. Lounis,[116] J. Love,[6] P. A. Love,[71] A. J. Lowe,[144,f] F. Lu,[33a]

H. J. Lubatti,[139] C. Luci,[133a,133b] A. Lucotte,[55] F. Luehring,[60] W. Lukas,[61] L. Luminari,[133a] O. Lundberg,[147a,147b] B. Lund-Jensen,[148] M. Lungwitz,[82] D. Lynn,[25] R. Lysak,[126] E. Lytken,[80] H. Ma,[25] L. L. Ma,[33d] G. Maccarrone,[47] A. Macchiolo,[100] J. Machado Miguens,[125a,125b] D. Macina,[30] D. Madaffari,[84] R. Madar,[48] H. J. Maddocks,[71] W. F. Mader,[44] A. Madsen,[167] M. Maeno,[8] T. Maeno,[25] E. Magradze,[54] K. Mahboubi,[48] J. Mahlstedt,[106] S. Mahmoud,[73] C. Maiani,[137] C. Maidantchik,[24a] A. A. Maier,[100] A. Maio,[125a,125b,125d] S. Majewski,[115] Y. Makida,[65] N. Makovec,[116] P. Mal,[137,z] B. Malaescu,[79] Pa. Malecki,[39] V. P. Maleev,[122] F. Malek,[55] U. Mallik,[62] D. Malon,[6] C. Malone,[144] S. Maltezos,[10] V. M. Malyshev,[108] S. Malyukov,[30] J. Mamuzic,[13b] B. Mandelli,[30] L. Mandelli,[90a] I. Mandić,[74] R. Mandrysch,[62] J. Maneira,[125a,125b] A. Manfredini,[100] L. Manhaes de Andrade Filho,[24b] J. A. Manjarres Ramos,[160b] A. Mann,[99] P. M. Manning,[138] A. Manousakis-Katsikakis,[9] B. Mansoulie,[137] R. Mantifel,[86] L. Mapelli,[30] L. March,[168] J. F. Marchand,[29] G. Marchiori,[79] M. Marcisovsky,[126] C. P. Marino,[170] M. Marjanovic,[13a] C. N. Marques,[125a] F. Marroquim,[24a] S. P. Marsden,[83] Z. Marshall,[15] L. F. Marti,[17] S. Marti-Garcia,[168] B. Martin,[30] B. Martin,[89] T. A. Martin,[171] V. J. Martin,[46] B. Martin dit Latour,[14] H. Martinez,[137] M. Martinez,[12,o] S. Martin-Haugh,[130] A. C. Martyniuk,[77] M. Marx,[139] F. Marzano,[133a] A. Marzin,[30] L. Masetti,[82] T. Mashimo,[156] R. Mashinistov,[95] J. Masik,[83] A. L. Maslennikov,[108] I. Massa,[20a,20b] N. Massol,[5] P. Mastrandrea,[149] A. Mastroberardino,[37a,37b] T. Masubuchi,[156] P. Mättig,[176] J. Mattmann,[82] J. Maurer,[26a] S. J. Maxfield,[73] D. A. Maximov,[108,u] R. Mazini,[152] L. Mazzaferro,[134a,134b] G. Mc Goldrick,[159] S. P. Mc Kee,[88] A. McCarn,[88] R. L. McCarthy,[149] T. G. McCarthy,[29] N. A. McCubbin,[130] K. W. McFarlane,[56,a] J. A. Mcfayden,[77] G. Mchedlidze,[54] S. J. McMahon,[130] R. A. McPherson,[170,j] A. Meade,[85] J. Mechnich,[106] M. Medinnis,[42] S. Meehan,[31] S. Mehlhase,[99] A. Mehta,[73] K. Meier,[58a] C. Meineck,[99] B. Meirose,[80] C. Melachrinos,[31] B. R. Mellado Garcia,[146c] F. Meloni,[17] A. Mengarelli,[20a,20b] S. Menke,[100] E. Meoni,[162] K. M. Mercurio,[57] S. Mergelmeyer,[21] N. Meric,[137] P. Mermod,[49] L. Merola,[103a,103b] C. Meroni,[90a] F. S. Merritt,[31] H. Merritt,[110] A. Messina,[30,aa] J. Metcalfe,[25] A. S. Mete,[164] C. Meyer,[82] C. Meyer,[31] J-P. Meyer,[137] J. Meyer,[30] R. P. Middleton,[130] S. Migas,[73] L. Mijović,[21] G. Mikenberg,[173] M. Mikestikova,[126] M. Mikuž,[74] A. Milic,[30] D. W. Miller,[31] C. Mills,[46] A. Milov,[173] D. A. Milstead,[147a,147b] D. Milstein,[173] A. A. Minaenko,[129] I. A. Minashvili,[64] A. I. Mincer,[109] B. Mindur,[38a] M. Mineev,[64] Y. Ming,[174] L. M. Mir,[12] G. Mirabelli,[133a] T. Mitani,[172] J. Mitrevski,[99] V. A. Mitsou,[168] S. Mitsui,[65] A. Miucci,[49] P. S. Miyagawa,[140] J. U. Mjörnmark,[80] T. Moa,[147a,147b] K. Mochizuki,[84] S. Mohapatra,[35] W. Mohr,[48] S. Molander,[147a,147b] R. Moles-Valls,[168] K. Mönig,[42] C. Monini,[55] J. Monk,[36] E. Monnier,[84] J. Montejo Berlingen,[12] F. Monticelli,[70] S. Monzani,[133a,133b] R. W. Moore,[3] A. Moraes,[53] N. Morange,[62] D. Moreno,[82] M. Moreno Llácer,[54] P. Morettini,[50a] M. Morgenstern,[44] M. Morii,[57] S. Moritz,[82] A. K. Morley,[148] G. Mornacchi,[30] J. D. Morris,[75] L. Morvaj,[102] H. G. Moser,[100] M. Mosidze,[51b] J. Moss,[110] K. Motohashi,[158] R. Mount,[144] E. Mountricha,[25] S. V. Mouraviev,[95,a] E. J. W. Moyse,[85] S. Muanza,[84] R. D. Mudd,[18] F. Mueller,[58a] J. Mueller,[124] K. Mueller,[21] T. Mueller,[28] T. Mueller,[82] D. Muenstermann,[49] Y. Munwes,[154] J. A. Murillo Quijada,[18] W. J. Murray,[171,130] H. Musheghyan,[54] E. Musto,[153] A. G. Myagkov,[129,bb] M. Myska,[127] O. Nackenhorst,[54] J. Nadal,[54] K. Nagai,[61] R. Nagai,[158] Y. Nagai,[84] K. Nagano,[65] A. Nagarkar,[110] Y. Nagasaka,[59] M. Nagel,[100] A. M. Nairz,[30] Y. Nakahama,[30] K. Nakamura,[65] T. Nakamura,[156] I. Nakano,[111] H. Namasivayam,[41] G. Nanava,[21] R. Narayan,[58b] T. Nattermann,[21] T. Naumann,[42] G. Navarro,[163] R. Nayyar,[7] H. A. Neal,[88] P. Yu. Nechaeva,[95] T. J. Neep,[83] P. D. Nef,[144] A. Negri,[120a,120b] G. Negri,[30] M. Negrini,[20a] S. Nektarijevic,[49] A. Nelson,[164] T. K. Nelson,[144] S. Nemecek,[126] P. Nemethy,[109] A. A. Nepomuceno,[24a] M. Nessi,[30,cc] M. S. Neubauer,[166] M. Neumann,[176] R. M. Neves,[109] P. Nevski,[25] P. R. Newman,[18] D. H. Nguyen,[6] R. B. Nickerson,[119] R. Nicolaidou,[137] B. Nicquevert,[30] J. Nielsen,[138] N. Nikiforou,[35] A. Nikiforov,[16] V. Nikolaenko,[129,bb] I. Nikolic-Audit,[79] K. Nikolics,[49] K. Nikolopoulos,[18] P. Nilsson,[8] Y. Ninomiya,[156] A. Nisati,[133a] R. Nisius,[100] T. Nobe,[158] L. Nodulman,[6] M. Nomachi,[117] I. Nomidis,[155] S. Norberg,[112] M. Nordberg,[30] O. Novgorodova,[44] S. Nowak,[100] M. Nozaki,[65] L. Nozka,[114] K. Ntekas,[10] G. Nunes Hanninger,[87] T. Nunnemann,[99] E. Nurse,[77] F. Nuti,[87] B. J. O'Brien,[46] F. O'grady,[7] D. C. O'Neil,[143] V. O'Shea,[53] F. G. Oakham,[29,e] H. Oberlack,[100] T. Obermann,[21] J. Ocariz,[79] A. Ochi,[66] M. I. Ochoa,[77] S. Oda,[69] S. Odaka,[65] H. Ogren,[60] A. Oh,[83] S. H. Oh,[45] C. C. Ohm,[30] H. Ohman,[167] T. Ohshima,[102] W. Okamura,[117] H. Okawa,[25] Y. Okumura,[31] T. Okuyama,[156] A. Olariu,[26a] A. G. Olchevski,[64] S. A. Olivares Pino,[46] D. Oliveira Damazio,[25] E. Oliver Garcia,[168] A. Olszewski,[39] J. Olszowska,[39] A. Onofre,[125a,125e] P. U. E. Onyisi,[31,p] C. J. Oram,[160a] M. J. Oreglia,[31] Y. Oren,[154] D. Orestano,[135a,135b] N. Orlando,[72a,72b] C. Oropeza Barrera,[53] R. S. Orr,[159] B. Osculati,[50a,50b] R. Ospanov,[121] G. Otero y Garzon,[27] H. Otono,[69] M. Ouchrif,[136d] E. A. Ouellette,[170] F. Ould-Saada,[118] A. Ouraou,[137] K. P. Oussoren,[106] Q. Ouyang,[33a] A. Ovcharova,[15] M. Owen,[83] V. E. Ozcan,[19a] N. Ozturk,[8] K. Pachal,[119] A. Pacheco Pages,[12] C. Padilla Aranda,[12] M. Pagáčová,[48] S. Pagan Griso,[15] E. Paganis,[140] C. Pahl,[100] F. Paige,[25] P. Pais,[85] K. Pajchel,[118] G. Palacino,[160b] S. Palestini,[30] M. Palka,[38b] D. Pallin,[34] A. Palma,[125a,125b] J. D. Palmer,[18] Y. B. Pan,[174] E. Panagiotopoulou,[10]

J. G. Panduro Vazquez,[76] P. Pani,[106] N. Panikashvili,[88] S. Panitkin,[25] D. Pantea,[26a] L. Paolozzi,[134a,134b] Th. D. Papadopoulou,[10] K. Papageorgiou,[155,m] A. Paramonov,[6] D. Paredes Hernandez,[34] M. A. Parker,[28] F. Parodi,[50a,50b] J. A. Parsons,[35] U. Parzefall,[48] E. Pasqualucci,[133a] S. Passaggio,[50a] A. Passeri,[135a] F. Pastore,[135a,135b,a] Fr. Pastore,[76] G. Pásztor,[29] S. Pataraia,[176] N. D. Patel,[151] J. R. Pater,[83] S. Patricelli,[103a,103b] T. Pauly,[30] J. Pearce,[170] M. Pedersen,[118] S. Pedraza Lopez,[168] R. Pedro,[125a,125b] S. V. Peleganchuk,[108] D. Pelikan,[167] H. Peng,[33b] B. Penning,[31] J. Penwell,[60] D. V. Perepelitsa,[25] E. Perez Codina,[160a] M. T. Pérez García-Estañ,[168] V. Perez Reale,[35] L. Perini,[90a,90b] H. Pernegger,[30] R. Perrino,[72a] R. Peschke,[42] V. D. Peshekhonov,[64] K. Peters,[30] R. F. Y. Peters,[83] B. A. Petersen,[30] T. C. Petersen,[36] E. Petit,[42] A. Petridis,[147a,147b] C. Petridou,[155] E. Petrolo,[133a] F. Petrucci,[135a,135b] N. E. Pettersson,[158] R. Pezoa,[32b] P. W. Phillips,[130] G. Piacquadio,[144] E. Pianori,[171] A. Picazio,[49] E. Piccaro,[75] M. Piccinini,[20a,20b] R. Piegaia,[27] D. T. Pignotti,[110] J. E. Pilcher,[31] A. D. Pilkington,[77] J. Pina,[125a,125b,125d] M. Pinamonti,[165a,165c,dd] A. Pinder,[119] J. L. Pinfold,[3] A. Pingel,[36] B. Pinto,[125a] S. Pires,[79] M. Pitt,[173] C. Pizio,[90a,90b] L. Plazak,[145a] M.-A. Pleier,[25] V. Pleskot,[128] E. Plotnikova,[64] P. Plucinski,[147a,147b] S. Poddar,[58a] F. Podlyski,[34] R. Poettgen,[82] L. Poggioli,[116] D. Pohl,[21] M. Pohl,[49] G. Polesello,[120a] A. Policicchio,[37a,37b] R. Polifka,[159] A. Polini,[20a] C. S. Pollard,[45] V. Polychronakos,[25] K. Pommès,[30] L. Pontecorvo,[133a] B. G. Pope,[89] G. A. Popeneciu,[26b] D. S. Popovic,[13a] A. Poppleton,[30] X. Portell Bueso,[12] S. Pospisil,[127] K. Potamianos,[15] I. N. Potrap,[64] C. J. Potter,[150] C. T. Potter,[115] G. Poulard,[30] J. Poveda,[60] V. Pozdnyakov,[64] P. Pralavorio,[84] A. Pranko,[15] S. Prasad,[30] R. Pravahan,[8] S. Prell,[63] D. Price,[83] J. Price,[73] L. E. Price,[6] D. Prieur,[124] M. Primavera,[72a] M. Proissl,[46] K. Prokofiev,[47] F. Prokoshin,[32b] E. Protopapadaki,[137] S. Protopopescu,[25] J. Proudfoot,[6] M. Przybycien,[38a] H. Przysiezniak,[5] E. Ptacek,[115] D. Puddu,[135a,135b] E. Pueschel,[85] D. Puldon,[149] M. Purohit,[25,ee] P. Puzo,[116] J. Qian,[88] G. Qin,[53] Y. Qin,[83] A. Quadt,[54] D. R. Quarrie,[15] W. B. Quayle,[165a,165b] M. Queitsch-Maitland,[83] D. Quilty,[53] A. Qureshi,[160b] V. Radeka,[25] V. Radescu,[42] S. K. Radhakrishnan,[149] P. Radloff,[115] P. Rados,[87] F. Ragusa,[90a,90b] G. Rahal,[179] S. Rajagopalan,[25] M. Rammensee,[30] A. S. Randle-Conde,[40] C. Rangel-Smith,[167] K. Rao,[164] F. Rauscher,[99] T. C. Rave,[48] T. Ravenscroft,[53] M. Raymond,[30] A. L. Read,[118] N. P. Readioff,[73] D. M. Rebuzzi,[120a,120b] A. Redelbach,[175] G. Redlinger,[25] R. Reece,[138] K. Reeves,[41] L. Rehnisch,[16] H. Reisin,[27] M. Relich,[164] C. Rembser,[30] H. Ren,[33a] Z. L. Ren,[152] A. Renaud,[116] M. Rescigno,[133a] S. Resconi,[90a] O. L. Rezanova,[108,u] P. Reznicek,[128] R. Rezvani,[94] R. Richter,[100] M. Ridel,[79] P. Rieck,[16] J. Rieger,[54] M. Rijssenbeek,[149] A. Rimoldi,[120a,120b] L. Rinaldi,[20a] E. Ritsch,[61] I. Riu,[12] F. Rizatdinova,[113] E. Rizvi,[75] S. H. Robertson,[86,j] A. Robichaud-Veronneau,[86] D. Robinson,[28] J. E. M. Robinson,[83] A. Robson,[53] C. Roda,[123a,123b] L. Rodrigues,[30] S. Roe,[30] O. Røhne,[118] S. Rolli,[162] A. Romaniouk,[97] M. Romano,[20a,20b] E. Romero Adam,[168] N. Rompotis,[139] L. Roos,[79] E. Ros,[168] S. Rosati,[133a] K. Rosbach,[49] M. Rose,[76] P. L. Rosendahl,[14] O. Rosenthal,[142] V. Rossetti,[147a,147b] E. Rossi,[103a,103b] L. P. Rossi,[50a] R. Rosten,[139] M. Rotaru,[26a] I. Roth,[173] J. Rothberg,[139] D. Rousseau,[116] C. R. Royon,[137] A. Rozanov,[84] Y. Rozen,[153] X. Ruan,[146c] F. Rubbo,[12] I. Rubinskiy,[42] V. I. Rud,[98] C. Rudolph,[44] M. S. Rudolph,[159] F. Rühr,[48] A. Ruiz-Martinez,[30] Z. Rurikova,[48] N. A. Rusakovich,[64] A. Ruschke,[99] J. P. Rutherfoord,[7] N. Ruthmann,[48] Y. F. Ryabov,[122] M. Rybar,[128] G. Rybkin,[116] N. C. Ryder,[119] A. F. Saavedra,[151] S. Sacerdoti,[27] A. Saddique,[3] I. Sadeh,[154] H. F-W. Sadrozinski,[138] R. Sadykov,[64] F. Safai Tehrani,[133a] H. Sakamoto,[156] Y. Sakurai,[172] G. Salamanna,[135a,135b] A. Salamon,[134a] M. Saleem,[112] D. Salek,[106] P. H. Sales De Bruin,[139] D. Salihagic,[100] A. Salnikov,[144] J. Salt,[168] B. M. Salvachua Ferrando,[6] D. Salvatore,[37a,37b] F. Salvatore,[150] A. Salvucci,[105] A. Salzburger,[30] D. Sampsonidis,[155] A. Sanchez,[103a,103b] J. Sánchez,[168] V. Sanchez Martinez,[168] H. Sandaker,[14] R. L. Sandbach,[75] H. G. Sander,[82] M. P. Sanders,[99] M. Sandhoff,[176] T. Sandoval,[28] C. Sandoval,[163] R. Sandstroem,[100] D. P. C. Sankey,[130] A. Sansoni,[47] C. Santoni,[34] R. Santonico,[134a,134b] H. Santos,[125a] I. Santoyo Castillo,[150] K. Sapp,[124] A. Sapronov,[64] J. G. Saraiva,[125a,125d] B. Sarrazin,[21] G. Sartisohn,[176] O. Sasaki,[65] Y. Sasaki,[156] G. Sauvage,[5,a] E. Sauvan,[5] P. Savard,[159,e] D. O. Savu,[30] C. Sawyer,[119] L. Sawyer,[78,n] D. H. Saxon,[53] J. Saxon,[121] C. Sbarra,[20a] A. Sbrizzi,[3] T. Scanlon,[77] D. A. Scannicchio,[164] M. Scarcella,[151] V. Scarfone,[37a,37b] J. Schaarschmidt,[173] P. Schacht,[100] D. Schaefer,[121] R. Schaefer,[42] S. Schaepe,[21] S. Schaetzel,[58b] U. Schäfer,[82] A. C. Schaffer,[116] D. Schaile,[99] R. D. Schamberger,[149] V. Scharf,[58a] V. A. Schegelsky,[122] D. Scheirich,[128] M. Schernau,[164] M. I. Scherzer,[35] C. Schiavi,[50a,50b] J. Schieck,[99] C. Schillo,[48] M. Schioppa,[37a,37b] S. Schlenker,[30] E. Schmidt,[48] K. Schmieden,[30] C. Schmitt,[82] C. Schmitt,[99] S. Schmitt,[58b] B. Schneider,[17] Y. J. Schnellbach,[73] U. Schnoor,[44] L. Schoeffel,[137] A. Schoening,[58b] B. D. Schoenrock,[89] A. L. S. Schorlemmer,[54] M. Schott,[82] D. Schouten,[160a] J. Schovancova,[25] S. Schramm,[159] M. Schreyer,[175] C. Schroeder,[82] N. Schuh,[82] M. J. Schultens,[21] H.-C. Schultz-Coulon,[58a] H. Schulz,[16] M. Schumacher,[48] B. A. Schumm,[138] Ph. Schune,[137] C. Schwanenberger,[83] A. Schwartzman,[144] Ph. Schwegler,[100] Ph. Schwemling,[137] R. Schwienhorst,[89] J. Schwindling,[137] T. Schwindt,[21] M. Schwoerer,[5] F. G. Sciacca,[17] E. Scifo,[116] G. Sciolla,[23] W. G. Scott,[130] F. Scuri,[123a,123b] F. Scutti,[21] J. Searcy,[88] G. Sedov,[42] E. Sedykh,[122] S. C. Seidel,[104]

A. Seiden,[138] F. Seifert,[127] J. M. Seixas,[24a] G. Sekhniaidze,[103a] S. J. Sekula,[40] K. E. Selbach,[46] D. M. Seliverstov,[122,a] G. Sellers,[73] N. Semprini-Cesari,[20a,20b] C. Serfon,[30] L. Serin,[116] L. Serkin,[54] T. Serre,[84] R. Seuster,[160a] H. Severini,[112] T. Sfiligoj,[74] F. Sforza,[100] A. Sfyrla,[30] E. Shabalina,[54] M. Shamim,[115] L. Y. Shan,[33a] R. Shang,[166] J. T. Shank,[22] M. Shapiro,[15] P. B. Shatalov,[96] K. Shaw,[165a,165b] C. Y. Shehu,[150] P. Sherwood,[77] L. Shi,[152,ff] S. Shimizu,[66] C. O. Shimmin,[164] M. Shimojima,[101] M. Shiyakova,[64] A. Shmeleva,[95] M. J. Shochet,[31] D. Short,[119] S. Shrestha,[63] E. Shulga,[97] M. A. Shupe,[7] S. Shushkevich,[42] P. Sicho,[126] O. Sidiropoulou,[155] D. Sidorov,[113] A. Sidoti,[133a] F. Siegert,[44] Dj. Sijacki,[13a] J. Silva,[125a,125d] Y. Silver,[154] D. Silverstein,[144] S. B. Silverstein,[147a] V. Simak,[127] O. Simard,[5] Lj. Simic,[13a] S. Simion,[116] E. Simioni,[82] B. Simmons,[77] R. Simoniello,[90a,90b] M. Simonyan,[36] P. Sinervo,[159] N. B. Sinev,[115] V. Sipica,[142] G. Siragusa,[175] A. Sircar,[78] A. N. Sisakyan,[64,a] S. Yu. Sivoklokov,[98] J. Sjölin,[147a,147b] T. B. Sjursen,[14] H. P. Skottowe,[57] K. Yu. Skovpen,[108] P. Skubic,[112] M. Slater,[18] T. Slavicek,[127] K. Sliwa,[162] V. Smakhtin,[173] B. H. Smart,[46] L. Smestad,[14] S. Yu. Smirnov,[97] Y. Smirnov,[97] L. N. Smirnova,[98,gg] O. Smirnova,[80] K. M. Smith,[53] M. Smizanska,[71] K. Smolek,[127] A. A. Snesarev,[95] G. Snidero,[75] S. Snyder,[25] R. Sobie,[170,j] F. Socher,[44] A. Soffer,[154] D. A. Soh,[152,ff] C. A. Solans,[30] M. Solar,[127] J. Solc,[127] E. Yu. Soldatov,[97] U. Soldevila,[168] E. Solfaroli Camillocci,[133a,133b] A. A. Solodkov,[129] A. Soloshenko,[64] O. V. Solovyanov,[129] V. Solovyev,[122] P. Sommer,[48] H. Y. Song,[33b] N. Soni,[1] A. Sood,[15] A. Sopczak,[127] B. Sopko,[127] V. Sopko,[127] V. Sorin,[12] M. Sosebee,[8] R. Soualah,[165a,165c] P. Soueid,[94] A. M. Soukharev,[108] D. South,[42] S. Spagnolo,[72a,72b] F. Spanò,[76] W. R. Spearman,[57] F. Spettel,[100] R. Spighi,[20a] G. Spigo,[30] M. Spousta,[128] T. Spreitzer,[159] B. Spurlock,[8] R. D. St. Denis,[53,a] S. Staerz,[44] J. Stahlman,[121] R. Stamen,[58a] E. Stanecka,[39] R. W. Stanek,[6] C. Stanescu,[135a] M. Stanescu-Bellu,[42] M. M. Stanitzki,[42] S. Stapnes,[118] E. A. Starchenko,[129] J. Stark,[55] P. Staroba,[126] P. Starovoitov,[42] R. Staszewski,[39] P. Stavina,[145a,a] P. Steinberg,[25] B. Stelzer,[143] H. J. Stelzer,[30] O. Stelzer-Chilton,[160a] H. Stenzel,[52] S. Stern,[100] G. A. Stewart,[53] J. A. Stillings,[21] M. C. Stockton,[86] M. Stoebe,[86] G. Stoicea,[26a] P. Stolte,[54] S. Stonjek,[100] A. R. Stradling,[8] A. Straessner,[44] M. E. Stramaglia,[17] J. Strandberg,[148] S. Strandberg,[147a,147b] A. Strandlie,[118] E. Strauss,[144] M. Strauss,[112] P. Strizenec,[145b] R. Ströhmer,[175] D. M. Strom,[115] R. Stroynowski,[40] S. A. Stucci,[17] B. Stugu,[14] N. A. Styles,[42] D. Su,[144] J. Su,[124] HS. Subramania,[3] R. Subramaniam,[78] A. Succurro,[12] Y. Sugaya,[117] C. Suhr,[107] M. Suk,[127] V. V. Sulin,[95] S. Sultansoy,[4c] T. Sumida,[67] X. Sun,[33a] J. E. Sundermann,[48] K. Suruliz,[140] G. Susinno,[37a,37b] M. R. Sutton,[150] Y. Suzuki,[65] M. Svatos,[126] S. Swedish,[169] M. Swiatlowski,[144] I. Sykora,[145a] T. Sykora,[128] D. Ta,[89] C. Taccini,[135a,135b] K. Tackmann,[42] J. Taenzer,[159] A. Taffard,[164] R. Tafirout,[160a] N. Taiblum,[154] Y. Takahashi,[102] H. Takai,[25] R. Takashima,[68] H. Takeda,[66] T. Takeshita,[141] Y. Takubo,[65] M. Talby,[84] A. A. Talyshev,[108,u] J. Y. C. Tam,[175] K. G. Tan,[87] J. Tanaka,[156] R. Tanaka,[116] S. Tanaka,[132] S. Tanaka,[65] A. J. Tanasijczuk,[143] B. B. Tannenwald,[110] N. Tannoury,[21] S. Tapprogge,[82] S. Tarem,[153] F. Tarrade,[29] G. F. Tartarelli,[90a] P. Tas,[128] M. Tasevsky,[126] T. Tashiro,[67] E. Tassi,[37a,37b] A. Tavares Delgado,[125a,125b] Y. Tayalati,[136d] F. E. Taylor,[93] G. N. Taylor,[87] W. Taylor,[160b] F. A. Teischinger,[30] M. Teixeira Dias Castanheira,[75] P. Teixeira-Dias,[76] K. K. Temming,[48] H. Ten Kate,[30] P. K. Teng,[152] J. J. Teoh,[117] S. Terada,[65] K. Terashi,[156] J. Terron,[81] S. Terzo,[100] M. Testa,[47] R. J. Teuscher,[159,j] J. Therhaag,[21] T. Theveneaux-Pelzer,[34] J. P. Thomas,[18] J. Thomas-Wilsker,[76] E. N. Thompson,[35] P. D. Thompson,[18] P. D. Thompson,[159] A. S. Thompson,[53] L. A. Thomsen,[36] E. Thomson,[121] M. Thomson,[28] W. M. Thong,[87] R. P. Thun,[88,a] F. Tian,[35] M. J. Tibbetts,[15] V. O. Tikhomirov,[95,hh] Yu. A. Tikhonov,[108,u] S. Timoshenko,[97] E. Tiouchichine,[84] P. Tipton,[177] S. Tisserant,[84] T. Todorov,[5] S. Todorova-Nova,[128] B. Toggerson,[7] J. Tojo,[69] S. Tokár,[145a] K. Tokushuku,[65] K. Tollefson,[89] L. Tomlinson,[83] M. Tomoto,[102] L. Tompkins,[31] K. Toms,[104] N. D. Topilin,[64] E. Torrence,[115] H. Torres,[143] E. Torró Pastor,[168] J. Toth,[84,ii] F. Touchard,[84] D. R. Tovey,[140] H. L. Tran,[116] T. Trefzger,[175] L. Tremblet,[30] A. Tricoli,[30] I. M. Trigger,[160a] S. Trincaz-Duvoid,[79] M. F. Tripiana,[12] N. Triplett,[25] W. Trischuk,[159] B. Trocmé,[55] C. Troncon,[90a] M. Trottier-McDonald,[143] M. Trovatelli,[135a,135b] P. True,[89] M. Trzebinski,[39] A. Trzupek,[39] C. Tsarouchas,[30] J. C-L. Tseng,[119] P. V. Tsiareshka,[91] D. Tsionou,[137] G. Tsipolitis,[10] N. Tsirintanis,[9] S. Tsiskaridze,[12] V. Tsiskaridze,[48] E. G. Tskhadadze,[51a] I. I. Tsukerman,[96] V. Tsulaia,[15] S. Tsuno,[65] D. Tsybychev,[149] A. Tudorache,[26a] V. Tudorache,[26a] A. N. Tuna,[121] S. A. Tupputi,[20a,20b] S. Turchikhin,[98,gg] D. Turecek,[127] I. Turk Cakir,[4d] R. Turra,[90a,90b] P. M. Tuts,[35] A. Tykhonov,[49] M. Tylmad,[147a,147b] M. Tyndel,[130] K. Uchida,[21] I. Ueda,[156] R. Ueno,[29] M. Ughetto,[84] M. Ugland,[14] M. Uhlenbrock,[21] F. Ukegawa,[161] G. Unal,[30] A. Undrus,[25] G. Unel,[164] F. C. Ungaro,[48] Y. Unno,[65] D. Urbaniec,[35] P. Urquijo,[87] G. Usai,[8] A. Usanova,[61] L. Vacavant,[84] V. Vacek,[127] B. Vachon,[86] N. Valencic,[106] S. Valentinetti,[20a,20b] A. Valero,[168] L. Valery,[34] S. Valkar,[128] E. Valladolid Gallego,[168] S. Vallecorsa,[49] J. A. Valls Ferrer,[168] W. Van Den Wollenberg,[106] P. C. Van Der Deijl,[106] R. van der Geer,[106] H. van der Graaf,[106] R. Van Der Leeuw,[106] D. van der Ster,[30] N. van Eldik,[30] P. van Gemmeren,[6] J. Van Nieuwkoop,[143] I. van Vulpen,[106] M. C. van Woerden,[30] M. Vanadia,[133a,133b] W. Vandelli,[30] R. Vanguri,[121] A. Vaniachine,[6] P. Vankov,[42] F. Vannucci,[79] G. Vardanyan,[178] R. Vari,[133a] E. W. Varnes,[7] T. Varol,[85] D. Varouchas,[79]

A. Vartapetian,[8] K. E. Varvell,[151] F. Vazeille,[34] T. Vazquez Schroeder,[54] J. Veatch,[7] F. Veloso,[125a,125c] S. Veneziano,[133a] A. Ventura,[72a,72b] D. Ventura,[85] M. Venturi,[170] N. Venturi,[159] A. Venturini,[23] V. Vercesi,[120a] M. Verducci,[133a,133b] W. Verkerke,[106] J. C. Vermeulen,[106] A. Vest,[44] M. C. Vetterli,[143,e] O. Viazlo,[80] I. Vichou,[166] T. Vickey,[146c,jj] O. E. Vickey Boeriu,[146c] G. H. A. Viehhauser,[119] S. Viel,[169] R. Vigne,[30] M. Villa,[20a,20b] M. Villaplana Perez,[90a,90b] E. Vilucchi,[47] M. G. Vincter,[29] V. B. Vinogradov,[64] J. Virzi,[15] I. Vivarelli,[150] F. Vives Vaque,[3] S. Vlachos,[10] D. Vladoiu,[99] M. Vlasak,[127] A. Vogel,[21] M. Vogel,[32a] P. Vokac,[127] G. Volpi,[123a,123b] M. Volpi,[87] H. von der Schmitt,[100] H. von Radziewski,[48] E. von Toerne,[21] V. Vorobel,[128] K. Vorobev,[97] M. Vos,[168] R. Voss,[30] J. H. Vossebeld,[73] N. Vranjes,[137] M. Vranjes Milosavljevic,[106] V. Vrba,[126] M. Vreeswijk,[106] T. Vu Anh,[48] R. Vuillermet,[30] I. Vukotic,[31] Z. Vykydal,[127] P. Wagner,[21] W. Wagner,[176] H. Wahlberg,[70] S. Wahrmund,[44] J. Wakabayashi,[102] J. Walder,[71] R. Walker,[99] W. Walkowiak,[142] R. Wall,[177] P. Waller,[73] B. Walsh,[177] C. Wang,[152,kk] C. Wang,[45] F. Wang,[174] H. Wang,[15] H. Wang,[40] J. Wang,[42] J. Wang,[33a] K. Wang,[86] R. Wang,[104] S. M. Wang,[152] T. Wang,[21] X. Wang,[177] C. Wanotayaroj,[115] A. Warburton,[86] C. P. Ward,[28] D. R. Wardrope,[77] M. Warsinsky,[48] A. Washbrook,[46] C. Wasicki,[42] P. M. Watkins,[18] A. T. Watson,[18] I. J. Watson,[151] M. F. Watson,[18] G. Watts,[139] S. Watts,[83] B. M. Waugh,[77] S. Webb,[83] M. S. Weber,[17] S. W. Weber,[175] J. S. Webster,[31] A. R. Weidberg,[119] P. Weigell,[100] B. Weinert,[60] J. Weingarten,[54] C. Weiser,[48] H. Weits,[106] P. S. Wells,[30] T. Wenaus,[25] D. Wendland,[16] Z. Weng,[152,ff] T. Wengler,[30] S. Wenig,[30] N. Wermes,[21] M. Werner,[48] P. Werner,[30] M. Wessels,[58a] J. Wetter,[162] K. Whalen,[29] A. White,[8] M. J. White,[1] R. White,[32b] S. White,[123a,123b] D. Whiteson,[164] D. Wicke,[176] F. J. Wickens,[130] W. Wiedenmann,[174] M. Wielers,[130] P. Wienemann,[21] C. Wiglesworth,[36] L. A. M. Wiik-Fuchs,[21] P. A. Wijeratne,[77] A. Wildauer,[100] M. A. Wildt,[42,ll] H. G. Wilkens,[30] J. Z. Will,[99] H. H. Williams,[121] S. Williams,[28] C. Willis,[89] S. Willocq,[85] A. Wilson,[88] J. A. Wilson,[18] I. Wingerter-Seez,[5] F. Winklmeier,[115] B. T. Winter,[21] M. Wittgen,[144] T. Wittig,[43] J. Wittkowski,[99] S. J. Wollstadt,[82] M. W. Wolter,[39] H. Wolters,[125a,125c] B. K. Wosiek,[39] J. Wotschack,[30] M. J. Woudstra,[83] K. W. Wozniak,[39] M. Wright,[53] M. Wu,[55] S. L. Wu,[174] X. Wu,[49] Y. Wu,[88] E. Wulf,[35] T. R. Wyatt,[83] B. M. Wynne,[46] S. Xella,[36] M. Xiao,[137] D. Xu,[33a] L. Xu,[33b,mm] B. Yabsley,[151] S. Yacoob,[146b,nn] M. Yamada,[65] H. Yamaguchi,[156] Y. Yamaguchi,[117] A. Yamamoto,[65] K. Yamamoto,[63] S. Yamamoto,[156] T. Yamamura,[156] T. Yamanaka,[156] K. Yamauchi,[102] Y. Yamazaki,[66] Z. Yan,[22] H. Yang,[33e] H. Yang,[174] U. K. Yang,[83] Y. Yang,[110] S. Yanush,[92] L. Yao,[33a] W-M. Yao,[15] Y. Yasu,[65] E. Yatsenko,[42] K. H. Yau Wong,[21] J. Ye,[40] S. Ye,[25] A. L. Yen,[57] E. Yildirim,[42] M. Yilmaz,[4b] R. Yoosoofmiya,[124] K. Yorita,[172] R. Yoshida,[6] K. Yoshihara,[156] C. Young,[144] C. J. S. Young,[30] S. Youssef,[22] D. R. Yu,[15] J. Yu,[8] J. M. Yu,[88] J. Yu,[113] L. Yuan,[66] A. Yurkewicz,[107] I. Yusuff,[28,oo] B. Zabinski,[39] R. Zaidan,[62] A. M. Zaitsev,[129,bb] A. Zaman,[149] S. Zambito,[23] L. Zanello,[133a,133b] D. Zanzi,[100] C. Zeitnitz,[176] M. Zeman,[127] A. Zemla,[38a] K. Zengel,[23] O. Zenin,[129] T. Ženiš,[145a] D. Zerwas,[116] G. Zevi della Porta,[57] D. Zhang,[88] F. Zhang,[174] H. Zhang,[89] J. Zhang,[6] L. Zhang,[152] X. Zhang,[33d] Z. Zhang,[116] Z. Zhao,[33b] A. Zhemchugov,[64] J. Zhong,[119] B. Zhou,[88] L. Zhou,[35] N. Zhou,[164] C. G. Zhu,[33d] H. Zhu,[33a] J. Zhu,[88] Y. Zhu,[33b] X. Zhuang,[33a] K. Zhukov,[95] A. Zibell,[175] D. Zieminska,[60] N. I. Zimine,[64] C. Zimmermann,[82] R. Zimmermann,[21] S. Zimmermann,[21] S. Zimmermann,[48] Z. Zinonos,[54] M. Ziolkowski,[142] G. Zobernig,[174] A. Zoccoli,[20a,20b] M. zur Nedden,[16] G. Zurzolo,[103a,103b] V. Zutshi,[107] and L. Zwalinski[30]

(ATLAS Collaboration)

[1]*Department of Physics, University of Adelaide, Adelaide, Australia*
[2]*Physics Department, SUNY Albany, Albany, New York, USA*
[3]*Department of Physics, University of Alberta, Edmonton, AB, Canada*
[4a]*Department of Physics, Ankara University, Ankara, Turkey*
[4b]*Department of Physics, Gazi University, Ankara, Turkey*
[4c]*Division of Physics, TOBB University of Economics and Technology, Ankara, Turkey*
[4d]*Turkish Atomic Energy Authority, Ankara, Turkey*
[5]*LAPP, CNRS/IN2P3 and Université de Savoie, Annecy-le-Vieux, France*
[6]*High Energy Physics Division, Argonne National Laboratory, Argonne, Illinois, USA*
[7]*Department of Physics, University of Arizona, Tucson, Arizona, USA*
[8]*Department of Physics, The University of Texas at Arlington, Arlington, Texas, USA*
[9]*Physics Department, University of Athens, Athens, Greece*
[10]*Physics Department, National Technical University of Athens, Zografou, Greece*
[11]*Institute of Physics, Azerbaijan Academy of Sciences, Baku, Azerbaijan*
[12]*Institut de Física d'Altes Energies and Departament de Física de la Universitat Autònoma de Barcelona, Barcelona, Spain*

[13a]*Institute of Physics, University of Belgrade, Belgrade, Serbia*
[13b]*Vinca Institute of Nuclear Sciences, University of Belgrade, Belgrade, Serbia*
[14]*Department for Physics and Technology, University of Bergen, Bergen, Norway*
[15]*Physics Division, Lawrence Berkeley National Laboratory and University of California, Berkeley, California, USA*
[16]*Department of Physics, Humboldt University, Berlin, Germany*
[17]*Albert Einstein Center for Fundamental Physics and Laboratory for High Energy Physics, University of Bern, Bern, Switzerland*
[18]*School of Physics and Astronomy, University of Birmingham, Birmingham, United Kingdom*
[19a]*Department of Physics, Bogazici University, Istanbul, Turkey*
[19b]*Department of Physics, Dogus University, Istanbul, Turkey*
[19c]*Department of Physics Engineering, Gaziantep University, Gaziantep, Turkey*
[20a]*INFN Sezione di Bologna, Italy*
[20b]*Dipartimento di Fisica e Astronomia, Università di Bologna, Bologna, Italy*
[21]*Physikalisches Institut, University of Bonn, Bonn, Germany*
[22]*Department of Physics, Boston University, Boston, Massachusetts, USA*
[23]*Department of Physics, Brandeis University, Waltham, Massachusetts, USA*
[24a]*Universidade Federal do Rio De Janeiro COPPE/EE/IF, Rio de Janeiro, Brazil*
[24b]*Federal University of Juiz de Fora (UFJF), Juiz de Fora, Brazil*
[24c]*Federal University of Sao Joao del Rei (UFSJ), Sao Joao del Rei, Brazil*
[24d]*Instituto de Fisica, Universidade de Sao Paulo, Sao Paulo, Brazil*
[25]*Physics Department, Brookhaven National Laboratory, Upton, New York, USA*
[26a]*National Institute of Physics and Nuclear Engineering, Bucharest, Romania*
[26b]*National Institute for Research and Development of Isotopic and Molecular Technologies, Physics Department, Cluj Napoca, Romania*
[26c]*University Politehnica Bucharest, Bucharest, Romania*
[26d]*West University in Timisoara, Timisoara, Romania*
[27]*Departamento de Física, Universidad de Buenos Aires, Buenos Aires, Argentina*
[28]*Cavendish Laboratory, University of Cambridge, Cambridge, United Kingdom*
[29]*Department of Physics, Carleton University, Ottawa, ON, Canada*
[30]*CERN, Geneva, Switzerland*
[31]*Enrico Fermi Institute, University of Chicago, Chicago, Illinois, USA*
[32a]*Departamento de Física, Pontificia Universidad Católica de Chile, Santiago, Chile*
[32b]*Departamento de Física, Universidad Técnica Federico Santa María, Valparaíso, Chile*
[33a]*Institute of High Energy Physics, Chinese Academy of Sciences, Beijing, China*
[33b]*Department of Modern Physics, University of Science and Technology of China, Anhui, China*
[33c]*Department of Physics, Nanjing University, Jiangsu, China*
[33d]*School of Physics, Shandong University, Shandong, China*
[33e]*Physics Department, Shanghai Jiao Tong University, Shanghai, China*
[34]*Laboratoire de Physique Corpusculaire, Clermont Université and Université Blaise Pascal and CNRS/IN2P3, Clermont-Ferrand, France*
[35]*Nevis Laboratory, Columbia University, Irvington, New York, USA*
[36]*Niels Bohr Institute, University of Copenhagen, Kobenhavn, Denmark*
[37a]*INFN Gruppo Collegato di Cosenza, Laboratori Nazionali di Frascati, Italy*
[37b]*Dipartimento di Fisica, Università della Calabria, Rende, Italy*
[38a]*AGH University of Science and Technology, Faculty of Physics and Applied Computer Science, Krakow, Poland*
[38b]*Marian Smoluchowski Institute of Physics, Jagiellonian University, Krakow, Poland*
[39]*The Henryk Niewodniczanski Institute of Nuclear Physics, Polish Academy of Sciences, Krakow, Poland*
[40]*Physics Department, Southern Methodist University, Dallas, Texas, USA*
[41]*Physics Department, University of Texas at Dallas, Richardson, Texas, USA*
[42]*DESY, Hamburg and Zeuthen, Germany*
[43]*Institut für Experimentelle Physik IV, Technische Universität Dortmund, Dortmund, Germany*
[44]*Institut für Kern- und Teilchenphysik, Technische Universität Dresden, Dresden, Germany*
[45]*Department of Physics, Duke University, Durham, North Carolina, USA*
[46]*SUPA - School of Physics and Astronomy, University of Edinburgh, Edinburgh, United Kingdom*
[47]*INFN Laboratori Nazionali di Frascati, Frascati, Italy*
[48]*Fakultät für Mathematik und Physik, Albert-Ludwigs-Universität, Freiburg, Germany*
[49]*Section de Physique, Université de Genève, Geneva, Switzerland*
[50a]*INFN Sezione di Genova, Italy*

[50b]Dipartimento di Fisica, Università di Genova, Genova, Italy
[51a]E. Andronikashvili Institute of Physics, Iv. Javakhishvili Tbilisi State University, Tbilisi, Georgia
[51b]High Energy Physics Institute, Tbilisi State University, Tbilisi, Georgia
[52]II Physikalisches Institut, Justus-Liebig-Universität Giessen, Giessen, Germany
[53]SUPA - School of Physics and Astronomy, University of Glasgow, Glasgow, United Kingdom
[54]II Physikalisches Institut, Georg-August-Universität, Göttingen, Germany
[55]Laboratoire de Physique Subatomique et de Cosmologie, Université Grenoble-Alpes, CNRS/IN2P3, Grenoble, France
[56]Department of Physics, Hampton University, Hampton, Virginia, USA
[57]Laboratory for Particle Physics and Cosmology, Harvard University, Cambridge, Massachusetts, USA
[58a]Kirchhoff-Institut für Physik, Ruprecht-Karls-Universität Heidelberg, Heidelberg, Germany
[58b]Physikalisches Institut, Ruprecht-Karls-Universität Heidelberg, Heidelberg, Germany
[58c]ZITI Institut für technische Informatik, Ruprecht-Karls-Universität Heidelberg, Mannheim, Germany
[59]Faculty of Applied Information Science, Hiroshima Institute of Technology, Hiroshima, Japan
[60]Department of Physics, Indiana University, Bloomington, Indiana, USA
[61]Institut für Astro- und Teilchenphysik, Leopold-Franzens-Universität, Innsbruck, Austria
[62]University of Iowa, Iowa City, Iowa, USA
[63]Department of Physics and Astronomy, Iowa State University, Ames, Iowa, USA
[64]Joint Institute for Nuclear Research, JINR Dubna, Dubna, Russia
[65]KEK, High Energy Accelerator Research Organization, Tsukuba, Japan
[66]Graduate School of Science, Kobe University, Kobe, Japan
[67]Faculty of Science, Kyoto University, Kyoto, Japan
[68]Kyoto University of Education, Kyoto, Japan
[69]Department of Physics, Kyushu University, Fukuoka, Japan
[70]Instituto de Física La Plata, Universidad Nacional de La Plata and CONICET, La Plata, Argentina
[71]Physics Department, Lancaster University, Lancaster, United Kingdom
[72a]INFN Sezione di Lecce, Italy
[72b]Dipartimento di Matematica e Fisica, Università del Salento, Lecce, Italy
[73]Oliver Lodge Laboratory, University of Liverpool, Liverpool, United Kingdom
[74]Department of Physics, Jožef Stefan Institute and University of Ljubljana, Ljubljana, Slovenia
[75]School of Physics and Astronomy, Queen Mary University of London, London, United Kingdom
[76]Department of Physics, Royal Holloway University of London, Surrey, United Kingdom
[77]Department of Physics and Astronomy, University College London, London, United Kingdom
[78]Louisiana Tech University, Ruston, Louisiana, USA
[79]Laboratoire de Physique Nucléaire et de Hautes Energies, UPMC and Université Paris-Diderot and CNRS/IN2P3, Paris, France
[80]Fysiska institutionen, Lunds universitet, Lund, Sweden
[81]Departamento de Fisica Teorica C-15, Universidad Autonoma de Madrid, Madrid, Spain
[82]Institut für Physik, Universität Mainz, Mainz, Germany
[83]School of Physics and Astronomy, University of Manchester, Manchester, United Kingdom
[84]CPPM, Aix-Marseille Université and CNRS/IN2P3, Marseille, France
[85]Department of Physics, University of Massachusetts, Amherst, Massachusetts, USA
[86]Department of Physics, McGill University, Montreal, QC, Canada
[87]School of Physics, University of Melbourne, Victoria, Australia
[88]Department of Physics, The University of Michigan, Ann Arbor, Michigan, USA
[89]Department of Physics and Astronomy, Michigan State University, East Lansing, Michigan, USA
[90a]INFN Sezione di Milano, Italy
[90b]Dipartimento di Fisica, Università di Milano, Milano, Italy
[91]B.I. Stepanov Institute of Physics, National Academy of Sciences of Belarus, Minsk, Republic of Belarus
[92]National Scientific and Educational Centre for Particle and High Energy Physics, Minsk, Republic of Belarus
[93]Department of Physics, Massachusetts Institute of Technology, Cambridge, Massachusetts, USA
[94]Group of Particle Physics, University of Montreal, Montreal QC, Canada
[95]P.N. Lebedev Institute of Physics, Academy of Sciences, Moscow, Russia
[96]Institute for Theoretical and Experimental Physics (ITEP), Moscow, Russia
[97]Moscow Engineering and Physics Institute (MEPhI), Moscow, Russia
[98]D.V.Skobeltsyn Institute of Nuclear Physics, M.V.Lomonosov Moscow State University, Moscow, Russia
[99]Fakultät für Physik, Ludwig-Maximilians-Universität München, München, Germany
[100]Max-Planck-Institut für Physik (Werner-Heisenberg-Institut), München, Germany
[101]Nagasaki Institute of Applied Science, Nagasaki, Japan

[102]*Graduate School of Science and Kobayashi-Maskawa Institute, Nagoya University, Nagoya, Japan*
[103a]*INFN Sezione di Napoli, Italy*
[103b]*Dipartimento di Fisica, Università di Napoli, Napoli, Italy*
[104]*Department of Physics and Astronomy, University of New Mexico, Albuquerque, New Mexico, USA*
[105]*Institute for Mathematics, Astrophysics and Particle Physics, Radboud University Nijmegen/Nikhef, Nijmegen, Netherlands*
[106]*Nikhef National Institute for Subatomic Physics and University of Amsterdam, Amsterdam, Netherlands*
[107]*Department of Physics, Northern Illinois University, DeKalb, Illinois, USA*
[108]*Budker Institute of Nuclear Physics, SB RAS, Novosibirsk, Russia*
[109]*Department of Physics, New York University, New York, New York, USA*
[110]*Ohio State University, Columbus, Ohio, USA*
[111]*Faculty of Science, Okayama University, Okayama, Japan*
[112]*Homer L. Dodge Department of Physics and Astronomy, University of Oklahoma, Norman, Oklahoma, USA*
[113]*Department of Physics, Oklahoma State University, Stillwater, Oklahoma, USA*
[114]*Palacký University, RCPTM, Olomouc, Czech Republic*
[115]*Center for High Energy Physics, University of Oregon, Eugene, Oregon, USA*
[116]*LAL, Université Paris-Sud and CNRS/IN2P3, Orsay, France*
[117]*Graduate School of Science, Osaka University, Osaka, Japan*
[118]*Department of Physics, University of Oslo, Oslo, Norway*
[119]*Department of Physics, Oxford University, Oxford, United Kingdom*
[120a]*INFN Sezione di Pavia, Italy*
[120b]*Dipartimento di Fisica, Università di Pavia, Pavia, Italy*
[121]*Department of Physics, University of Pennsylvania, Philadelphia, Pennsylvania, USA*
[122]*Petersburg Nuclear Physics Institute, Gatchina, Russia*
[123a]*INFN Sezione di Pisa, Italy*
[123b]*Dipartimento di Fisica E. Fermi, Università di Pisa, Pisa, Italy*
[124]*Department of Physics and Astronomy, University of Pittsburgh, Pittsburgh, Pennsylvania, USA*
[125a]*Laboratorio de Instrumentacao e Fisica Experimental de Particulas - LIP, Lisboa, Portugal*
[125b]*Faculdade de Ciências, Universidade de Lisboa, Lisboa, Portugal*
[125c]*Department of Physics, University of Coimbra, Coimbra, Portugal*
[125d]*Centro de Física Nuclear da Universidade de Lisboa, Lisboa, Portugal*
[125e]*Departamento de Fisica, Universidade do Minho, Braga, Portugal*
[125f]*Departamento de Fisica Teorica y del Cosmos and CAFPE, Universidad de Granada, Granada (Spain), Portugal*
[125g]*Dep Fisica and CEFITEC of Faculdade de Ciencias e Tecnologia, Universidade Nova de Lisboa, Caparica, Portugal*
[126]*Institute of Physics, Academy of Sciences of the Czech Republic, Praha, Czech Republic*
[127]*Czech Technical University in Prague, Praha, Czech Republic*
[128]*Faculty of Mathematics and Physics, Charles University in Prague, Praha, Czech Republic*
[129]*State Research Center Institute for High Energy Physics, Protvino, Russia*
[130]*Particle Physics Department, Rutherford Appleton Laboratory, Didcot, United Kingdom*
[131]*Physics Department, University of Regina, Regina SK, Canada*
[132]*Ritsumeikan University, Kusatsu, Shiga, Japan*
[133a]*INFN Sezione di Roma, Italy*
[133b]*Dipartimento di Fisica, Sapienza Università di Roma, Roma, Italy*
[134a]*INFN Sezione di Roma Tor Vergata, Italy*
[134b]*Dipartimento di Fisica, Università di Roma Tor Vergata, Roma, Italy*
[135a]*INFN Sezione di Roma Tre, Italy*
[135b]*Dipartimento di Matematica e Fisica, Università Roma Tre, Roma, Italy*
[136a]*Faculté des Sciences Ain Chock, Réseau Universitaire de Physique des Hautes Energies - Université Hassan II, Casablanca, Morocco*
[136b]*Centre National de l'Energie des Sciences Techniques Nucleaires, Rabat, Morocco*
[136c]*Faculté des Sciences Semlalia, Université Cadi Ayyad, LPHEA-Marrakech, Morocco*
[136d]*Faculté des Sciences, Université Mohamed Premier and LPTPM, Oujda, Morocco*
[136e]*Faculté des sciences, Université Mohammed V-Agdal, Rabat, Morocco*
[137]*DSM/IRFU (Institut de Recherches sur les Lois Fondamentales de l'Univers), CEA Saclay (Commissariat à l'Energie Atomique et aux Energies Alternatives), Gif-sur-Yvette, France*

[138]*Santa Cruz Institute for Particle Physics, University of California Santa Cruz, Santa Cruz, California, USA*
[139]*Department of Physics, University of Washington, Seattle, Washington, USA*
[140]*Department of Physics and Astronomy, University of Sheffield, Sheffield, United Kingdom*
[141]*Department of Physics, Shinshu University, Nagano, Japan*
[142]*Fachbereich Physik, Universität Siegen, Siegen, Germany*
[143]*Department of Physics, Simon Fraser University, Burnaby BC, Canada*
[144]*SLAC National Accelerator Laboratory, Stanford, California, USA*
[145a]*Faculty of Mathematics, Physics & Informatics, Comenius University, Bratislava, Slovak Republic*
[145b]*Department of Subnuclear Physics, Institute of Experimental Physics of the Slovak Academy of Sciences, Kosice, Slovak Republic*
[146a]*Department of Physics, University of Cape Town, Cape Town, South Africa*
[146b]*Department of Physics, University of Johannesburg, Johannesburg, South Africa*
[146c]*School of Physics, University of the Witwatersrand, Johannesburg, South Africa*
[147a]*Department of Physics, Stockholm University, Sweden*
[147b]*The Oskar Klein Centre, Stockholm, Sweden*
[148]*Physics Department, Royal Institute of Technology, Stockholm, Sweden*
[149]*Departments of Physics & Astronomy and Chemistry, Stony Brook University, Stony Brook, New York, USA*
[150]*Department of Physics and Astronomy, University of Sussex, Brighton, United Kingdom*
[151]*School of Physics, University of Sydney, Sydney, Australia*
[152]*Institute of Physics, Academia Sinica, Taipei, Taiwan*
[153]*Department of Physics, Technion: Israel Institute of Technology, Haifa, Israel*
[154]*Raymond and Beverly Sackler School of Physics and Astronomy, Tel Aviv University, Tel Aviv, Israel*
[155]*Department of Physics, Aristotle University of Thessaloniki, Thessaloniki, Greece*
[156]*International Center for Elementary Particle Physics and Department of Physics, The University of Tokyo, Tokyo, Japan*
[157]*Graduate School of Science and Technology, Tokyo Metropolitan University, Tokyo, Japan*
[158]*Department of Physics, Tokyo Institute of Technology, Tokyo, Japan*
[159]*Department of Physics, University of Toronto, Toronto, ON, Canada*
[160a]*TRIUMF, Vancouver, BC, Canada*
[160b]*Department of Physics and Astronomy, York University, Toronto, ON, Canada*
[161]*Faculty of Pure and Applied Sciences, University of Tsukuba, Tsukuba, Japan*
[162]*Department of Physics and Astronomy, Tufts University, Medford, Massachusetts, USA*
[163]*Centro de Investigaciones, Universidad Antonio Narino, Bogota, Colombia*
[164]*Department of Physics and Astronomy, University of California Irvine, Irvine, California, USA*
[165a]*INFN Gruppo Collegato di Udine, Sezione di Trieste, Udine, Italy*
[165b]*ICTP, Trieste, Italy*
[165c]*Dipartimento di Chimica, Fisica e Ambiente, Università di Udine, Udine, Italy*
[166]*Department of Physics, University of Illinois, Urbana, Illinois, USA*
[167]*Department of Physics and Astronomy, University of Uppsala, Uppsala, Sweden*
[168]*Instituto de Física Corpuscular (IFIC) and Departamento de Física Atómica, Molecular y Nuclear and Departamento de Ingeniería Electrónica and Instituto de Microelectrónica de Barcelona (IMB-CNM), University of Valencia and CSIC, Valencia, Spain*
[169]*Department of Physics, University of British Columbia, Vancouver, BC, Canada*
[170]*Department of Physics and Astronomy, University of Victoria, Victoria, BC, Canada*
[171]*Department of Physics, University of Warwick, Coventry, United Kingdom*
[172]*Waseda University, Tokyo, Japan*
[173]*Department of Particle Physics, The Weizmann Institute of Science, Rehovot, Israel*
[174]*Department of Physics, University of Wisconsin, Madison, Wisconsin, USA*
[175]*Fakultät für Physik und Astronomie, Julius-Maximilians-Universität, Würzburg, Germany*
[176]*Fachbereich C Physik, Bergische Universität Wuppertal, Wuppertal, Germany*
[177]*Department of Physics, Yale University, New Haven, Connecticut, USA*
[178]*Yerevan Physics Institute, Yerevan, Armenia*
[179]*Centre de Calcul de l'Institut National de Physique Nucléaire et de Physique des Particules (IN2P3), Villeurbanne, France*

[a]Deceased.
[b]Also at Department of Physics, King's College London, London, United Kingdom.

[c]Also at Institute of Physics, Azerbaijan Academy of Sciences, Baku, Azerbaijan.
[d]Also at Particle Physics Department, Rutherford Appleton Laboratory, Didcot, United Kingdom.
[e]Also at TRIUMF, Vancouver, BC, Canada.
[f]Also at Department of Physics, California State University, Fresno, CA, USA.
[g]Also at Tomsk State University, Tomsk, Russia.
[h]Also at CPPM, Aix-Marseille Université and CNRS/IN2P3, Marseille, France.
[i]Also at Università di Napoli Parthenope, Napoli, Italy.
[j]Also at Institute of Particle Physics (IPP), Canada.
[k]Also at Department of Physics, St. Petersburg State Polytechnical University, St. Petersburg, Russia.
[l]Also at Chinese University of Hong Kong, China.
[m]Also at Department of Financial and Management Engineering, University of the Aegean, Chios, Greece.
[n]Also at Louisiana Tech University, Ruston, LA, USA.
[o]Also at Institucio Catalana de Recerca i Estudis Avancats, ICREA, Barcelona, Spain.
[p]Also at Department of Physics, The University of Texas at Austin, Austin, TX, USA.
[q]Also at Institute of Theoretical Physics, Ilia State University, Tbilisi, Georgia.
[r]Also at CERN, Geneva, Switzerland.
[s]Also at Ochadai Academic Production, Ochanomizu University, Tokyo, Japan.
[t]Also at Manhattan College, New York, NY, USA.
[u]Also at Novosibirsk State University, Novosibirsk, Russia.
[v]Also at Institute of Physics, Academia Sinica, Taipei, Taiwan.
[w]Also at LAL, Université Paris-Sud and CNRS/IN2P3, Orsay, France.
[x]Also at Academia Sinica Grid Computing, Institute of Physics, Academia Sinica, Taipei, Taiwan.
[y]Also at Laboratoire de Physique Nucléaire et de Hautes Energies, UPMC and Université Paris-Diderot and CNRS/IN2P3, Paris, France.
[z]Also at School of Physical Sciences, National Institute of Science Education and Research, Bhubaneswar, India.
[aa]Also at Dipartimento di Fisica, Sapienza Università di Roma, Roma, Italy.
[bb]Also at Moscow Institute of Physics and Technology State University, Dolgoprudny, Russia.
[cc]Also at Section de Physique, Université de Genève, Geneva, Switzerland.
[dd]Also at International School for Advanced Studies (SISSA), Trieste, Italy.
[ee]Also at Department of Physics and Astronomy, University of South Carolina, Columbia, SC, USA.
[ff]Also at School of Physics and Engineering, Sun Yat-sen University, Guangzhou, China.
[gg]Also at Faculty of Physics, M.V.Lomonosov Moscow State University, Moscow, Russia.
[hh]Also at Moscow Engineering and Physics Institute (MEPhI), Moscow, Russia.
[ii]Also at Institute for Particle and Nuclear Physics, Wigner Research Centre for Physics, Budapest, Hungary.
[jj]Also at Department of Physics, Oxford University, Oxford, United Kingdom.
[kk]Also at Department of Physics, Nanjing University, Jiangsu, China.
[ll]Also at Institut für Experimentalphysik, Universität Hamburg, Hamburg, Germany.
[mm]Also at Department of Physics, The University of Michigan, Ann Arbor, MI, USA.
[nn]Also at Discipline of Physics, University of KwaZulu-Natal, Durban, South Africa.
[oo]Also at University of Malaya, Department of Physics, Kuala Lumpur, Malaysia.